INSIGHTS INTO VIRUS-HOST INTERACTIONS: REGULATION OF CYTOKINE SIGNALING IS A VIRULENCE DETERMINANT OF WEST NILE VIRUS

APPROVED BY SUPERVISORY COMMITTEE

Michael Gale, Jr., Ph.D.
Supervising Professor

Donald Sodora, Ph.D.
Chair, Examining Committee

J. David Farrar, Ph.D.
Committee Member

Julie Pfeiffer, Ph.D.
Committee Member

DEDICATION

This dissertation is dedicated to my family.

To my parents, Jim and Sherry, you instilled in me a fundamental desire to learn, a never-give-up work ethic and personal values that can only be taught by people who they, themselves, possess. You have always loved and supported me in whatever decision I made and for that, I am truly grateful. To my sister, Krista, you are a true inspiration to me. The differences you are making in kids' lives and the love of science you are instilling in your students will last forever. Thank you for always caring about what was going on in my life and for providing words of encouragement when I needed them most.

To my wife and best friend, Amber, your love and support can never be measured. You have always been by my side, helping me through the difficult times and celebrating the wonderful times. The daily joy and inspiration you provide give me the will to always push ahead; I could not have accomplished half of what I have without your love. Finally, I want to dedicate this dissertation to the light of my life, my beautiful daughter, Anna. You are my never-ending source of love and laughter and always serve to remind me of what is truly important in life. Coming home to your little, smiling face after a long day in the lab makes it all worth it.

ACKNOWLEDGMENTS

As with any significant research project, many people contributed to the final version of my dissertation through their insightful comments, helpful suggestions and technical assistance. First and foremost, I want to thank my mentor, Dr. Michael Gale, for giving me a chance to pursue a new avenue of research in his lab. What started out as a seemingly orphan project has blossomed into a significant focus in his lab. Mike was a great mentor because he led by his actions. Whether through his probing questions at meetings, his determined work ethic or his persistence in the face of adversity, Mike demonstrated what it takes to be a respected scientist. He also taught me to always ask the next question, to never be satisfied with results achieved but to look for questions to be answered and of course, to always find the positive in whatever the outcome. It is these attributes, in addition to the scientific knowledge gained, that I will take with me as I progress through my career.

I also want to thank the members, both past and present, of the Gale lab for providing a wonderful environment to do science. Dr. Brenda Fredericksen was critical to my training in BSL-3 techniques and protocols. Cindy Johnson and Andrea Erickson were always there with suggestions and comments for my experiments, presentations and publications. Cindy also provided me with several of the illustrations used in figures throughout this work. Mehul Suthar, the newest member of the Gale lab, was instrumental in helping me finish experiments for the SOCS story. I also want to thank Kristan Hagan, David Owen, Dr. Yueh-Ming Loo and Dr. Junichi Tanabe for their

support over the past few years. Past Gale lab members who contributed both intellectually and technically to my project include Dr. Eileen Foy, Dr. Rhea Sumpter, Dr. Chunfu Wang, Penny Fish, Dr. Spencer Carney and Jill Pflugheber. Finally, my dissertation would not be complete without thanking Dr. Takeshi Saito and Nanette Crochet for all of the wonderful laughs and fun times they provided. It was always easy to come to the lab because I knew they would be there to brighten the day. To the members of the Gale lab, I say "Thank you for everything. You are great scientists, and it was a pleasure working with each and every one of you."

My project would not have even been possible without Dr. Richard Mock at the Texas A&M Veterinary Medical Diagnostics Laboratory who isolated and sent us the TX02 strain. Melanie Samuel and Dr. Michael Diamond at Washington University conducted the IFNAR mouse studies. Dr. Peter Mason at the UT Medical Branch carried out the initial in vivo characterization of TX02. I am most grateful to Dr. Lisa Kinch for her amazing assistance with the phylogenetic analyses. The functional genomics experiment would not have been possible without Dr. Michael Katze, Dr. Jamie Fornek and Sean Proll at the University of Washington. I also need to thank the UT Southwestern Sequencing Core for their assistance.

I would also like to thank the members of my dissertation committee, Drs. Donald Sodora, David Farrar and Julie Pfeiffer. The comments they provided and the questions they asked were extremely valuable in furthering my scientific training. I need to thank the Department of Microbiology for awarding me a training grant to support my studies.

Rachel Cassady in the department office deserves a special thank you for all of the assistance she provided in regards to travel for the numerous conferences the Gale lab attends. Finally, I would like to thank the UT Southwestern Medical Scientist Training Program, especially Robin Downing and Stephanie Robertson, for their support over the course of my studies.

INSIGHTS INTO VIRUS-HOST INTERACTIONS: REGULATION OF CYTOKINE SIGNALING IS A VIRULENCE DETERMINANT OF WEST NILE VIRUS

by

BRIAN CHRISTOPHER KELLER

DISSERTATION

Presented to the Faculty of the Graduate School of Biomedical Sciences

The University of Texas Southwestern Medical Center at Dallas

In Partial Fulfillment of the Requirements

For the Degree of

DOCTOR OF PHILOSOPHY

The University of Texas Southwestern Medical Center at Dallas

Dallas, Texas

May, 2007

INSIGHTS INTO VIRUS-HOST INTERACTIONS: REGULATION OF CYTOKINE SIGNALING IS A VIRULENCE DETERMINANT OF WEST NILE VIRUS

Publication No. _____

Brian Christopher Keller, Ph.D.

The University of Texas Southwestern Medical Center at Dallas, 2007

Supervising Professor: Michael Gale, Jr., Ph.D.

West Nile virus (WNV) has rapidly become a pathogen of global importance over the past two decades. Its recent association with severe neurological disease and emergence in the Western Hemisphere suggest that the virus has acquired the ability to effectively evade host immune defenses. One of the earliest steps in controlling viral infection occurs through the action of interferon (IFN) and its downstream activation of an antiviral state within the infected cell and neighboring tissue. To begin to understand how WNV evades host defenses, studies were initiated to examine the interaction of virulent (TX02) and avirulent (MAD78) WNV strains with the host IFN system. Compared to TX02, MAD78 replicated at

lower levels in cultured human cells, was highly sensitive to the antiviral actions of IFN in vitro and demonstrated a completely avirulent phenotype in wild-type mice. In contrast to TX02 and other pathogenic forms of WNV, MAD78 was defective in its ability to disrupt IFN-induced JAK-STAT signaling. However, replication of MAD78 was rescued in cells lacking a functional IFNα/β receptor (IFNAR). Consistent with this, MAD78 virulence was unmasked upon infection of mice lacking IFNAR. The regulation of IFN signaling was multifactorial involving a combination of viral and host factors. In particular, overexpression of various proteins from the pathogenic TX02 strain and the nonpathogenic MAD78 strain attenuated signaling to an IFN-responsive promoter, suggesting that viral products from both strains are capable of contributing to the IFN signal block. Differences between TX02 and MAD78 were identified, however, when host suppressors of cytokine signaling (SOCS) proteins were shown to be differentially upregulated by the two strains. Furthermore, expression of a dominant-negative form of SOCS1 partially restored IFN signaling during TX02 infection indicating that SOCS proteins do in fact participate in virus-induced signaling suppression. Importantly, WNV regulation of signaling was not restricted to IFNα/β but included IFNγ and IL-6, cytokines that similarly utilize JAK-STAT. These studies demonstrate novel insights into the complex interactions that occur between a virus and its infected host cell and may allow for the identification of viral and cellular targets for the development of improved therapeutics and new vaccine strategies.

TABLE OF CONTENTS

PUBLICATIONS

Keller BC, Suthar M and Gale M Jr. (2007) Viral and cellular regulation of cytokine signaling during West Nile virus infection. (*In preparation*)

Fredericksen BL, **Keller BC**, Fornek J, Katze MG, and Gale M Jr. (2007) Establishment and maintenance of the innate antiviral response to West Nile virus requires both RIG-I and MDA5 signaling through IPS-1. (*In preparation*)

Daffis S, Samuel MA, **Keller BC**, Gale M Jr., and Diamond MS. (2007) IRF-3 protects from lethal West Nile virus infection by controlling infection in peripheral tissues through an IFN-independent mechanism. *PLOS Pathogens*. (*In press*)

Keller BC, Johnson CL, Erickson A, and Gale M Jr. (2007) Innate immune evasion by hepatitis C virus and West Nile virus. *Cytokine & Growth Factor Reviews.* (*In press*)

Keller BC, Fredericksen BL, Samuel MA, Mock RE, Mason PW, Diamond MS, and Gale M Jr. (2006) Resistance to alpha/beta interferon is a determinant of West Nile virus replication fitness and virulence. *Journal of Virology*. 80(19):9424-34.

Samuel MA, Whitby K, **Keller BC**, Marri A, Barchet W, Williams BRG, Silverman RH, Gale M. Jr., and Diamond MS. (2006) PKR and RNase L contribute to protection against lethal West Nile Virus infection by controlling early viral spread in the periphery and replication in neurons. *Journal of Virology*. 80(14):7009-7019.

Wang C, Gale M Jr., **Keller BC**, Huang H, Brown MS, Goldstein JL, and Ye J. (2005) Identification of FBL2 as a geranylgeranylated cellular protein required for Hepatitis C virus RNA replication. *Molecular Cell*. 18(4):425-34.

Cornillot E, **Keller B**, Cushion MT, Metenier G, and Vivares CP. (2002) Fine analysis of the *Pneumocystis carinii* f. sp. *carinii* genome by two-dimensional pulsed-field gel electrophoresis. *Gene.* 293:87-95.

Kumar M, **Keller B**, Makalou N, and Sutton RE. (2001) Systematic Determination of the Packaging Limit of Lentiviral Vectors. *Human Gene Therapy.* 12:1893-1905.

LIST OF FIGURES

LIST OF TABLES

ABBREVIATIONS

AFP – acute flaccid paralysis

CARD – caspase activation and recruitment domain

CNS – central nervous system

DENV – Dengue virus

DN – dominant negative

FITC – fluorescein isothiocyanate

GAPDH – glyceraldehyde 3-phosphate dehydrogenase

HA – hemagglutinin

HCV – hepatitis C virus

IFN – interferon

IFNAR – interferon alpha/beta receptor

IPS-1 – interferon-beta promoter stimulator 1

ISRE – interferon stimulated response element

JEV – Japanese encephalitis virus

LB/amp –Luria-Bertani bacteria culture media (agar or broth) containing 50 μg/ml ampicillin

LGTV – Langat virus

MAD78 – WNV Madagascar-AnMg798

MEF – mouse embryo fibroblast

MVEV – Murray Valley encephalitis virus

MOI – multiplicity of infection

NFDM – non-fat dried milk

NS – nonstructural

NTR – nontranslated region

NY 3356 – WNV NY 2000-crow3356

PAMP – pathogen associated molecular pattern

poly(I:C) – polyinosinic:polycytidylic acid

PRR – pathogen recognition receptor

SDS – sodium dodecyl sulfate

SF-DMEM – serum-free Dulbecco's modified eagle medium

SLEV – St. Louis encephalitis virus

TBEV – tick-borne encephalitis virus

TLR – toll-like receptor

TX02 – WNV TX 2002-HC

VSV – vesicular stomatitis virus

WT – wild-type

YFV – Yellow fever virus

CHAPTER ONE
Introduction & Literature Review

An old virus learns new tricks

Entebbè, Uganda, 1937:

> An African woman, aged 37 years, was seen by one of us (A. W. B.) in December 1937 at Omogo, West Nile district, Northern Province of Uganda. This woman reported to the officers of the sleeping sickness survey and was not subjected to other examination than that which is usual in the routine survey, except that her temperature was taken. Her oral temperature was 100.6ºF. She denied feeling ill, perhaps to avoid hospitalization. Nevertheless a sample of her blood was taken, and serum from it was inoculated intracerebrally into mice. The woman was not seen again until 3 months later, when another specimen of her blood was taken. At this time she denied that she had been ill at or near the time she was seen in December. She was not altogether co-operative and it is possible that she withheld pertinent facts.
>
> Of the ten mice inoculated with the original blood serum of the woman, only one survived. The others became ill 6 to 8 days after inoculation and either died or were sacrificed for subinoculation. The infectious agent was readily established in mice and was preserved for months in the frozen state. Subinoculations in series have been done by injecting each mouse intracerebrally with 0.03 cc. of the supernatant from a suspension of infected mouse brain in saline. The virus is now (September 15, 1939) in its 53rd passage, and there have been no survivors since the first mouse passage. . . (as reported by Smithburn, Hughes, Burke and Paul in (245))

Smithburn and colleagues, in their seminal article, went on to demonstrate that the infectious agent isolated from the febrile woman was filterable down to a limiting membrane with pore diameter of 62 nm suggesting the presence of a virus. Furthermore, they characterized in detail, the pathogenicity of the virus in mice, rhesus macaques, rabbits, guinea pigs and hedgehogs using multiple inoculation routes. Through histological studies they described the pathology of central nervous system (CNS) lesions. Finally, using serum neutralization tests, they proposed that the virus, which they named the West Nile virus (WNV), was related to Japanese B encephalitis viruses (JEV), a relationship that still holds true today.

Since its discovery in 1937, WNV has become a pathogen of global importance (Figure 1-1). Although first identified in Uganda, WNV was most likely endemic to the African subcontinent long before (173). However, over the course of the next 50 years, the virus would be identified in geographically distant countries throughout the Eastern Hemisphere. For most of this time though, human cases of WNV infection were sporadic and consisted of a mild, flu-like illness (WN fever), if symptoms appeared at all. In fact, the presence of WNV in these regions was usually determined by serological detection of WNV-specific antibodies in healthy humans, birds and other animals or by isolation of the virus from wild animals. Exceptions to the sporadic nature of cases include several localized

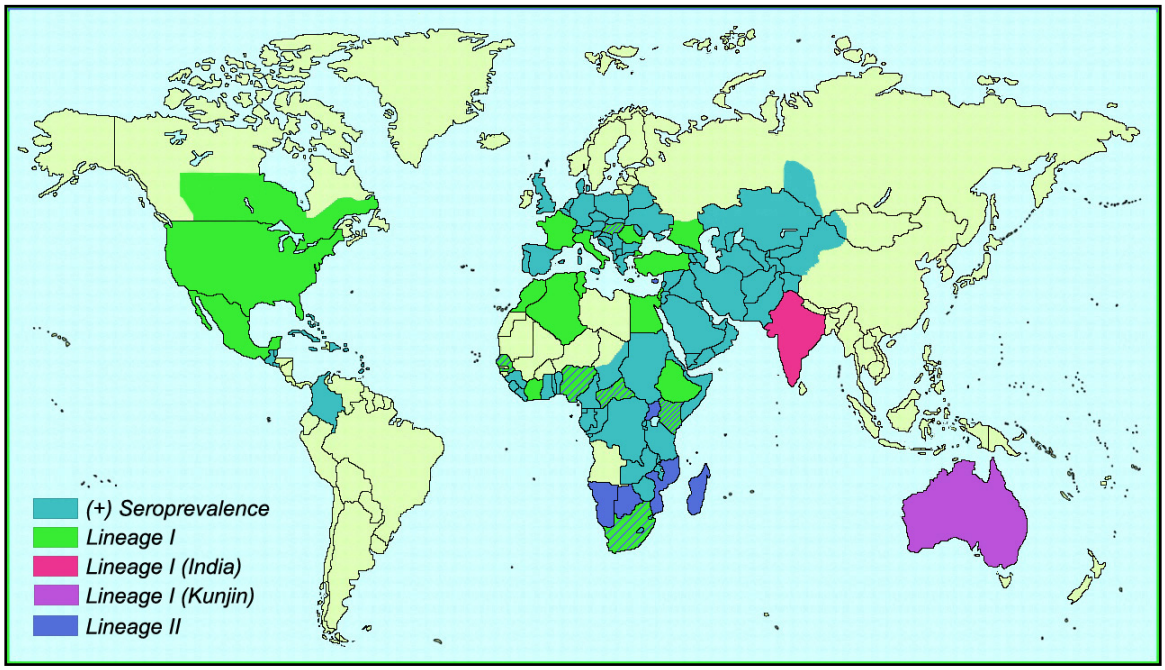

Figure 1-1. Global WNV distribution.
Locations of WNV seroprevalence as determined by the presence of neutralizing antibodies are depicted in light blue. WNV lineage I (clades a, b and c) are shown in green, purple and pink, respectively. Dark blue represents the presence of WNV lineage II isolates. Lineage I and lineage II co-circulate in countries colored with blue/green stripes. Map was adapted from (246).

summertime epidemics of WN fever in Israel in the 1950s (89) and a widespread epidemic of WN fever in South Africa from 1973-1974 affecting thousands of people (178). Beginning in the late 1980s, outbreaks of epidemic WNV suddenly began occurring at a higher frequency and with significantly more severe disease manifestations including death of infected individuals. Outbreaks of meningitis and encephalitis were documented in India in 1987 (82), Romania in 1996 (226), Tunisia in 1997 (71), Russia in 1999 (208) and Israel in 2000 (134). In addition to the increased propensity for the virus to cause CNS disease, these outbreaks highlighted another change in the epidemiology of WNV: for the first time, WNV caused large scale deaths among infected birds and horses. The dramatic shift in WNV pathogenesis was most clearly realized in 1999 when the virus made its entrée into the ecology of North America. From 1999 on, WNV spread from New York City, where it was first detected, west across the United States, north into Canada, and most recently, south into Mexico, the Caribbean and Central and South America. In the U.S. alone, the expansion of WNV across the country has resulted in nearly 24,000 documented cases and 950 deaths, mostly occurring over the last 5 years (Figure 1-2) (48). However, data from a household survey conducted shortly after the appearance of WNV in 1999 suggest that the actual number of human WNV infections over the course of the epidemic may be closer to 1.4 million (189). In either case, the number of human WNV cases has remained relatively stable over the past few years, and it appears that WNV has firmly established itself in the ecology of North America.

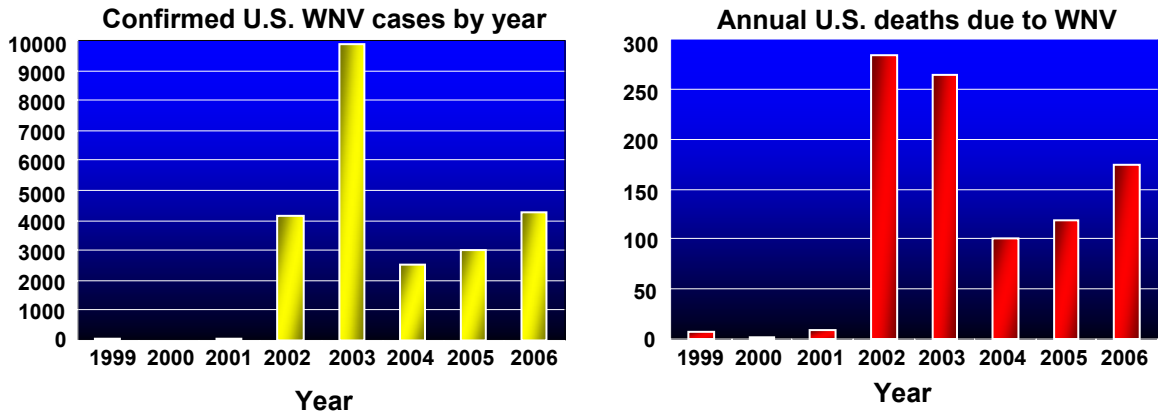

Figure 1-2. Epidemiology of WNV in the U.S. 1999-2006.
The graph on the left shows the number of confirmed WNV cases by year as reported to the Centers for Disease Control and Prevention (48). Annual deaths due to WNV infection are depicted in the graph to the right. The large increase in number of cases and deaths in 2002-2003 was most likely due to a greater public awareness of the epidemic resulting in better use of diagnostic tests in the clinic. After a dramatic drop in cases/deaths in 2004, there now appears to be a trend for increasing numbers of severe cases of WNV.

The work of Smithburn and colleagues laid the groundwork for a field of study on a novel, emerging, neurotropic virus. Little did they know that the virus they isolated at the Yellow Fever Research Institute in Uganda would eventually be detected throughout Africa, Europe, the Middle East, Asia and Australia before its arrival in North America some 70 years later. The expansion of WNV, especially to North America, has proved to be an excellent natural experiment for the study of virus-host interactions in naïve populations of humans, birds, insects and other animals.

The enhanced lethality of WNV during recent epidemics suggests that the virus has acquired characteristics that provide it with an advantage in the battle against host immune defenses. What these new traits are exactly is the focus of intense study in many labs across

the globe. Since viruses interact with infected hosts on many different levels (i.e. entry, replication, translation, maturation and egress), there exist many opportunities for a virus to acquire an advantage over its host resulting in a successful infection. For example, viruses must counteract host innate and cell-mediated immune defenses as well as compete for host components needed for replication of viral nucleic acid, all-the-while maintaining elements absolutely required for the virus' natural transmission life cycle in nature. It is the interaction of WNV with the innate immune response in the infected cell that forms the basis of the studies described in this dissertation.

Biology of WNV

WNV is a member of the *Flaviviridae* family of positive-sense single-stranded RNA viruses which also includes the neurotropic viruses JEV, St. Louis encephalitis virus (SLEV) and Murray Valley encephalitis virus (MVEV) as well as the more distantly related Dengue viruses (DENV), Yellow fever virus (YFV), Tick-borne encephalitis virus (TBEV) and Hepatitis C virus (HCV) (216) (Figure 1-3). WNV strains are separated into two lineages, lineage I and lineage II, on the basis of their nucleotide and amino acid sequences. Strains associated with the recent outbreaks of neuroinvasive disease are in lineage I, while the original isolate of WNV is a lineage II form of the virus. WNV is a spherical, enveloped virus with an icosahedral virion 40-60 nm in diameter (35,191,216). Unlike some other enveloped viruses, the surface of the WNV envelope is relatively smooth and lacks spike-like projections (191).

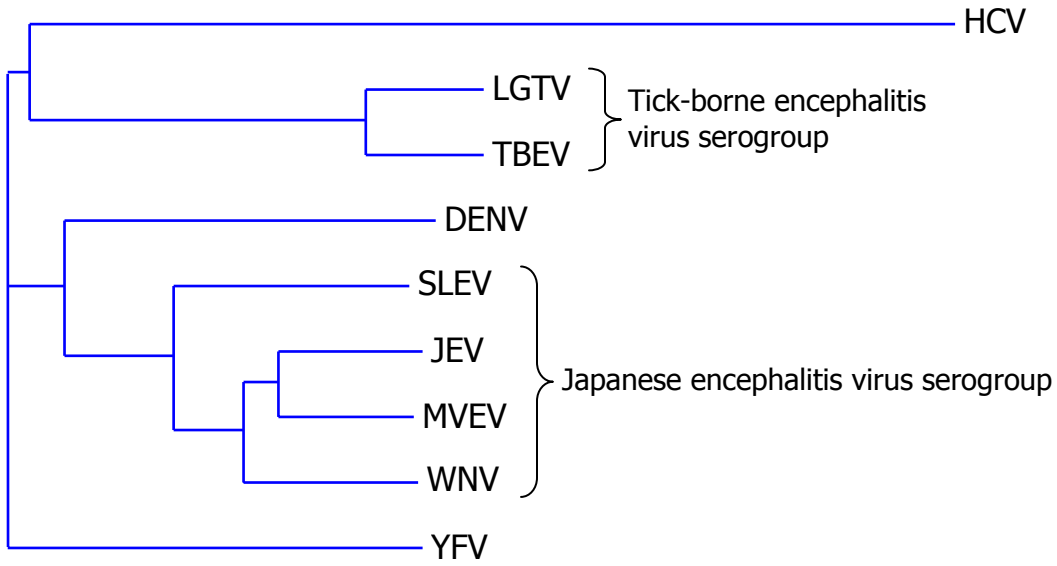

Figure 1-3. Phylogenetic relationships of the *Flaviviridae*
Complete amino acid sequences of representative members of the *Flaviviridae* were aligned using Clustal W and assembled into a tree with the Neighbor Joining method. DV, Dengue virus serotype 2 strain 16681 (GenBank #U87411); HCV, Hepatitis C virus genotype 1A strain H77 (GenBank # NC_004102); JEV, Japanese encephalitis virus strain HW (GenBank #AY849939); LGTV, Langat virus strain TP21 (GenBank #AF253419); MVEV, Murray Valley encephalitis virus (GenBank #NC_000943); SLEV, St. Louis encephalitis virus strain Kern 217 (GenBank #NC_007580); TBEV, Tick-borne encephalitis virus strain Vasilchenko (GenBank #L40361); WNV, West Nile virus lineage I strain NY99 (GenBank #AF196835); YFV, Yellow Fever virus strain Couma (GenBank #DQ235229).

Genome organization and viral proteins

The genome of WNV is approximately 11 kb in length and encodes a single open reading frame (ORF) of 10.3 kb. The WNV ORF is translated as a single polyprotein (NH_2-C-prM-E-NS1-NS2A-NS2B-NS3-NS4A-NS4B-NS5-COOH) with structural genes occupying the first 25% of the ORF and nonstructural (NS) genes in the remainder (Figure 1-4). Co- and post-translational cleavage by the viral NS2B3 serine protease as well as host furin and Golgi-localized proteases yields at least 10 viral proteins. The extreme 5' and 3' ends of the viral genome flanking the ORF are referred to as nontranslated regions (NTR) and encode highly conserved secondary structural elements responsible for proper replication and translation of the viral genome. The 3 genes immediately downstream from the 5' NTR encode the viral structural genes: capsid (C), premembrane (prM) and envelope (E). C encodes the viral capsid protein and contains a short hydrophobic membrane tether at its C-terminus (anchored C or anchC). The mature C protein is liberated from its anchor by NS2B3 during subsequent processing steps. Likewise prM is further processed to the mature

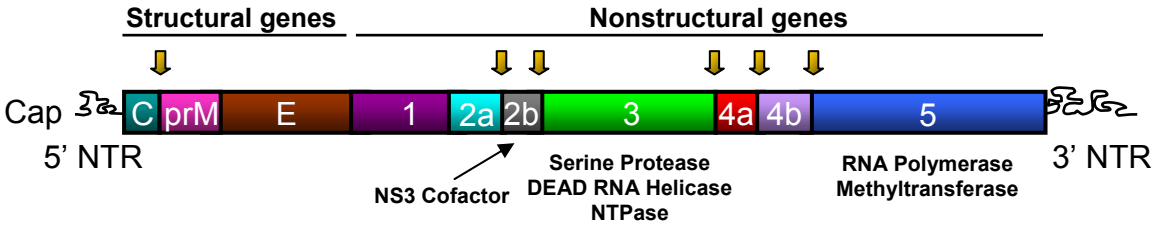

Figure 1-4. WNV Genome Organization.
The WNV ORF is flanked by 5' and 3' NTRs. Proteins made from the 5' structural genes (C, prM and E) form the virion particle. NS proteins are involved in replication and translation of the the viral genome. Gold arrows indicate sites of polyprotein cleavage by the WNV NS2B3 serine protease.

membrane (M) form by an unidentified host protease shortly before virion release from the cell (216). Upstream signal peptides for prM, E and NS1 are targeted for cleavage by a host signal protease, while downstream cleavages of most of the NS proteins are mediated by the viral NS2B3 protease. Functions of most of the nonstructural genes have still not been described. NS1 is a glycosylated protein that appears to be secreted from infected cells (35). NS3 encodes serine protease activity in its N-terminus and DEAD family RNA helicase and nucleoside triphosphatase (NTPase) activities in the C-terminal part of the protein (35). However, full functionality of NS3 protease activity requires the small, hydrophobic NS2B protein as a cofactor (162). NS5 serves as the viral RNA-dependent RNA polymerase in addition to containing methyltransferase activity in its N-terminus (35). NS2A, NS4A and NS4B are small, hydrophobic proteins containing numerous transmembrane domains that appear to be involved in viral RNA synthesis, possibly by rearranging cytoplasmic membranes and assisting in the formation of replication complexes (273).

Intracellular life cycle

WNV enters cells by binding to an as yet undefined cellular receptor resulting in clathrin-dependent endocytosis of the viral particle (52). Once inside the cell WNV appears to traffic to the early endosome in a Rab5-dependent manner where it subsequently undergoes uncoating and release of the viral nucleic acid into the cytoplasm (142). Viral replication occurs on virus-induced membranes (273), which may act to hide the replication complex machinery from cellular pattern recognition receptors (PRR; see below). As mentioned above, the viral RNA is transcribed as a single polyprotein that is subsequently

processed by viral and cellular proteases to yield individual viral proteins. Virion assembly then occurs on the rough endoplasmic reticulum with virion maturation occurring as the particle is trafficked through the Golgi network (172) before budding from the cell in an actin-dependent manner (51).

Ecology and host-range

In nature, WNV is maintained in an enzoonotic cycle between birds and ornithophilic mosquitos and is thus an arbovirus (Figure 1-5). Transmission to humans occurs by the bite

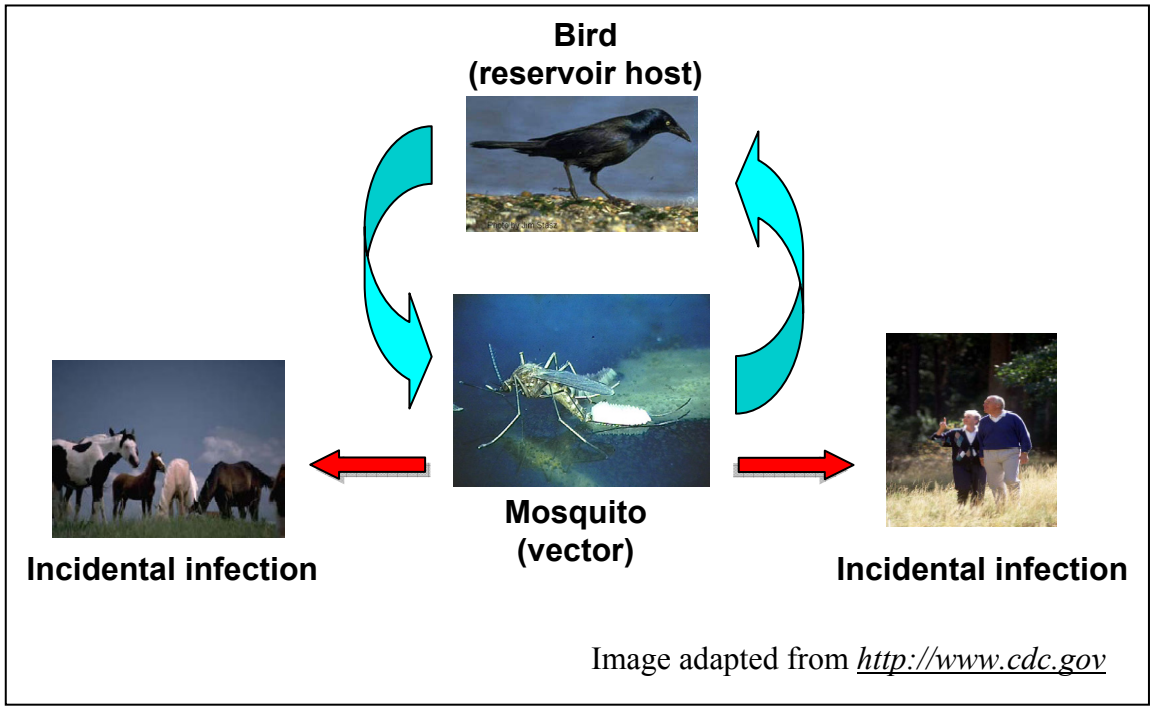

Figure 1-5. Transmission cycle of WNV.
WNV is maintained in nature through an amplification loop between avian hosts and mosquitos. Switches in mosquito feeding behavior during bird migration seasons results in an increase in dead-end infections of humans, horses and other mammals.

of an infected mosquito. Humans and other animals are generally not, with a few exceptions, able to further transmit the virus back to mosquitos because the virus is incapable of replicating in these species to the high levels required for transmission. As a virus, WNV is rather promiscuous in its host range. To date, natural exposure to the virus has been detected either directly (by viral isolation/sequencing) or serologically (by neutralizing antibody) in approximately 450 avian species, 134 insect species, 70 mammalian species and 3 reptilian species (see Appendices A through D). Experimental infection of other animal species has also been performed. It should be noted, however, that the virus is transmitted efficiently by only a very small number of species. For instance, *Culex* mosquitos seem to be particularly efficient vectors, probably due to their promiscuous feeding behavior on birds and humans (133), their capacity to maintain viral loads while they overwinter (195), and their ability to transmit virus vertically from female to offspring (15,184). Passeriform birds appear to be the most competent reservoirs for the maintenance of the virus in nature (136). While the virus is passed from infected mosquitos to birds primarily during bloodmeals, birds can also acquire WNV by eating infected mosquitos or by coming into close contact with virus shed from other birds (136). Transmission to humans occurs through the bite of a mosquito. However, for the mosquito to become initially infected, it must feed on a viremic bird. Since not all mosquitos feed on birds and mammals, one might think this would serve to limit transmission to humans. However, the *Culex* mosquitos found in the U.S. not only feed on both birds and humans but other species of mammals as well. Studies of mosquito feeding behavior have yielded insights into the now-annual outbreaks of human WNV cases in the U.S. Human cases peak in late summer, early autumn (38), the time at which certain bird

species begin migrating southward. With the loss of their preferred meal source, mosquitos switch their feeding pattern from bird to mammal thus resulting in a spike in WNV transmissions to humans (133).

Clinical spectrum

When humans are bitten by an infected mosquito the virus is inoculated intradermally. From the skin, the virus traffics via Langerhans cells to draining lymph nodes where the initial round of viral replication occurs (61). Virus then disseminates hematogenously (viremia) albeit at a low level. Although infected mosquitos are the primary mode of WNV transmission, infection with WNV has also occurred through contaminated blood products (206), transplacental fetal infection (6,42), organ transplantation (114), infected breast milk (44) and laboratory exposure (43). Renal dialysis has also been reported as a potential route of exposure (45).

WN fever

According to a serological survey of households in New York, approximately 80% of WNV infections were asymptomatic, 20% involved WN fever and <1% resulted in CNS disease (189). Of cases reported to the Centers for Disease Control (CDC), 41% included CNS involvement (48) suggesting that generally, only the most severe cases of WNV infection seek medical attention and are subsequently reported. Patients infected with WNV typically present with fever, headache and fatigue; although malaise, myalgia,

lymphadenopathy, nonpruritic rash, weakness and nausea are also fairly common symptoms (46,57,100). Viremia is usually absent by the time of symptom onset, and symptoms generally begin to resolve in about a week, although it can take weeks or months for complete resolution in some cases. Rarely, WNV infection involves other visceral organs resulting in uveitis, hepatitis, myocarditis, pancreatitis, orchitis and in one case hemorrhagic fever (140,143,202).

WN neuroinvasive disease

Patients in whom the virus crosses the blood-brain barrier can present with any or all of the symptoms of WN fever. Additionally, symptoms of CNS involvement such as altered mental status, stiff neck, photophobia, seizures, myelitis, polyradiculitis, optic neuritis, chorioretinitis, flaccid paralysis, ataxia or extrapyrimadal signs are present in various combinations (46,57,100). WNV infection of the CNS results in meningitis, encephalitis, or poliomyelitis/acute flaccid paralysis (AFP), although mixed disease presentations are not uncommon (57). Generally, patients with meningitis have a very good prognosis with complete recovery in most cases (100). Cases of encephalitis and AFP are much more severe and result in less favorable outcomes including intubation/mechanical ventilation, coma and death (38). Encephalitic/AFP patients who survive face a long road to recovery with some neurologic deficits persisting indefinitely. Risk factors for CNS involvement during WNV infection include age > 50 years, alcohol abuse, diabetes and immunosuppression (57). Interestingly, AFP seems to be more predominant in younger patients compared to patients who develop encephalitis (57).

Treatment

Currently, there is no approved therapy for WNV infection. Interferon (IFN) α, corticosteroids and WNV-specific antibodies have been used in some cases with variable efficacy (100). It does appear, though, that IFN treatment initiated early after the onset of symptoms provides a much greater benefit than therapy begun late in the course of disease (49,124). Treatment for HCV, a distantly related flavivirus, involves the combination of IFNα with ribavirin. Ribavirin has been shown to be effective at reducing WNV levels in neural cells in vitro (120) possibly through error catastrophe (58). In a hamster model of infection, ribavirin did not have any effect on WNV and actually resulted in increased mortality in WNV-infected hamsters (186). During the 2000 WNV epidemic in Israel, ribavirin therapy was used on a subset of patients with no detectable benefit (134), although the ribavirin was not used in conjunction with IFN therapy. To date, there have been no studies of combination IFN/ribavirin therapy in humans infected with WNV, but recently a report described the onset of WNV infection in two HCV-infected males who had just begun combination therapy (108). Both patients cleared the WNV infection, but no conclusions could be drawn regarding the impact of the combination therapy other than it did not prevent infection with WNV. It is possible, however, that the combination IFN/ribavirin had not reached therapeutic levels by the time the patients were infected with WNV. It is clear from the data presented here that further study is required to understand the interactions of WNV with the IFN system in order to develop better antiviral therapies.

Animal models of infection

WNV is a promiscuous virus when it comes to infecting various species of animals as demonstrated by Appendices A through D. The variety of animal models for studying WNV pathogenesis in vivo is therefore not surprising. The initial studies of Smithburn and colleagues included infections of mice, rhesus macaques, rabbits, guinea pigs and hedgehogs (245). Mice have remained the most common animal model for WNV primarily because of the ease of genetic manipulation, efficient infection by numerous routes (subcutaneous, intraperitoneal, intracerebral, intranasal, intravenous), rapid expansion of mouse colonies, and economic reasons. Monkeys, especially rhesus macaques have been utilized in the study of WNV persistence following resolution of disease symptoms (209) and in evaluating the levels and duration of antibody responses (213). More recently, studies have looked at WNV infection of hamsters (as a model of encephalitis) (277), crows and other birds (since recent outbreaks involved massive avian deaths) (32) and mosquitos (68,252) (to determine which species are efficient vectors and to analyze the amount of WNV inoculated during a single bloodmeal). Animal models have also been used to evaluate the therapeutic potential of various antiviral treatments, some of which will be discussed later.

Overview of the host innate antiviral response

The interplay between a virus and its infected host is, at its essence, a war with battles waged on many fronts. The front lines in this engagement, however, lie within the infected cell itself (Figure 1-6). Coevolution with viruses over thousands of years has forced

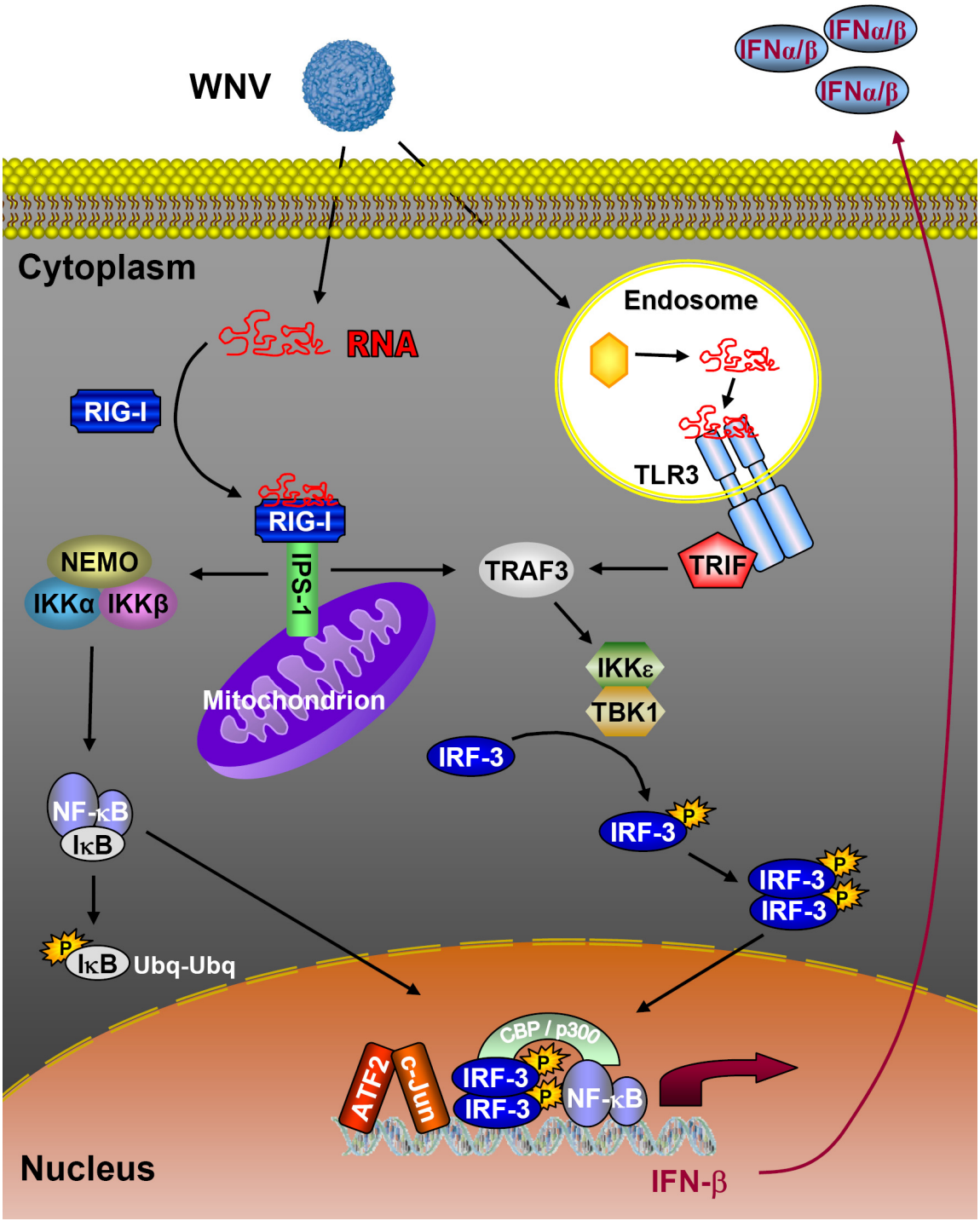

Figure 1-6. The Innate Intracellular Response to Virus Infection.
Intermediates of viral replication (dsRNA) are recognized by cytoplasmic (RIG-I, MDA5) or endosomal (TLR3) pathogen recognition receptors. Downstream signaling activates IRF-3 and NF-κB leading to the production of IFNα/β. The WNV particle image was adapted from (191).

susceptible hosts to develop antiviral countermeasures to block, or at least attenuate, infection. Meanwhile, viruses have evolved traits that allow them to counteract or evade these defenses. What follows is a brief overview of our current understanding of the intracellular antiviral response and the unique ways in which some viruses deal with this issue.

The initial step a cell must take in mounting an antiviral defense is to detect the invading virus. All pathogens, be it viruses, bacteria, or fungi, possess conserved pathogen associated molecular patterns (PAMPs), elements unique to the particular microbe that are absolutely required for the microbe's life cycle. PAMPs are detected by pathogen recognition receptors (PRRs) including toll-like receptors (TLRs), retinoic acid inducible gene I (RIG-I) and melanoma differentiation-associated gene 5 (MDA5). Since WNV is a positive-sense RNA virus, this section will only cover aspects related to the host response to RNA viruses.

RIG-I—IPS-1—IRF-3 axis

When a virus enters a cell and begins to replicate, it produces double-stranded RNA (dsRNA) intermediates. dsRNA in the cytosol is detected by RIG-I or MDA5, which bind dsRNA via C-terminal DExD/H box RNA helicase domains. Binding of dsRNA to RIG-I or MDA5 induces a conformational change in the protein allowing it to dimerize and translocate to the outer mitochondrial membrane where it interacts with interferon beta promoter stimulator 1 (IPS-1) through its N-terminal caspase activation and recruitment domain

(CARD). IPS-1 then recruits a large complex of signaling and scaffolding proteins leading to the activation of TANK-binding kinase 1 (TBK1) and inhibitor of kappa B kinase epsilon (IKKε). TBK1 phosphorylates the latent cytoplasmic transcription factor interferon regulatory factor 3 (IRF-3) on multiple serine residues resulting in its dimerization, translocation to the nucleus and transcriptional activation of IFNβ through binding to PRDIII elements in the IFNβ enhanceosome. IRF-3 is also capable of binding to interferon stimulated response elements (ISRE) to initiate transcription of other antiviral genes. IFNβ secretion and signaling results in an auto-activation loop leading to amplified IFNα/β expression as well as the production of hundreds of interferon stimulated genes (ISG), the antiviral effectors of the cell (see below).

NF-κB

In addition to IRF-3, stimulation of IPS-1 also leads to the downstream activation of the canonical nuclear factor kappa B (NF-κB) pathway. NF-κB is normally held quiescent through an interaction with inhibitor of kappa B alpha (IκBα). Phosphorylation of IκBα by an IKK complex consisting of IKKα, IKKβ and NEMO results in the ubiquitination of IκBα and its subsequent degradation. Once released from IκBα, NF-κB is free to translocate to the nucleus and bind to consensus NF-κB promoter binding sites stimulating transcription of a variety of genes. Along with IRF-3, c-Jun and ATF-2, NF-κB also participates in the initial induction of IFNβ expression during viral infection.

TLR signaling

In addition to the cytoplasmic sensors RIG-I and MDA5, cells also possess cell surface or endosomal PRRs, the TLRs. TLRs implicated in host responses to viruses include TLR3, TLR7, TLR8 and TLR9 (153,183). TLRs bind their ligand via leucine-rich regions (LRR) in the extracellular part of the protein (20). Signaling occurs through cytoplasmic Toll-interleukin-1 receptor (TIR) domain interactions with various adaptor molecules (153). TLR3/7/8/9 are generally expressed on endosomes where they sense their respective ligand (129). Cellular expression of TLRs varies by cell type: TLR3 is expressed in conventional dendritic cells (cDC), natural killer (NK) cells, macrophages (Mϕ), neural cells, astrocytes and endothelial/epithelial cells; TLR7 is expressed in plasmacytoid dendritic cells (pDC), B cells, monocytes, neutrophils and eosinophils; TLR8 is expressed in monocytes, cDCs, T cells, B cells, NK cells, mast cells and neutrophils; and TLR9 is expressed in pDCs, NK cells, B cells, epithelial cells, eosinophils and neutrophils (153,241). The specificity of the TLR response is determined by the particular ligand bound by each family member and the downstream adaptor activated in response to binding. dsRNA is detected by TLR3, which signals via the adaptor protein TIR-domain-containing adaptor inducing IFNβ (TRIF) to activate the IRF-3 and NF-κB pathways, leading to the induction of IFNβ expression (153). TLR7 and TLR8 detect viral ssRNA, and TLR9 detects viral CpG DNA, yet all three of these TLRs signal through MyD88 and IL-1 receptor-associated kinase 4 (IRAK4) to activate IRF-5 and IRF-7 (IRF-3-related transcription factors). The end result of all three TLR pathways is the induction of IFNs and other proinflammatory cytokines (153,183).

Overview of the IFN system

IFN was discovered 50 years ago by Isaacs and Lindenmann as a component in the supernatant of infected cells that "interfered" with subsequent virus infection (112). Since then much work has been done to characterize this mediator of viral interference. Mammalian IFNs encompass three families: type I IFN which includes IFNs α (13 subtypes), β, ω, κ, ε, τ, ζ, δ, and ν; type II IFN, of which IFNγ is the sole member; and the recently discovered type III IFN or IFNλ (3 subtypes) (9,263). Many of the type I IFN subtypes exhibit restricted expression across species, with only α and β IFNs found in all mammalian species. All type I IFNs initiate signaling by binding to the IFNα/β receptor (IFNAR) which is composed of the IFNAR1 and IFNAR2 subunits (Figure 1-7). IFNγ signals through binding to the IFNγ receptor (IFNGR) and its 2 chains, IFNGR1 and IFNGR2, while IFNλ signals through the IL-28Rα and IL-10Rβ chains which comprise the IFNλ receptor (IFNLR). Receptors for all IFNs appear to be expressed on numerous cell types, yet only type I IFNs are produced by all nucleated cells in response to viral infection. Data on the expression of IFNλ is just being gathered, but initial results suggest significant overlap in the expression of IFNα/β and IFNλ. However, production of IFNγ is restricted mainly to NK cells, T cells, macrophages and other myeloid cells (219).

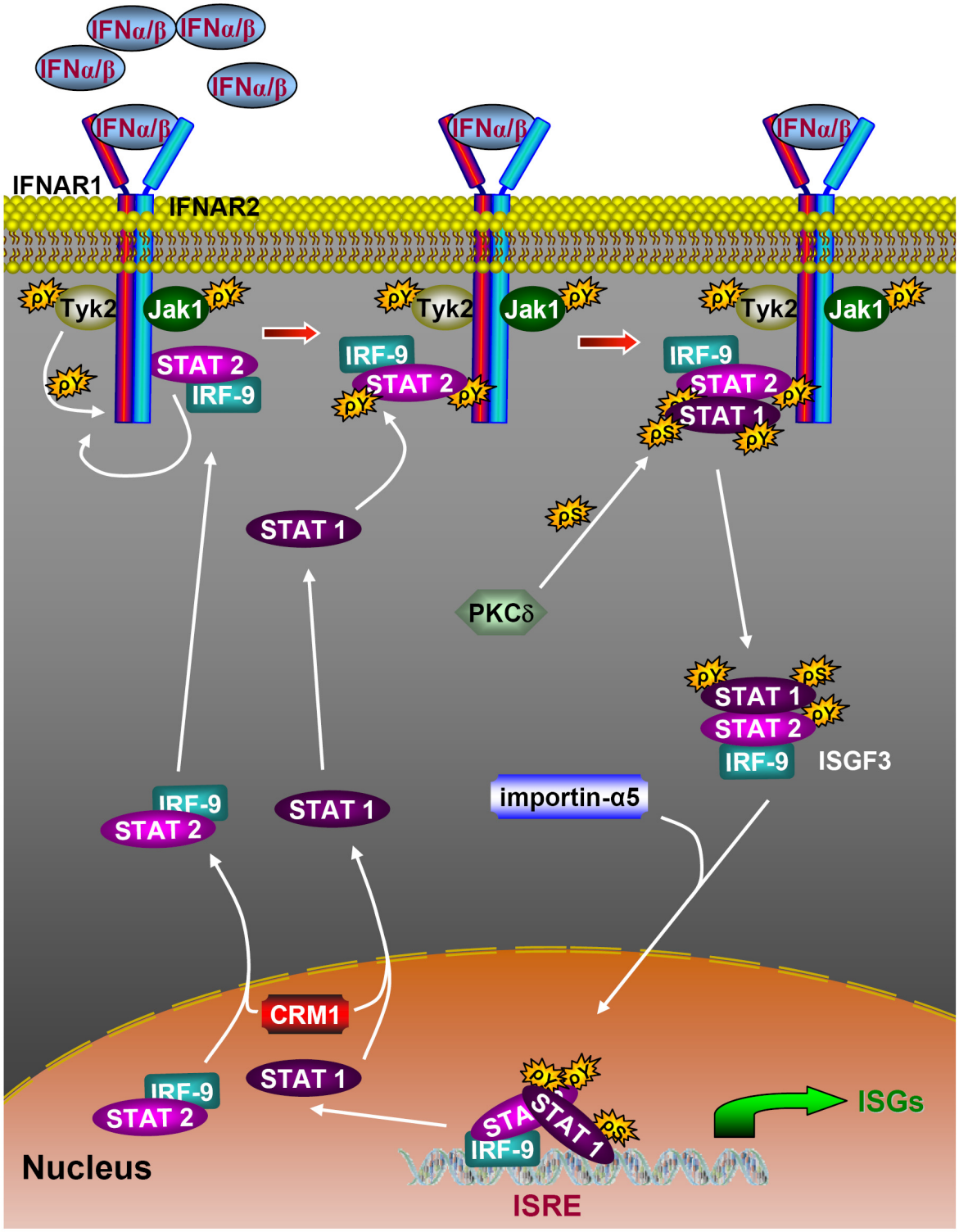

Figure 1-7. Classical IFNα/β signaling pathway.

Activation of intracellular innate antiviral defenses, whether it be through the cytoplasmic sensors RIG-I and MDA5 or through endosomal TLR sensors, all converge at the production of IFNα/β. Secreted IFNα/β binding to IFNAR brings together the two receptor chains and initiates a cascade of phosphorylation steps beginning with the autophosphorylation of the receptor-associated Janus kinases (JAKs) JAK1 and TYK2 which interact with IFNAR2 and IFNAR1, respectively (207). The JAKs then phosphorylate multiple residues on IFNAR leading to the recruitment and activation of signal transducer and activator of transcription (STAT) proteins including STAT1, STAT2, STAT3 and STAT5 (207).

STAT2 and IRF-9 are thought to constitutively bind the IFNAR2 chain (90), although there is evidence for shuttling of this complex in and out of the nucleus in the absence of receptor activation (14). Phosphorylation of IFNAR1 at Tyr466 recruits STAT2/IRF-9 from its preactivation location on IFNAR2 (34,90). Upon binding IFNAR1, STAT2 is phosphorylated at Tyr690 by TYK2 (34,90) forming a docking site for STAT1 (34). STAT1 is subsequently phosphorylated at Tyr701 leading to its activation. Full transcriptional activity requires a further phosphorylation on Ser727 of STAT1 by protein kinase C delta (PKCδ) (207). The fully active STAT1/STAT2/IRF-9 complex (termed ISGF3 for interferon stimulated gene factor 3) then translocates to the nucleus where it binds to ISREs in the promoters of ISGs.

In addition to the formation of STAT1:STAT2 heterodimers, IFNα/β also induces the formation of STAT1:STAT1, STAT3:STAT3, STAT4:STAT4, STAT5:STAT5 and STAT6:STAT6 homodimers as well as heterodimers of STAT1:STAT3, STAT1:STAT4, STAT1:STAT5, STAT2:STAT3 and STAT5:STAT6 (207). The exact complex(es) formed depends on the cell type and specific IFN stimulus. These alternate STAT complexes bind to IFNγ-activated site (GAS) elements in the promoters of some ISGs allowing for a very complex, yet tailored response to IFN stimulation in each cell.

Since STAT1 and STAT2 do not contain classical nuclear localization sequences (NLS), their constitutive nuclear import is precluded (14,34). STAT1 binding to STAT2 induces a conformational shift in the proteins that confers NLS activity and their subsequent import into the nucleus via importin-α5 (177). After binding to DNA, STATs are dephosphorylated by yet-to-be-identified phosphatases, reducing the affinity of the STATs for DNA binding. Release from DNA results in dissociation of the STAT complex and exposes STAT nuclear export sequences which are bound by CRM1, a nuclear exportin (14,34,177). The shuttling of inactive STATs out of the nucleus allows for their recycling.

Viral antagonism of IFN signaling

IFN signaling through JAK-STAT is critical for the induction of the antiviral state within the infected cell and as such is a prime target for viruses to dampen the immune response. Viruses have evolved numerous ways of antagonizing JAK-STAT signaling at

nearly every point in the pathway. The poxviruses Vaccinia virus and Myxomavirus encode IFNAR and IFNGR homologues, respectively that compete for binding to IFN (80,90,221,232). The T antigen from murine polyomavirus binds JAK1 to suppress downstream signaling, while Sendai virus and human parainfluenza virus 3 (hPIV3) prevent STAT phosphorylation (90). Some viruses (adenovirus, human cytomegalovirus, SV5, mumps, hPIV2) simply target JAK-STAT signaling components for degradation via the proteasome (39,80,90), while others (varicella zoster virus) prevent expression of JAK-STAT components (221). Others, like Hepatitis B virus, prevent formation of active ISGF3 complexes (39). Human herpesvirus-8 encodes homologues of IRFs that bind to and sequester critical cellular proteins (221). Further downstream, STAT nuclear accumulation and DNA binding are inhibited by the V protein of rabies virus (266). Finally, some viruses, including herpes simplex virus, act directly on the downstream products of IFN signaling, the ISGs (127,232).

It is clear from the examples cited above that viruses of all types place an emphasis on modulating signaling through JAK-STAT. The flaviviruses, too, have been shown to attenuate IFN signaling, and this will be discussed in detail later. Although the mechanisms may differ greatly, the end result is the same – the down-regulation of critical innate immune defenses. Viral interference with IFN signaling has consequences not only for the natural course of infection, but also for the efficacy of IFN-based antiviral therapies. It is therefore, of the utmost importance that viral interactions with the JAK-STAT pathway be dissected carefully to aid in the development of better therapeutics for treating viral infections.

WNV delays activation of IRF-3

Although RIG-I and MDA5 are closely related members of the DExD/H box family of RNA helicases with high homology to each other, it is clear from recent work that they exhibit different functionalities in infected cells. RIG-I has been shown to be critical for the antiviral response to flaviviruses (JEV), paramyxoviruses and orthomyxoviruses, while MDA5 is essential for the detection of picornaviruses and polyinosine-polycytidylic acid (poly(I:C)) (125). Unlike HCV which antagonizes RIG-I signaling by cleaving IPS-1 (116), WNV appears to simply delay activation of the pathway long enough to gain a replicative advantage (76). This was demonstrated by Brenda Fredericksen, a former post-doctoral researcher in our lab, in two elegant papers. The first paper showed a delay in IRF-3 phosphorylation and downstream IFNβ expression with the initial appearance of both at 24 hours post-infection (hpi) (76). Furthermore, ISG mRNA and protein expression were also delayed until 24 hpi, which interestingly, coincided with the onset of WNV protein expression. In the second paper, Fredericksen and Gale demonstrated that the delay in IRF-3 activation was not due to active inhibition of IRF-3 signaling by WNV (75). Coinfection of cells with WNV and vesicular stomatitis virus (VSV) confirmed that WNV is not capable of preventing VSV-induced IRF-3 phosphorylation. Additionally, WNV was unable to block poly(I:C) signaling through TLR3 to IFNβ, demonstrating that the delayed IRF-3 response was not due to viral inhibition of RIG-I-dependent or -independent signaling pathways in WNV-infected cells.

Why study WNV-host interactions?

The emergence and subsequent spread of WNV in North America highlighted a need to better understand the basic interactions of a new pathogen with its infected host. Since the introduction of WNV in the U.S. in 1999, research on WNV has exploded. A significant portion of this work included epidemiological surveys, description of WNV-induced pathology, analysis of potential vectors/susceptible species, and molecular characterization of basic functions in the viral life cycle. All of these types of studies are needed in their own way, but it is unfortunate that research into the interface between health and disease, that of WNV's interaction with the infected cell, has lagged behind the previously mentioned studies. It was, therefore, with great anticipation and excitement that I undertook the following studies as part of my dissertation examining WNV regulation of cytokines signaling. In the beginning the field was wide open. Several studies had looked at the role of WNV proteins in apoptosis and the induction of major histocompatibility complex proteins in response to WNV, yet the interaction of WNV with other pathways, including RIG-I, TLR, NF-κB and IFN had hardly been touched. Importantly, previous studies laid the groundwork for testable hypotheses to be made, and the hardest part, initially, was in deciding what aspect of the WNV-host interaction to examine. Still today, there are many unanswered and even more unasked questions still to be addressed. It is my hope and belief that the studies presented here contribute to our understanding of how certain WNV strains are capable of causing severe, life-threatening disease while others cause no detectable disease at all. What follows is an examination of WNV's interactions with cytokine signaling networks,

beginning with the IFN pathway and expanding to include other cytokines that utilize JAK-STAT in their signal transduction.

CHAPTER TWO
Materials & Methods[§]

Cell culture

A549, Huh7 (R. Bartenschlager), HEK-293, Vero, wild-type (WT) 129 Sv/Ev mouse embryo fibroblast (MEF) (H. Virgin), WT C57BL/6 MEF (T. Fujita), IFNAR-/- MEF (H. Virgin), IPS1-/- MEF (S. Akira), U3A (G. Stark) and U5A (G. Stark) cells were maintained in Dulbecco's modified eagle medium (DMEM) supplemented with 10% fetal bovine serum (FBS) (Hyclone), 2 mM L-glutamine (Cellgro), antibiotic/antimycotic solution (Cellgro), 1mM sodium pyruvate (Cellgro), 1X non-essential amino acids (Cellgro) and 25mM HEPES (Cellgro) (complete DMEM). All cells were grown at 37°C under 5% CO_2 in H_2O-jacketed incubators. Many of these cells lines were generously provided by other labs, and the source of the cells is listed following the cell line.

IFNs, cytokines and inhibitors

IFNα-2a was obtained from PBL Biomedical Laboratories. Consensus IFN (CIFN; IFN alphacon-1) and IFNγ (Actimmune) were provided by Intermune. Pegylated IFNα-2b (PEG-Intron) was purchased from Schering. IFNβ (Betaseron) was obtained from Berlex. Recombinant human IL-6, Actinomycin D and cycloheximide were purchased from Sigma.

[§] Portions of Chapter 2 are copyrighted to ASM Journals [J Virol. (2006) Oct;80(19)9424-34] and used with permission.

Chemical inhibitors used in these studies include PD98059 (Sigma), SB203580 (Biosource), U0126 (Cell Signaling), LY294002 (Cell Signaling).

Viruses

WNV TX 2002-HC (TX02) was isolated on Vero cells inoculated with brain homogenate from an infected grackle (Quiscalus quiscula) recovered in Hall County, TX in 2002. Virus was amplified once in HEK-293 cells, and supernatants were collected and stored frozen for further analyses of viral stocks. WNV strain Madagascar-AnMg798 (MAD78) was obtained from the World Reference Center of Emerging Viruses and Arboviruses (18) and passaged once in Vero cells. Working stocks of TX02 and MAD78 were obtained by plaque purifying virus and amplifying one time in HEK-293 cells at a low multiplicity of infection (MOI). Supernatants were cleared of cell debris by low speed centrifugation, aliquoted and stored at -80ºC. Preparation of WNV strain NY 2000-crow3356 (NY 3356) (GenBank accession #AF404756) working stocks from plasmid pFLWNV was done as previously described (76,76). For all virus infections, cells were washed twice in serum-free DMEM (SF-DMEM) and infected with the respective virus in SF-DMEM for 1 hour at 37ºC with rocking. Following the 1 hour virus adsorption, the SF-DMEM containing virus was replaced with complete DMEM at 37ºC until collection of samples.

Sequencing and phylogenetic analysis

Monolayers of Vero cells were infected (MOI = 0.5) with TX02 or MAD78 for 1 hour at 37°C with rocking. At 24 (TX02) or 48 (MAD78) hpi, total RNA was collected using Trizol LS (Invitrogen) according to the manufacturer's instructions. cDNA synthesis was performed on 2 μg RNA using random nonamers (IDT) and Omniscript reverse transcriptase (Qiagen) for 90 minutes at 37°C. Overlapping PCR products were obtained initially using primers designed from the sequence of NY 3356 (for TX02) or a lineage II consensus sequence created from the alignment of the Uganda 1937, B956 and Sarafend sequences (for MAD78). Secondary internal sequence-specific primers were used to amplify PCR fragments spanning the initial primer regions to eliminate any bias from the NY 3356- or lineage II consensus-specific primers. Primers used for PCR and sequencing or TX02 and MAD78 are listed in Tables 2-1 and 2-2, respectively. Sequencing was performed on PCR products using Applied Biosystems Inc. (ABI) Big Dye Terminator 3.1 chemistry and ABI capillary instruments at the DNA Sequencing Core Facility in the UT Southwestern McDermott Center for Human Growth and Development. This protocol was repeated for both viruses to confirm sequence data. Alignment of the amino acid sequences encoding the entire WNV open reading frame was done using ClustalW (258). Distances were estimated with the amino acid transition probability matrix of Jones, Taylor and Thornton (117). Neighbor-joining phylogenetic trees were constructed using MOLPHY, version 2.3 with maximum likelihood rearrangement (1). Bootstrap values in support of branches are the result of 1000 neighbor-joining replicates. All published complete WNV genomes were gathered from GenBank (through 06/08/2005) and used in the phylogenetic analysis.

Japanese encephalitis virus isolate HW (GenBank accession #AY849939) was used as the outgroup.

Plaque assays and virus growth analysis

Monolayers of Vero, A549, Huh7 or 2fTGH cells were washed twice in SF-DMEM. Cells were infected with 10-fold serial dilutions of virus for 1 hour at 37°C with rocking. Inoculum was removed and replaced with a 0.9% agarose-complete DMEM overlay. Forty-eight hours later, a second 0.9% agarose overlay containing 2% Neutral Red (ICN Biomedicals) was added to the cells. Plaques were counted at 48 (TX02) or 96 (MAD78) hours after the second overlay. All plaque assays were performed in duplicate. For analysis of virus growth kinetics, A549 or Huh7 cells were infected with NY 3356, TX02 or MAD78 at an MOI of 1 based on titers determined on the respective cell line. At indicated times, culture supernatants were recovered from infected cultures and the level of infectious virus was determined by plaque assay on Vero cells. In parallel, cells were harvested and whole-cell lysates were prepared for immunoblot analysis. All growth curves were performed multiple times and viral titration analyses were conducted in duplicate for each sample.

Plasmid construction and Site-directed mutagenesis

Plasmids pCAGGS-HA, pCAGGS-DEN(NS4b), pCAGGS-WNV(NS4b) and pCAGGS-NipV were kindly provided by Adolfo Garcia-Sastre (194). Each gene from TX02

Table 2-1: Primers used for sequencing of TX02 viral genome

Name	Sequence
WNV 12s	5'-TGTGTGAGCTGACAAACTTAG
WNV (5'UTR)	5'-TGACAAACTTAGTAGTGTTTGTGAGGATTAAC
WNV (Core) 97s	5'-AGTGATATCGATGTCTAAGAAACCAGGAGGGCCC
WNV 173a	5'-GCCCTCTTCAGTCCAATCAAGG
WNV (Core)	5'-ATCATCACCTTCCCTTGGAAGTTA
WNV (M) 771s	5'-CACCAAGGCCACAAGGTATTTG
WNV (E) 1700a	5'-ATTCCACAGGAATGGCTCCA
WNV (E) 2201s	5'-TCAAAGGAGCGCAGAGACTAGCCG
WNV (E) 2469a	5'-GATTCTAGATTAAGCGTGCACGTTCACGGAGAGG
WNV (NS1)	5'-CTGGATATCGGACACTGGGTGTGCCATAGACAT
WNV (NS1)	5'-GGACATTCCTTGGTCTCCGGACCA
WNV (NS1)	5'-AGTCACACTGGCGGGACCACGAAGCAA
WNV (NS1)	5'-GGCTCTAGACTAAGCATTCACTTGTGACTGCACG
WNV (NS2a) 5'	5'-GATCGATATCGTATAATGCTGATATGATTGACCC
WNV (NS2a) 3'	5'-TCAGTCTAGACTAGCGTTTACGGTTGGGATCAC
WNV (NS2b)	5'-AAAGATATCGGGATGGCCCGCAACTGAAGTGA
WNV (NS2b)	5'-GAAATGTCCGCCGTTCTCTCAATC
WNV (NS2b)	5'-GGGTCTAGATCATCTCTTTGTGTATTGGAGAGTT
WNV (NS3)	5'-AAAGATATCGGGAGGCGTGTTGTGGGAC
WNV (NS3)	5'-GGAAATTGCAGCACAAGTGG
WNV (NS3)	5'-GCCCCCATTTCAGATATGTC
WNV (NS3)	5'-GAGAAAAAACTTTCTGGAACTGTTG
WNV (NS3)	5'-CAGTCTAGATCAACGTTTTCCCGAGGCGAAGT
WNV (NS4a)	5'-GCGGATATCGTCTCAGATAGGGCTCATTGAGGTTC
WNV (NS4a)	5'-TTTTCTAGATTAGGCTGCCACTGCGCTCACAAGG
WNV (NS4b)	5'-TTTGATATCGAACGAGATGGGTTGGCTAG
WNV (NS4b)	5'-GACGTGATCAAATGCTTTAGCAGT
WNV (NS4b)	5'-AGAGCGCACCACACCCATCATGCA
WNV (NS4b)	5'-GCCTCTAGATCATCTTTTTAGTCCTGGTTTTTCC
WNV (NS5)	5'-AAAGATATCGGGTGGGGCAAAAGGACGCA
WNV (NS5)	5'-CCGGTTCGAGAAACCTCCGTTCGA
WNV 8706s	5'-CATGGCCATGACTGACACTACTC
WNV 9072a	5'-CTTGGCCTTTCCGAACTCTCCG
WNV (NS5)	5'-GTGGATGACAACAGAGGACATGTTG
WNV (NS5)	5'-CCCTCTAGACTACAGTACTGTGTCCTCAACCAA
WNV 10529s	5'-CCGGAAGTTGAGTAGACGGTGCTGCC
WNV 10694a	5'-TGGGGCACTATCGCAGACTGCACTCTCCGC
WNV (3'UTR)	5'-CTTTCGCCCTGGTTAACGCCATTA

Table 2-2: Primers used for sequencing of MAD78 viral genome

Name	Sequence
WNV (1) s	5'-AGTAGTTCGCCTGTGTGAGC
WNV 12s	5'-TGTGTGAGCTGACAAACTTAG
WNV-MAD (579s)	5'-CATGGACGTGGGATACCTCTG
WNV-MAD (1871as)	5'-GAGCACACTCCATATGTCGTTCC
WNV(lin2) 2541as	5'-ATCGTTGTGGATAAACACTCC
WNV-MAD (2305s)	5'-AGATCACTCTTTGGAGGGATGTCCT
WNV-MAD (3071s)	5'-GGATAGAAAGTGGGTTTAATGAGACCTGGAAG
WNV-MAD (4242as)	5'-CATGACTTCTGTAGCAGGCCATCCC
WNV (lin2) 4761s	5'-GGGAGCTGCTCTCATGAGTGGTGAG
WNV-MAD (5003as)	5'-GGATAATCCAGTGTCACGGCTCC
WNV-MAD (5457s)	5'-CATAATGGATGAAGCCCACTTCAC
WNV-MAD (4b) sigseq fwd	5'-GCGAATTCACCATGCAGCGCTCACAGACTGATAAC
WNV-MAD (6835as)	5'-CAGGTTCTGGAATCAGAACAATC
WNV (lin2) 7221s	5'-GGTGACTCTGACTGTGACTGTGACT
WNV (lin2) 7500as	5'-GGCCTCTCTGACGGTTCTCACTGAT
WNV-MAD (7709s)	5'-GTGAGGTCTGGAAGGAAAGGCTTAAC
WNV-MAD (9185as)	5'-CCTAACCAGTGGTCCTCGTTGAG
WNV-MAD (9617s)	5'-GACCAAAAGTCAGGACTTGGCTG
WNV (lin2) 9840as	5'-CATGATCAGTTCCGTGAAATGGTTT
WNV 10529s	5'-CCGGAAGTTGAGTAGACGGTGCTGCC
WNV 10694a	5'-TGGGGCACTATCGCAGACTGCACTCTCCGC
WNV (lin2) 10990as	5'-GTTGTGCAGAGCAGAAGATCCCCTA
WNV (11029) as	5'-AGATCCTGTGTTCTCGCACC

or MAD78 was cloned from cDNA generated during sequencing of the viral genomes (see above) into the mammalian expression vector pCAGGS-HA under the control of a β-actin promoter yielding the plasmids pCAGGS WNV-TX02 (gene) or pCAGGS WNV-MAD78 (gene). 5'-end PCR primers included either EcoRI, NsiI, or SacI restriction sites followed by an AUG start codon while 3'-end PCR primers contained KpnI or NsiI restriction sites for insertion into the multiple cloning site of pCAGGs-HA (Table 2-3, pCAGGS-TX02; Table 2-4, pCAGGS-MAD78). For the prM, E, NS1 and NS4b genes, 5'-end PCR primers were targeted to upstream gene regions to include the necessary signal peptide for ER translocation or signal peptidase cleavage of the encoded protein. WNV genes were cloned in-frame with the 3'-Hemagglutinin (HA) tag of pCAGGS-HA to yield C-terminal HA-tagged proteins. Since the amino acid sequence of WNV (NS4B) from pCAGGS-WNV(NS4B) (193) was identical to that of TX02 (NS4B), pCAGGS-WNV(NS4B) was used in these studies. PCR reactions contained 2 μl TX02 or MAD78 cDNA, 36 μl ddH_2O, 5 μl ExTaq Buffer, 4 μl 2.5 mM dNTPs, 1 μl forward primer, 1 μl reverse primer and 1 μl ExTaq DNA polymerase. Reaction conditions were denaturation at 95ºC for 1 min; 40 cycles at 95ºC for 30 s, 55ºC for 30 s and 68ºC for 3 min; and final extension at 68ºC for 5 min. PCR products were doubly digested with the respective enzymes (NEB or Promega) followed by gel extraction of the digestion product (Qiagen) and ligation into pCAGGS-HA with T4 DNA ligase (Promega). Ligations were transformed by heat-shock at 42ºC into *E. coli* (DH5α, Invitrogen) and plated on LB agar plates containing ampicillin (50 μg/ml) (referred to as LB/amp). Colonies were picked, cultured in LB/amp broth at 37ºC with agitation, and plasmid DNA was extracted using the Wizard *Plus* SV Minipreps Kit (Promega). Plasmids

were initially screened by diagnostic digestion with restriction endonucleases found in the primer sequences (5 μl plasmid, 2 μl Buffer (1, 2, 3, or 4; NEB), 1 μl enzyme, ddH2O to 20 μl final volume). Alternatively, colonies were screened by Rapid Disruption of Bacterial Colonies. Briefly, colonies were transferred with a toothpick to an Eppendorf tube containing 25 μl cracking buffer (50 mM NaOH, 0.5% SDS, 5 mM EDTA). Tubes were incubated at 65ºC for 45-60 min. 2.5 μl 10X TAE sample buffer was added, and tubes were vortexed for 30 s. Entire sample was run on a 0.7% TAE agarose gel with uncut plasmid run as a standard followed by staining in ethidium bromide (0.5 μg/ml ddH2O) for 45 min. Correct insertion of the viral gene into pCAGGS-HA was confirmed by sequencing (pCAGGS-COOH-TAG seq(f), 5'-GGCAGGGCGGGGT TCG and pCAGGS-HA seq(r), 5'-GCCAGAAGTCAGATGCTCAAG). Large-scale plasmid DNA extractions were done with the GenElute Endotoxin-free Plasmid Midiprep Kit (Sigma). Due to difficulty in cloning certain viral genes, cloning techniques were modified as follows. PCR conditions for amplifying MAD (NS5) from cDNA were changed to denaturation at 95ºC for 1 min; 40 cycles at 95ºC for 30 s, 55ºC for 30 s and 72ºC for 3 min; and final extension at 68ºC for 5 min. *E. coli* containing pCAGGS WNV-MAD (NS2b3) or pCAGGS WNV-MAD (NS5) was grown at 30ºC instead of 37ºC.

The mammalian expression plasmids pORF5, pORF5-hSOCS1 and pORF5-hSOCS3 were purchased from Invivogen. FLAG epitope tags were placed upstream of hSOCS1 or hSOCS3 with the QuikChange XL Site-Directed Mutagenesis Kit (Stratagene) to yield N-

Table 2-3: Primers used for cloning TX02 genes into pCAGGS-HA

Name	Sequence
WNV-TX EcoRI-(C) s	5'- GG**GAATTC**GCCATGTCTAAGAAACCAGGAGG
WNV-TX (C)-KpnI as	5'- CC**GGTACC**CCTCTTTTCTTTTGTTTTGAGC
WNV-TX (anchC)-KpnI as	5'- AT**GGTACC**CCTGCTCCTACGCTGGCGATCA
WNV-TX EcoRI-(prM) s	5'- GC**GAATTC**CATGAAAAGAGGAGGAAAGACCG
WNV-TX (prM)-KpnI as	5'- AT**GGTACC**CCGCTGTAAGCTGGGGCCAC
WNV-TX EcoRI-(E) s	5'- GC**GAATTC**ATGAGCAACACCATGCAGAGAGTTG
WNV-TX (E)-KpnI as	5'- TT**GGTACC**CCAGCATGCACGTTCACGG
WNV-TX EcoRI-(NS1) s	5'- GG**GAATTC**ATGATAGCTCTCACGTTTCTCGCAG
WNV-TX (NS1)-KpnI as	5'- AC**GGTACC**CCAGCATTCACTTGTGACTGCA
WNV-TX SacI-(NS2a) s	5'- CC**GAGCTC**ATGTATAATGCTGATATGATTGA
WNV-TX (NS2a)-KpnI as	5'- AT**GGTACC**CCGCGTTTACGGTTGG
WNV-TX EcoRI-(NS2b) s	5'- AA**GAATTC**ATGGGATGGCCCGCAACTG
WNV-TX (NS2b)-KpnI as	5'- CC**GGTACC**CCTCTCTTTGTGTATTGGAGAG
WNV-TX EcoRI-(NS3) s	5'- GA**GAATTC**ATGGGAGGCGTGTTGTGGGACAC
WNV-TX (NS3)-NsiI as	5'- ACC**ATGCAT**CCACGTTTTCCCGAGGCG
WNV-TX EcoRI-(NS4a) s	5'- CC**GAATTC**ATGTCTCAGATAGGGCTCATTGA
WNV-TX (NS4a)-KpnI as	5'- AT**GGTACC**CCCTTCTCTGGCTCAGGAATTA
WNV-TX NsiI-(NS5) s	5'- ATA**ATGCAT**ATGGGTGGGGCAAAAGGACGCAC
WNV-TX (NS5)-NsiI as	5'- CCC**ATGCAT**CCCAATACTGTGTCCTCAACCA

[1]Engineered restrictions sites are shown in bold font. [2]Viral nucleic acid is underlined.

Table 2-4: Primers used for cloning MAD78 genes into pCAGGS-HA

Name	Sequence
WNV-MAD EcoRI-(C) s	5'- GC**GAATTC**ACCATGTCTAAGAAACCAGGAGG
WNV-MAD (C)-KpnI as	5'- AC**GGTACC**CCTCTTTTCTTTTGTTTTGCGC
WNV-MAD (anchC)-KpnI as	5'- AT**GGTACC**CCAGCGCCTGCGCAG
WNV-MAD EcoRI-(prM) s	5'- GC**GAATTC**ATGAAAAGAGGAGGTACAGCGG
WNV-MAD (prM)-KpnI as	5'- AT**GGTACC**CCACTGTATGCCGGCGCTACTA
WNV-MAD EcoRI-(E) s	5'- AA**GAATTC**ATGAGCAACACGATGCAGCGAG
WNV-MAD (E)-KpnI as	5'- TA**GGTACC**CCCGCATGGACGTTAACTGAGA
WNV-MAD EcoRI-(NS1) s	5'- CC**GAATTC**ATGATTGCTATGACGTTCCTTGCTG
WNV-MAD (NS1)-KpnI as	5'- AA**GGTACC**CCCGCATTCACTCTCGATTGCA
WNV-MAD SacI-(NS2a) s	5'- CC**GAGCTC**ATGTACAATGCTGACATGATTGATCC
WNV-MAD (NS2a)-KpnI as	5'- TT**GGTACC**CCCCGCTTGCGGTTAGGGT
WNV-MAD SacI-(2b) s	5'- TT**GAGCTC**ATGGGATGGCCTGCTACAG
WNV-MAD (NS2b)-KpnI as	5'- TT**GGTACC**CCACGTTTCGTGTATTGAAG
WNV-MAD SacI-(NS3) s	5'- TT**GAGCTC**ATGGGTGGTGTCTTGTGGGAC
WNV-MAD (NS3)-KpnI as	5'- AA**GGTACC**CCGCGTTTCCCCGATGC
WNV-MAD EcoRI-(NS4a) s	5'- GG**GAATTC**ATGTCACAAATTGGGCTTGT
WNV-MAD (NS4a)-KpnI as	5'- TT**GGTACC**CCCTTTTCAGGTTCTGGAATCA
WNV-MAD EcoRI-(NS4b) s	5'-GC**GAATTC**ACCATGCAGCGCTCACAGACTGATAAC
WNV-MAD (NS4b)-NsiI as	5'-TACC**ATGCAT**CGTCTCTTCAGGCCAGGCTTCTCC
WNV-MAD EcoRI-(NS5) s	5'- TTAAA**GAATTC**ATGGGTGGGGCCAAAGGACGCAC
WNV-MAD (NS5)-KpnI as	5'- CCTCGG**GGTACC**AACAAAACAGTGTCCTCTACAAC

[1]Engineered restrictions sites are shown in bold font. [2]Viral nucleic acid is underlined.

terminal FLAG-tagged proteins (pORF5-FLAG-hSOCS1 and pORF5-FLAG-hSOCS3). Insertion of the FLAG tag was accomplished using primers specific for hSOCS1 (pORF5-FLAG-hSOCS1 fwd, 5'-GGATATCACAGAGGAGACCATGGACTACA AAGACGATGA CGACAAGGTAGCACACAACCAGGTGGCAG; and pORF5-FLAG-hSOCS1 rev, 5'- CT GCCACCTGGTTGTGTGCTACCTTGTCGTCATCGTCTTTGTAGTCCATGGTCTCCTC TGTGATATCC) or hSOCS3 (pORF5-FLAG-hSOCS3 fwd, 5'-GGATATCACAGAGGAG ACCATGGACTACAAAGACGATGACGACAAGGTCACCCACAGCAAGTTTCCCG; and pORF5-FLAG-hSOCS3 rev, 5'- CGGGAAACTTGCTGTGGGTGACCTTGTCGTCAT CGTCTTTGTAGTCCATGGTCTCCTCTGTGATATCC). FLAG epitope tag is denoted by underlined nucleotides. 50 μl PCR mutagenesis reactions were performed according to manufacturer's protocol with denaturation at 95ºC for 1 min; 18 cycles of 95ºC for 50 s, 60ºC for 50 s and 68ºC for 8 min; and final extension at 68ºC for 7 min. Following the PCR reaction, samples were treated with 1 μl DpnI at 37ºC to remove template DNA. XL10-Gold *E. coli* were transformed with 2 μl DpnI-treated samples and plated at 37ºC on LB/amp plates. Plasmids were miniprepped and sequenced to verify insertion of the N-terminal FLAG tag. Dominant negative forms of SOCS1 and SOCS3 have been previously described (95,225,280). Site-directed mutagenesis (described above) was performed on pORF5-FLAG-hSOCS1 or pORF5-FLAG-hSOCS3 to create pORF5-FLAG-hSOCS1 (F59D) [SOCS1 DN], pORF5-FLAG-hSOCS1 (R105K) [SOCS1 DN#2] and pORF5-FLAG-hSOCS3 (F25A) [SOCS3 DN]. The primers used in the creation of the dominant negative SOCS expression plasmids are listed in Table 2-5. Plasmids were sequenced to verify the presence of the desired mutation.

Table 2-5: Primers used for creation of SOCS dominant negative plasmids

Name	Sequence
SOCS1 (F59D) fwd	5'-GCGACACGCACTTCCGCACA**GA**CCGTTCGCACGCCGATTACC
SOCS1 (F59D) rev	5'- GGTAATCGGCGTGCGAACG**GTC**TGTGCGGAAGTGCGTGTCGC
SOCS1 (R105K) fwd	5'-CCGTGGGCACCTTCCTGGTG**AAG**GACAGCCGCCAGCGGAACTG
SOCS1 (R105K) rev	5'-CAGTTCCGCTGGCGGCTGTC**CTT**CACCAGGAAGGTGCCCACGG
SOCS3 (F25A) fwd	5'- CCAGCCTGCGCCTCAAGACC**GC**CAGCTCCAAGAGCGAGTACC
SOCS3 (F25A) rev	5'- GGTACTCGCTCTTGGAGCT**GGC**GGTCTTGAGGCGCAGGCTGG

[1]Bold nucleotides represent the targeted codon. Actual mutated nucleotides are underlined.

RNA analysis

Quantitative real-time RT-PCR analysis

SOCS1, SOCS3 and CISH gene expression were determined by quantitative real-time RT-PCR analysis on an ABI 7500 Real Time PCR System (Applied Biosystems) with 7500 System Sequence Detection Software v1.3.1 (Applied Biosystems). The reaction mixture contained 50 ng input RNA, 12.5 µl SYBR PCR Master Mix (Applied Biosystems), 1 µl 1.25 µM primer mix (see below), 0.5 µl RNase Inhibitor (Applied Biosystems), 0.125 µl Multiscribe reverse transcriptase (Applied Biosystems) and RNase-free ddH_2O to a final reaction volume of 20 µl. Human and murine SOCS1 and SOCS3 and human CISH primers were purchased from SuperArray. Human GAPDH (GAPDH_4 5', 5'-CTGGGCTACACTG AGCACCAG; GAPDH_4 3', 5'-CCAGCGTCAAAGGTGGAG) and murine GAPDH (mGAPDH 5', 5'-CAACTACATGGTCTACATGTTC; mGAPDH 3', 5'-CTCGCTCCTGGA AGATG) were purchased from IDT (Integrated DNA Technologies). Reaction conditions were as follows: 48º for 30 min; 95ºC for 10 min; and 40 cycles of 95ºC for 15 s, 60ºC for 1

min. Controls consisted of reactions lacking template or RT, and all samples were run in triplicate. GAPDH was used as the reference gene. Threshold cycles (C_t) were recorded for each gene and compared to the reference gene C_t (ΔC_t). Fold change values were calculated using the $\Delta\Delta C_t$ ($2^{-\Delta\Delta Ct}$).

Small interfering RNA transfection

A549 cells (2 x10^5 cells per well in a 6-well plate) were transfected with 3.2 μg per well of SOCS-1 siRNA (Dharmacon) and SOCS-3 siRNA (Dharmacon), or negative control siRNA (Ambion) using TransMessenger Transfection Reagent (Qiagen) per manufacturer's instructions. Twenty-four hours post-transfection, cells were mock infected (diluent alone) or infected with TX02 or MAD78 at an MOI of 1. Cells were equally divided into two aliquots, one for analysis by qRT-PCR and the second for Western blot analysis.

Northern blot

RNA was extracted with TRIzol (Invitrogen) per manufacturer's instructions, resuspended in RNase-free ddH2O, quantified by spectrometry and mixed with RNA loading buffer. After 10 min of denaturation at 50ºC, 5 μg RNA was separated on a 1% agarose gel containing 2.2 M formaldehyde, 20 mM MOPS (pH 7.0), 8 mM sodium acetate and 1 mM EDTA (pH 8.0). The gel was soaked in ddH2O for 15 min followed by 15 min in 20X SSC. RNA was transferred to a Nytran membrane using the Schleicher & Schuell Turboblotter downward transfer system per manufacturer's instructions. DNA probes for WNV, ISG15, ISG56, or GAPDH were made using Klenow DNA polymerase and random nonamers in a

reaction containing α^{32}P-dCTP. Hybridization was carried out with ULTRAhyb (Ambion) and 10^6 cpm/ml of radiolabeled probe overnight at 48ºC. The membrane was then rinsed once in preheated low-stringency wash buffer (LSWB; 2X SSC, 0.1% SDS) followed by two 5 min washes in LSWB and two 15 min washes in preheated high-stringency wash buffer (HSWB; 0.1X SSC, 0.1% SDS) at 48ºC. Blots were visualized by autoradiography and/or phosphorimage analysis.

Polyribosome distribution analysis

To analyze the effects of IFN treatment on polyribosome-WNV association in vitro, WNV 1.1 replicon cells (a kind gift from Peter Mason) in 15 cm dishes were left untreated or were treated with complete DMEM containing 100 U IFNα-2a/ml for 24 h. Following IFN treatment cells were treated with complete DMEM containing cycloheximide (CHX; 1 μg/ml) for 15 min at 37ºC. Cells were then rinsed twice in prewarmed PBS-CHX (100 μg/ml), trypsinized and washed off the plate in 10 ml prewarmed PBS-CHX containing 1 mM phenylmethlysulfonyl fluoride. The mixture was added to 10 ml frozen PBS-CHX and centrifuged for 5 min at 1000 x *g* at 4ºC. The supernatant was removed, and the pellet was washed with 10 ml ice-cold PBS-CHX and spun again for 5 min at 1000 x *g* at 4ºC. Again, the supernatant was discarded. After resuspension in 750 μl ice-cold low-salt buffer (LSB; 20 mM Tris [pH 7.5], 10 mM NaCl and 3 mM $MgCl_2$), cells were allowed to swell on ice for 3 min. Cells were then lysed with 250 μl detergent buffer (LSB containing 1.2% Triton-

N101), transferred to an ice-cold 7 ml Dounce homogenizer and homogenized with 8 strokes of the pestle. The homogenate was then transferred to an ice-cold microcentrifuge tube and subjected to centrifugation at 10,000 x *g* for 1 min at 4ºC. The supernatant was transferred to a new ice-cold tube containing 100 µl LSB supplemented with 1 mg heparin and NaCl (1.5 M final concentration). The lysates was carefully layered on top of a 0.5 M to 1.5 M sucrose gradient previously prepared in a polyallomer tube (14 x 95 mm) and subjected to ultra-centrifugation in a Beckman SW40 rotor at 36,000 rpm for 2 h at 4ºC. Gradients were collected into approximately ten 1 ml fractions with a Brandel syringe pump and ISCO density gradient fractionator. Fractions were monitored by optical density at a wavelength of 254 nm (OD_{254}) and collected into microcentrifuge tubes containing 100 µl 10% SDS. Fractions were then transferred to a new tube containing 11 µl Proteinase K and incubated at 37ºC for 30 min. RNA was extracted from fractions with TRIzol per manufacturer's instructions and resuspended in 30 µl ddH2O. RNA integrity was confirmed by separating 10 µl RNA on a 2% agarose gel and staining the rRNA with ethidium bromide. Polysome distribution was determined by monitoring distribution of the 18S and 28S rRNA bands which corresponded to the 40S and 60S ribosomal subunits, respectively.

The Titanium One-Step RT-PCR kit (Clontech) was used to measure the gradient distribution (ribosome association) of 1 µl of WNV and β-actin RNAs. RNA was amplified in a reaction with conditions of 50ºC for 60 min; 94ºC for 5 min; 22 cycles (for WNV) or 35 cycles (for β-actin) of 94ºC for 30 s, 65ºC for 30 s, 68ºC for 1 min; and 68ºC for 2 min. RT-

PCR reaction products were analyzed on a 2% agarose gel stained with ethidium bromide. Primers for WNV were directed to the 3'UTR of the viral genome (WNV 10529s, 5'-CCGG AAGTTGAGTAGACGGTGCTGCC; WNV 10694a, 5'-TGGGGCACTATCGCAGACTGC ACTCTCCGC). Primers for β-actin were previously described (253) (5' B-actin 303s, 5'-TTGTTACCAACTGGGACGACATGG; 3' B-actin 1067a, 5'-GATCTTGATCTTCATGG TGCTAGG).

Microarray

A549 cells were seeded (7.5×10^5) in 6 cm dishes and infected with TX02 or MAD78 (MOI = 5). Twenty-four or 48 h post-infection, media was replaced with complete DMEM or complete DMEM containing IFNα-2a (100 U/ml) for 6 h at 37ºC. Following IFN treatment, media was removed and cells were collected in TRIzol LS (Invitrogen). RNA was extracted according to manufacturer's instructions and analyzed by oligonucleotide expression array in Michael Katze's lab at the University of Washington.

Microarray format, protocols for probe labeling, and array hybridization are described at http://expression.viromics.washington.edu. Briefly, a single experiment comparing two mRNA samples was done with four replicate Human 1A (V2) 22K oligonucleotide expression arrays (Agilent Technologies) using the dye label reverse technique. This allows for the calculation of mean ratios between expression levels of each gene in the analyzed sample pair, standard deviation and *P* values for each experiment. Spot quantitation, normalization and application of a platform-specific error model was performed using

Agilent's Feature Extractor software (version 8.1.1) and all data was then entered into a custom-designed database, Expression Array Manager, and then uploaded into Rosetta Resolver System 6.0.0.2.8 Taqman (Rosetta Biosoftware, Kirkland, WA) and Spotfire DecisionSite for Functional Genomics 8.1 (Spotfire, Somerville, MA). Data normalization and the Resolver Error Model are described on the website http://expression.viromics.washington.edu. This website is also used to publish all primary data in accordance with the proposed MIAME standards (33). Selection of genes for data analysis was based on a greater than 99% probability of being differentially expressed ($P \leq 0.01$) and a fold change of 2 or greater.

Protein analysis

Western blot

For immunoblot analysis of proteins, cell extracts were prepared by washing cell monolayers twice in ice-cold PBS followed by lysis with radioimmunoprecipitation assay (RIPA) buffer (10 mM Tris, 150 mM NaCl, 0.02% sodium deoxycholate, 1% Triton X-100, 0.1% SDS) containing 1 μM okadaic acid (Calbiochem), 1 μM Phosphatase Inhibitor Cocktail II (Calbiochem) and 10 mM protease inhibitor (Sigma). Lysates were spun at >18,000 x *g* for 15 minutes at 4ºC, and protein concentrations were determined by the Bradford method. Proteins (20-35 μg) were resolved on 10% SDS-polyacrylamide gels, transferred to nitrocellulose at 110-120 V-hr and blocked in 5% non-fat dried milk (NFDM) in Western wash buffer (1X PBS, 0.1% Tween-20). Monoclonal and polyclonal primary antibodies used for immunoblot analysis are listed in Table 2-6. Secondary antibodies

included peroxidase-conjugated goat anti-rabbit and goat anti-mouse from Perkin Elmer and donkey anti-goat from Jackson Immunoresearch.

Immunoprecipitation

A549 cells were seeded at a density of 6 x 10^5 cells per 10 cm dish. Cells were infected with TX02 or MAD 78 (MOI = 5) as described above. Twenty-four h post-infection cells were pulsed with 1000 U IFNα-2a in complete DMEM for 0, 15, or 30 minutes, washed once in ice-cold PBS and lysed in 500 µl Buffer A (25 mM Tris-Cl [pH7.5], 150 mM NaCl, 1% NP-40) plus 1 µM okadaic acid, 1 µM Phosphatase Inhibitor Cocktail II (Calbiochem) and 10 µM protease inhibitor (Sigma). Lysates were homogenized through a 22G needle, rotated 30 min at 4ºC and spun for 15 min at top speed in a microcentrifuge. The supernatant was cleared with a 20 µl slurry of Protein A agarose beads (Roche) for 30 min at 4ºC. Protein concentration was determined by the Bradford method. Samples were split into 2 aliquots of 200 µg proteins in 200 µl Buffer A containing protease and phosphatase inhibitors. Immunoprecipitation was performed overnight at 4ºC with 25 µl Protein A agarose beads and mouse anti-phosphotyrosine (Cell Signaling) or mouse anti-JAK1 (BD Biosciences) antibodies. The beads were spun down at 350 x *g* for 3 min, and 75 µl of the supernatant was taken and stored at -80ºC (supernatant fraction). The beads were then washed 3 times in Buffer A, mixed with 1X SDS sample buffer, boiled for 5 min and pelleted at max speed in a microcentrifuge. The supernatant was transferred to a new tube (pellet fraction) and analyzed by immunoblotting.

Table 2-6: Monoclonal and polyclonal primary antibodies

Source[1]	Target	Company
G	actin	Santa cruz
R	eEF2	Cell Signaling Technology
M	FLAG	Sigma
G	GAPDH	Santa cruz
M	GAPDH	Abcam
M	HA	Sigma
R	HA (Y-11)	Santa cruz
R	IRF-3 (human)	Michael David, UCSD
R	IRF-3 (murine)	Zymed
R	IRF-9	Santa cruz
R	ISG15	Arthur Haas, Medical College of Wisconsin
R	ISG54 (murine)	Ganes Sen, Cleveland Clinic
R	ISG56	Ganes Sen, Cleveland Clinic
R	ISG56 (murine)	Ganes Sen, Cleveland Clinic
M	JAK1	BD Biosciences
R	JAK2	Upstate
R	MAVS	Zhijian Chen, UT Southwestern
R	MDA5 (murine)	Axxora
R	PARP	Cell Signaling Technology
R	phospho-eIF2α (S51)	Cell Signaling Technology
R	phospho-JAK1 (Y1022/1023)	Biosource
R	phospho-JAK2 (Y1007/1008)	Cell Signaling Technology
R	phospho-PKR (T451)	Biosource
R	phospho-STAT1 (Y701)	Cell Signaling Technology
R	phospho-STAT2 (Y689)	Upstate
R	phospho-STAT3 (Y705)	Cell Signaling Technology
R	phospho-TYK2 (Y1054/1055)	Cell Signaling Technology
M	phospho-Tyrosine	Cell Signaling Technology
M	PKR (B-10)	Santa cruz
R	RIG-I	Michael Gale, UT Southwestern
R	SOCS1 (J192) (human)	IBL
R	SOCS3 (C204) (human)	IBL
R	STAT1	Cell Signaling Technology
M	STAT1α	Sigma
R	STAT2	Santa cruz
R	STAT3	Cell Signaling Technology
R	TYK2	Upstate
M	WNV (strain Eg101)	CDC

[1]G, goat; M, mouse; R, rabbit

Cellular fractionation

For cell extract fractionation experiments, A549 cells were mock-infected or infected with TX02 or MAD78 (MOI = 5). Twenty-four h later the cells were pulse-treated with 1000 U IFNα-2a in complete DMEM for 1 h at 37ºC. Cells were collected in ice-cold PBS, washed and lysed in cytoplasmic lysis buffer (10 mM Tris-HCl, 60 mM KCl, 1 mM EDTA, 2 mM DTT, and 0.15% NP-40). Nuclei were pelleted at 9000 rpm for 15 min at 4ºC in a microcentrifuge, and the supernatant was collected (cytoplasmic fraction). Nuclear fractions were collected in nuclear extract buffer (20 mM Tris-Cl, 400 mM NaCl, 1.5 mM $MgCl_2$, 0.2 mM EDTA and glycerol) by sheering DNA through a 20G syringe, centrifuging sample at maximum speed for 15 min at 4ºC and collecting the supernatant (nuclear fraction). Cytoplasmic and nuclear fractions were analyzed by SDS-PAGE and immunoblotting.

Metabolic labeling

Huh7 or A549 cells were seeded in 6-well plates and infected the next day with TX02 (MOI ~ 5). Cells were washed twice in PBS and starved in DME lacking Cys, Met or Glu supplemented with 5% dialyzed FBS, L-Glu and L-Cys (starve media) at 37ºC for 2 h prior to labeling with ^{35}S-Met (200 μCi/ml) in starve media for 30 min at 37ºC. Following metabolic labeling, cells were collected in PBS, washed once in ice-cold PBS and lysed in RIPA buffer containing protease inhibitors. Protein concentrations were determined by the Bradford method and analyzed by SDS-PAGE. To control for protein loading, the gel was stained for 2 h with Coomassie Brilliant-Blue, destained (20% methanol, 10% glacial acetic acid) and imaged on a MultiImage Light Cabinet (Alpha Innotech Corp.). The gel was then

treated with Amplify fluorographic reagent (Amersham Biosciences) for 30 min, dried onto Whatman paper at 80ºC for 1.5 h and exposed to a Storage Phosphor Screen (Amersham Biosciences). Images were resolved on a Storm 820 imaging system (Amersham Biosciences) running ImageQuant software.

Transfection and luciferase reporter assay

pCAGGS WNV expression constructs

To analyze the ability of WNV genes to antagonize IFN signaling, Huh7 cells were seeded in 48-well plates at a confluency of 2 x 10^4 cells per well the day prior to transfection. On the day of transfection, cells were washed once in PBS and antibiotic/antimycotic-free media (DMEM, 10% FBS, 2 mM L-glutamine, 1mM sodium pyruvate, 1X non-essential amino acids and 25mM HEPES) was added. Ten ng pRL-CMV (*Renilla* luciferase transfection control plasmid) (74), 30 ng pISRE-TA-luc (Mercury Pathway Profiling Kit, Clontech) and the indicated amount of expression vector being tested were transfected into cells with Lipofectamine 2000 (L2000; Invitrogen) according to manufacturer's instructions. pISRE-TA-luc is a promoter reporter plasmid encoding 5 copies of the ISRE enhancer element located upstream of the minimal TA promoter driving transcription of the firefly luciferase gene. After 24 hrs of transfection, media was replaced with complete DMEM or complete DMEM containing IFNα-2a (1000 U/ml) for 6 hrs. Cells were then washed once in PBS, lysed in Passive Lysis Buffer (Dual-Luciferase Reporter Assay System, Promega) and analyzed for luciferase activity in a Centro LB 960 Luminometer (Berthold,

Technologies) running MikroWin 2000 software. For each experiment transfections were performed in triplicate.

Dominant negative SOCS expression constructs

SOCS1 and SOCS3 expression plasmids containing dominant negative mutations were used to determine the role of these proteins in signaling antagonism during WNV infection. Huh7 cells were seeded in a 48 well plate and transfected with 30 ng pISRE-TA-luc, 10ng pRL-CMV and 60g pORF5, SOCS1 DN, SOCS3 DN, or a combination of SOCS1 DN and SOCS3 DN using Fugene 6 (Roche). The transfected cells were infected 24 h later with TX02 (MOI ~ 5) for a further 24 h. IFNα (1000U/ml) or complete DMEM was then added to the cells for 6 h. Cells were washed once in PBS, lysed in Passive Lysis Buffer (Dual-Luciferase Reporter Assay System, Promega) and analyzed for luciferase activity as described above.

Confocal microscopy

For indirect immunofluorescence assay of protein localization, A549 cells were seeded on 4-chamber microscope slides (Nalge Nunc International) and infected (MOI = 2) with TX02 or MAD78 for 1 hour at 37ºC. Inoculum was replaced with complete DMEM and incubated for 24 hours, at which time cells were pulsed with complete DMEM or complete DMEM containing IFNα-2a (1000 U/ml) for 60 minutes at 37°C. Cells were washed once in PBS and fixed in 4% paraformaldehyde for 30 minutes at room temperature. Cells were

washed in PBS-Glycine for 15 minutes at 25°C, permeabilized with 0.2% Triton-X 100 in PBS for 15 minutes, blocked with 10% normal goat serum (Santa cruz) in PBS for 1 hour at 25°C and stained with fluorescein isothiocyanate-conjugated (FITC) human anti-WNV (1:400) (kindly provided by Jorge Munoz-Jordan) and rabbit anti-STAT2 (1:100) (Santa Cruz) primary antibodies for 1 hour at 25°C. Cells were then washed 3 times with 0.05% Tween-20 in PBS and incubated with goat anti-rabbit rhodamine-conjugated secondary antibody (1:1000) (Jackson Immunoresearch) and DAPI (1:100). Coverslips were mounted with Vectashield, and slides visualized in the UT Southwestern Pathogen Imaging Facility using a Zeiss Pascal Laser Scanning confocal microscope with Zeiss LSM software.

WNV Replicon

WNV Rluc/NeoRep

BHK-21 cells harboring the WNV subgenomic replicon Rluc/NeoRep was kindly provided by P.Y. Shi (165). Rluc/NeoRep contains a dual reporter system and was derived from the parental WNV Replicon (234) by replacing most of the structural gene region (nt 190 to 2379) with an in-frame *Renilla* luciferase (Rluc) reporter gene. A neomycin phospho-transferase (Neo) gene under the control of an encephalomyocarditis virus IRES was placed just downstream from the NS5 gene in the 3' UTR. Total RNA was isolated from these cells with TRIzol according to the manufacturer's instructions and stored at -80ºC. Rluc/NeoRep RNA was treated with DNaseI (Ambion) for 1 h at 37º according to the manufacturer's protocol and transferred to a new microcentrifuge tube after inactivation of the DNase

enzyme. Huh7 cells (4 x 10^5 cells/well) in 6-well plates were transfected with 1 μg, 2 μg, or 4 μg of DNaseI-treated Rluc/NeoRep RNA using Transmessenger Transfection Reagent (Qiagen) according to the manufacturer's instructions. After 3 h, transfection mix was replaced with complete DMEM for 16-20 h at 37ºC. Cells were then washed in PBS, trypsinized, transferred in 8 ml complete DMEM to a 10 cm plate and allowed to recover for 48 h at 37ºC. After recovery, complete DMEM was replaced with complete DMEM containing G418 (G418 DMEM, 400 μg/ml) for selection of resistant colonies. Resistant colonies were transferred to 24-well plates via colony selection discs and expanded in the presence of G418 (400 μg/ml). Once the cells were expanded to 75 cm^2 flasks (approximately 11 weeks after RNA transfection), WNV Rluc/NeoRep protein expression was examined by Western blot analysis of cell lysates collected in RIPA containing protease inhibitors as described above. *Renilla* luciferase activity of cells collected in PLB was also examined on a luminometer at this time (see luciferase assay above). In all, 14 distinct clones of WNV Rluc/NeoRep (WNV Rluc#1, #2, #4, #6, #7, #8, #9, #10, #11, #12, #13, #14, #17 and #18) with variable protein and luciferase expression were recovered in Huh7 cells.

Curing of WNV Rluc/NeoRep

To create a Huh7-derived control cell line for WNV Rluc/NeoRep, clones #2 and #8 were subjected to curing with IFN. Briefly, both cell lines (WNV Rluc#2 and WNV Rluc#8) were passaged in the presence of pegylated IFNα-2b (PEG-INTRON, Schering) at a concentration of 100 U/ml in complete DMEM. Controls consisted of WNV Rluc#2 and

WNV Rluc#8 cultured in the absence of PEG-INTRON and Huh7 cells lacking a replicon cultured in the presence or absence of PEG-INTRON. After 11 to 25 days of maintenance in PEG-INTRON, cells were collected and analyzed for *Renilla* luciferase activity. When *Renilla* luciferase activity was below the background level of Huh7 control cells, the cured WNV Rluc#2c and WNV Rluc#8c were switched to complete DMEM. Loss of the replicon from WNV Rluc#2c and WNV Rluc#8c was confirmed by reselecting the cells in G418 and staining the plates (Coomassie Brilliant Blue in a solution of 50% methanol and 10% glacial acetic acid). Selection was performed twice in G418 DMEM (800 μg/ml) and once in G418 DMEM (200 μg/ml). Curing of the replicons was also confirmed by RT-PCR analysis of RNA isolated from WNV Rluc#2c and WNV Rluc#8c as well as the control untreated WNV Rluc #2 and WNV Rluc#8 replicons and PEG-INTRON-treated Huh7 cells. cDNA was made from 2 μg RNA as described above. Primers directed against NS1 (WNV (NS1) 2470s, 5'- CTGGATATCGGACACTGGGTGTGCCATAGACAT; WNV (NS1) 3525a, 5'-GGCTCTAGACTAAGCATTCACTTGTGACTGCACG), NS4a (WNV (NS4a) 6469s, 5'-GCGGATATCGTCTCAGATAGGGCTCATTGAGGTTC; WNV (NS4a) 6915a, 5'-TTTTCTAGATTAGGCTGCCACTGCGCTCACAAGG), 3' UTR (WNV 10529s, 5'-CCGGAAGTTGAGTAGACGGTGCTGCC; WNV 10694a, 5'-TGGGGCACTATCGCAGACTGCACTCTCCGC) and β-actin (see above) were used in a PCR reaction with parameters of 95ºC for 1 min; 40 cycles of 95ºC for 30 s, 53ºC for 30 s, 68ºC for 2.5 min; and 68ºC for 5 min. RT-PCR products were analyzed on 1% agarose gels stained with ethidium bromide.

Mouse lethality experiments.

Commercially obtained four-week-old outbred Swiss-Webster mice were divided into 10 groups of 10 animals and inoculated intraperitoneally with 100 μl of virus diluted in PBS containing 10% FBS. The inocula consisted of a Vero passage 1 preparation of NY 385-99 (GenBank accession #AY842931) (kindly provided by Robert Tesh) or a Vero passage 2 preparation of plaque-purified TX02, in both cases diluted to give titers of 1000, 200, 40, 8 or 1.6 PFU per 100 μl. Following inoculation, animals were monitored for lethality. Moribund animals (defined as those not expected to survive for an additional 24 hours) were humanely euthanized and scored as "dead" the following day. Fifty percent lethal doses (LD_{50}) values were determined using the method of Reed and Muench (214). Wild-type C57BL/6J mice were obtained commercially. Interferon α/β receptor-deficient mice (IFNAR-/-) on a pure C57BL/6J background were obtained from Jonathan Sprent (Scripps Institute, San Diego, CA) and genotyped. For infection of wild-type C57BL/6J and IFNAR-/- mice, TX02 and MAD78 were plaque purified and passaged twice on Vero cells to generate viral stocks that were used in all experiments. Eight to ten week old wild-type and IFNAR-/- mice were infected by footpad inoculation with 10^2 PFU of each virus diluted in Hanks balanced salt solution (HBSS) with 1% heat inactivated FBS as described (222). Mice were monitored daily for lethality. Mouse experiments were approved and performed in accordance with the guidelines of the University of Texas Medical Branch Institutional Animal Care and Use Committee or the Washington University Animal Studies Committee.

Statistical analyses

Unless otherwise noted, the student's unpaired t-test in the Prism 4 software package (GraphPad Software, San Diego, CA) was used to determine statistical significance of experimental values.

CHAPTER THREE
Resistance to Alpha/Beta Interferon is a determinant of WNV replication fitness and virulence[§]

INTRODUCTION

After its introduction in New York City in 1999, WNV rapidly spread across the continent and now appears to have firmly established itself in the ecology of North America. The recent emergence of pathogenic WNV strains and their virulence within a naïve population suggests that epidemic forms of the virus may encode mechanisms to evade host immunity.

Infection with WNV triggers a delayed host response that includes the activation of IRF-3 and subsequent production of α/β interferons (IFN) (75,76,222). IFNs are a family of immunomodulatory cytokines that are produced in response to virus infection and serve as integral signal initiators of host intracellular defenses (232,270). Binding of IFN to the cognate IFN α/β receptor (IFNAR) on target cells results in the activation of the JAK-STAT pathway that includes the receptor-associated kinases JAK1 and TYK2, which in turn phosphorylate and activate their downstream effectors, STAT1 and STAT2. Activated phospho-STAT1/STAT2 heterodimers translocate to the nucleus to form a heterotrimeric complex with IRF-9 and induce transcription of hundreds of interferon stimulated genes (ISGs) whose products can direct antiviral and antiproliferative actions that limit virus replication and spread.

The importance of the IFN system in WNV infections has been demonstrated by a combination of in vivo studies and anecdotal evidence from off-label use of IFN in healthcare settings. In fact, this idea was first suggested by Isaacs and Westwood in 1959 when they observed that cells pre-treated with IFN were refractory to WNV infection (113). Later, studies in mice and hamsters demonstrated protection with IFN treatment, especially prophylactic therapy administered prior to infection (186,187). Several recent reports have demonstrated the efficacy of IFNα treatment in a variety of patients infected with WNV (124,227,271). The effectiveness of IFN on WNV and related flaviviruses was confirmed in vivo using chemical inducers of IFN production (83,254) and in vitro with exogenously added IFN (7,55,98,267). It should be noted, however, that there has been some dispute as to the actual effectiveness of IFN in controlling flaviviral infections with a couple of reports claiming treatment failure (49,246). The discrepancies in these reports are now beginning to be resolved. An elegant study by Diamond and colleagues described the modulation of DENV infection with IFNα/β and IFNγ and suggested that DENV may actively resist IFN since treatment before or shortly after infection was much more effective at controlling DENV than treatment initiated as little as 4 hpi (60). Additionally, of WNV patients treated with IFN, those whose treatment was initiated within 9-10 days after the onset of symptoms exhibited a much better response compared to those with delayed IFN therapy (49) indicating that WNV may also resist IFN later in the course of infection.

Many viruses encode proteins that direct mechanisms to disrupt innate antiviral defenses and IFN-induced JAK-STAT signaling, and these processes have been linked to

viral emergence in new host populations and species (90,127,268) and to pathogenic outcomes of infection (39,232,270). Importantly, virulent isolates of WNV have recently been shown to attenuate IFN actions by preventing STAT1 and STAT2 activation, though the mechanisms of this regulation and its influence in vivo were not defined (93,164). Here we describe in vitro and in vivo studies comparing the genetic and phenotypic properties of a lineage I/emergent strain and a lineage II/non-emergent strain of WNV. Our data show that viral control of IFN action and JAK-STAT signaling is critical for high replication fitness and virulence. We propose that WNV control of IFN defenses may provide a platform for pathogenesis and continual emergence within naïve host populations.

RESULTS

Genetic and phenotypic characterization of WNV isolates from Madagascar and Texas.

WNV Madagascar-AnMg798 (MAD78) was isolated from an infected parrot (*Coracopsis vasa*) in the Analabe region, Madagascar in May, 1978 (188). On the basis of a small region of the E gene, Berthet and colleagues proposed that MAD78 clusters with WNV lineage II (23). Expanding on their findings, we determined the complete coding sequence of MAD78 and compared it to other WNV strains. In agreement with previous studies (18,23,37,147), phylogenetic analysis of the entire open reading frame (ORF) clearly places MAD78 in lineage II (Figure 3-1), although MAD78 appears to cluster genetically distant

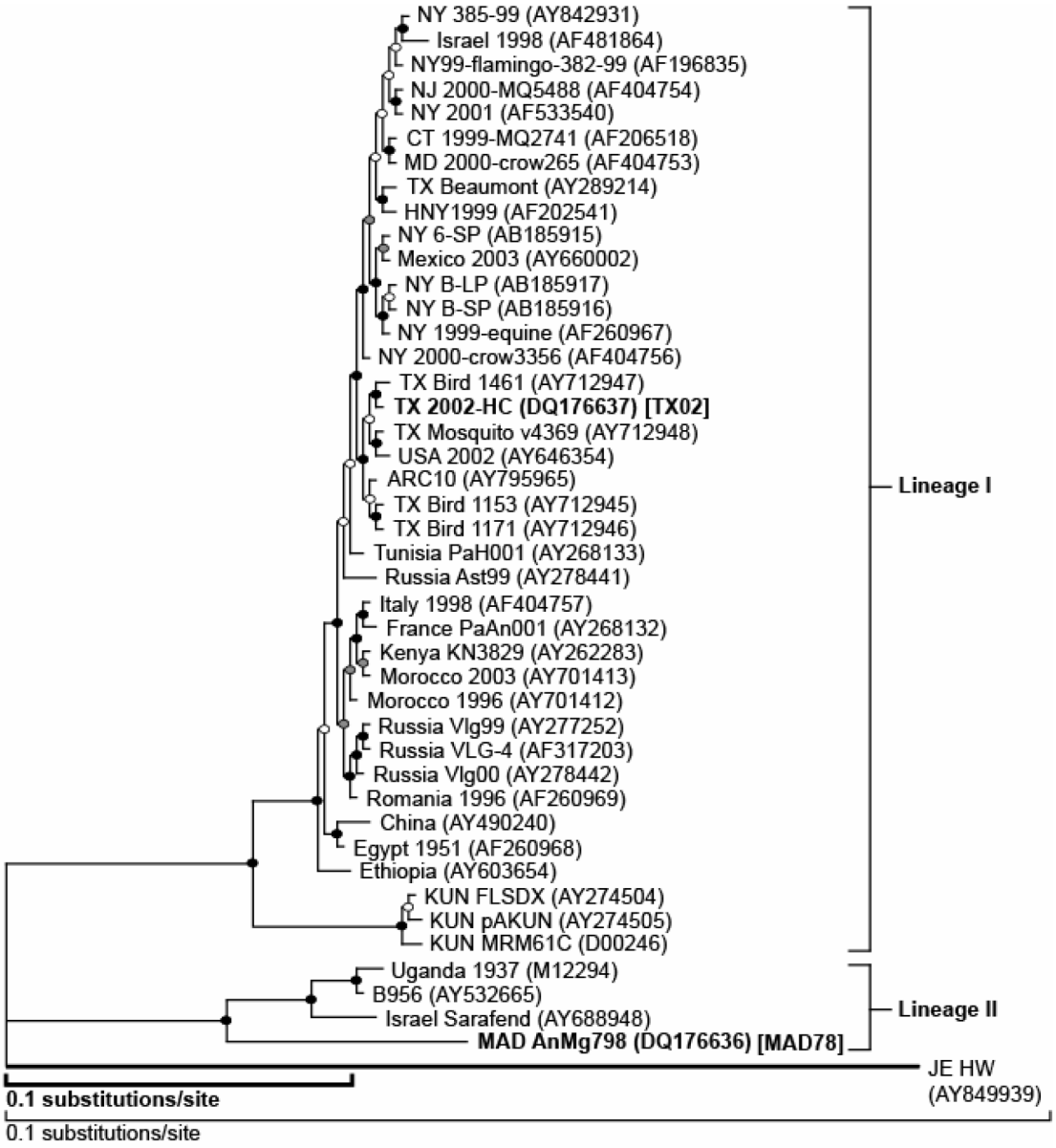

Figure 3-1. Phylogenetic analysis of complete WNV coding sequences.
Complete WNV genomic sequences were obtained from GenBank and aligned using ClustalW. The Neighbor-joining tree was created by maximum likelihood using Molphy, version 2.3 with sequence JE HW as the outgroup. Bootstrap values are the result of 1000 replicates and are represented by colored dots at the nodes (black = values ≥ 90; grey = values ≥ 75 but < 90; and white = values < 75). Scale bars are proportional to genetic distance. Because of the extreme divergence between the JE HW outgroup and the WNV isolates, two different scale bars are used. The thick line represents the scale for the JE outgroup, while the thin line depicts the relative scale for the WNV isolates.

from other lineage II strains. Across the complete ORF, MAD78 exhibits 83.9% (nucleotide) and 96.3% (amino acid) similarity to the lineage II prototype strain from Uganda (Table 3-1 and data not shown).

WNV-TX 2002-HC (TX02) was isolated in August, 2002 from the brain of an infected grackle (*Quiscalus quiscula*) in Hall County, Texas. Following plaque purification, the entire TX02 coding sequence was determined by overlapping RT-PCR. Sequence comparison with published complete WNV genomes demonstrated very little genetic divergence between TX02 and other lineage I WNV strains in North America (Figure 3-1). Relative to the prototypical lineage I isolate, WNV NY99-flamingo382-99 (NY99), only four amino acid substitutions (one each in the prM/M, E, NS2b and NS5 genes) were identified in TX02 (Table 3-1). However, TX02 is only 93.2% identical to MAD78 at the amino acid level with residue substitutions occurring throughout the coding region (Table 3-1).

One step growth analyses of virus replication in human lung carcinoma (A549, Figure 3-2 A) or human hepatoma (Huh7, data not shown) cells revealed that TX02 displays nearly

Table 3-1: Amino acid differences between TX02 and MAD78 and prototypical lineage I and lineage II WNV strains

Gene	Total	Core	prM/M[a]	E	NS1	NS2a	NS2b	NS3	NS4a	NS4b	NS5
TX02 & NY99											
# aa differences	4	0	1	1	0	0	1	0	0	0	1
% aa identity	99.9	100	99.4	99.8	100	100	99.2	100	100	100	99.9
MAD78 & Uganda 1937											
# aa differences	128	2	3	20	20	22	2	11	4	18	26
% identity	96.3	98.4	98.2	96.0	94.3	90.5	98.5	98.2	97.3	93.0	97.1
TX02 & MAD78											
# aa differences	234	12	7	34	37	26	6	28	9	23	52
% identity	93.2	82.9	95.8	93.2	89.5	88.7	95.4	95.5	94.0	91.0	94.3

[a]prM, premembrane; M, membrane; E, envelope; NS, nonstructural

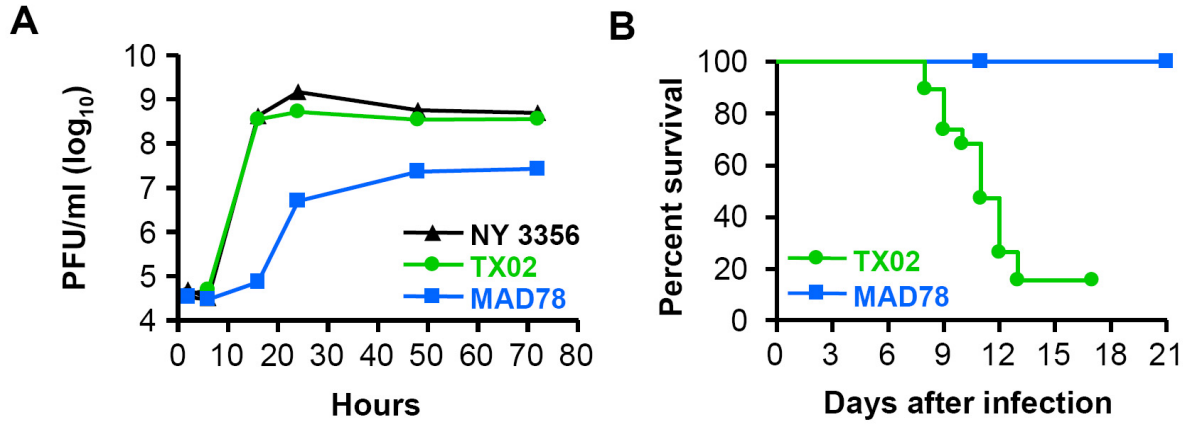

Figure 3-2. In vitro and in vivo characterization of MAD78 and TX02.
(A) A549 cells were infected (MOI = 1) with TX02, MAD78, or NY 3356. At 2, 6, 18, 24, 48 and 69 hours post-infection (TX02, NY 3356) or 2, 6, 16, 24, 48 and 72 hours post-infection (MAD78) culture supernatants were collected and titered by plaque assay on Vero cells. (B) Groups of wild-type C57BL/6 mice were infected by footpad inoculation with 10^2 PFU of MAD78 or TX02 and monitored for survival. Results are plotted as percent surviving mice.

identical growth kinetics and peak infectious virus production as WNV NY 2000-crow3356 (NY 3356), a well-characterized lineage I strain that is 99.9% identical (147) to the NY99 isolate. By comparison, growth of MAD78 was delayed, and peak infectious virus production was decreased 10-fold relative to the lineage I strains. To define the virulence phenotype of TX02, cohorts of outbred Swiss-Webster mice were inoculated by the intraperitoneal route with increasing doses of TX02 or NY 385-99 and monitored for survival (data not shown). We found that both TX02 and NY 385-99, a second control isolate from the 1999 New York outbreak (248), conferred lethality in mice challenged with a dose of 10^3 PFU, resulting in mortality of 90% (mean survival time of 7.7 days) and 100% (mean survival time of 7.5 days), respectively. Furthermore, we calculated LD_{50} values for TX02 and NY 385-99 of 7.1 and 5.8 PFU, respectively, thus confirming the lethality of TX02 in a

mouse model. On the other hand, MAD78 demonstrated a non-neuroinvasive, non-pathogenic phenotype in outbred Swiss-Webster mice when inoculated intraperitoneally with doses 10-fold higher than those used in our TX02 experiments (17,18), consistent with its reduced replication fitness in vitro. Further in vivo characterization of MAD78 and TX02 by footpad inoculation of inbred C57BL/6 mice with 10^2 PFU resulted in 0% and 86% lethality, respectively ($n = 19$, $P < 0.0001$) (Figure 3-2 B), confirming the attenuated nature of MAD78.

MAD78 and TX02 exhibit differential responses to interferon action.

We hypothesized that the different virulence phenotypes of MAD78 and TX02 may be due, in part, to variable interactions with IFN antiviral defense programs of the host cell. We therefore evaluated the influence of IFN on viral growth. One hour after infection with TX02 or MAD78, cultures of A549 cells were treated with 10 U IFNα-2a or media alone. We then examined infectious particle production and cell-associated viral protein abundance at various times post-infection and treatment. As shown in Figure 3-3 A, low-dose IFN treatment resulted in 8-fold ($P < 0.03$, paired t-test) and 1.5- ($P = 0.1$, paired t-test) reductions in peak infectious virus production of MAD78 and TX02, respectively. With low-dose IFN treatment, viral protein abundance was almost completely suppressed in MAD78-infected cells, but levels of TX02 proteins were only slightly affected, if at all, in the presence of IFN (Figure 3-3 B). Similar patterns of protein expression were observed with higher IFN doses (data not shown). These results demonstrate that MAD78 is highly sensitive to antiviral

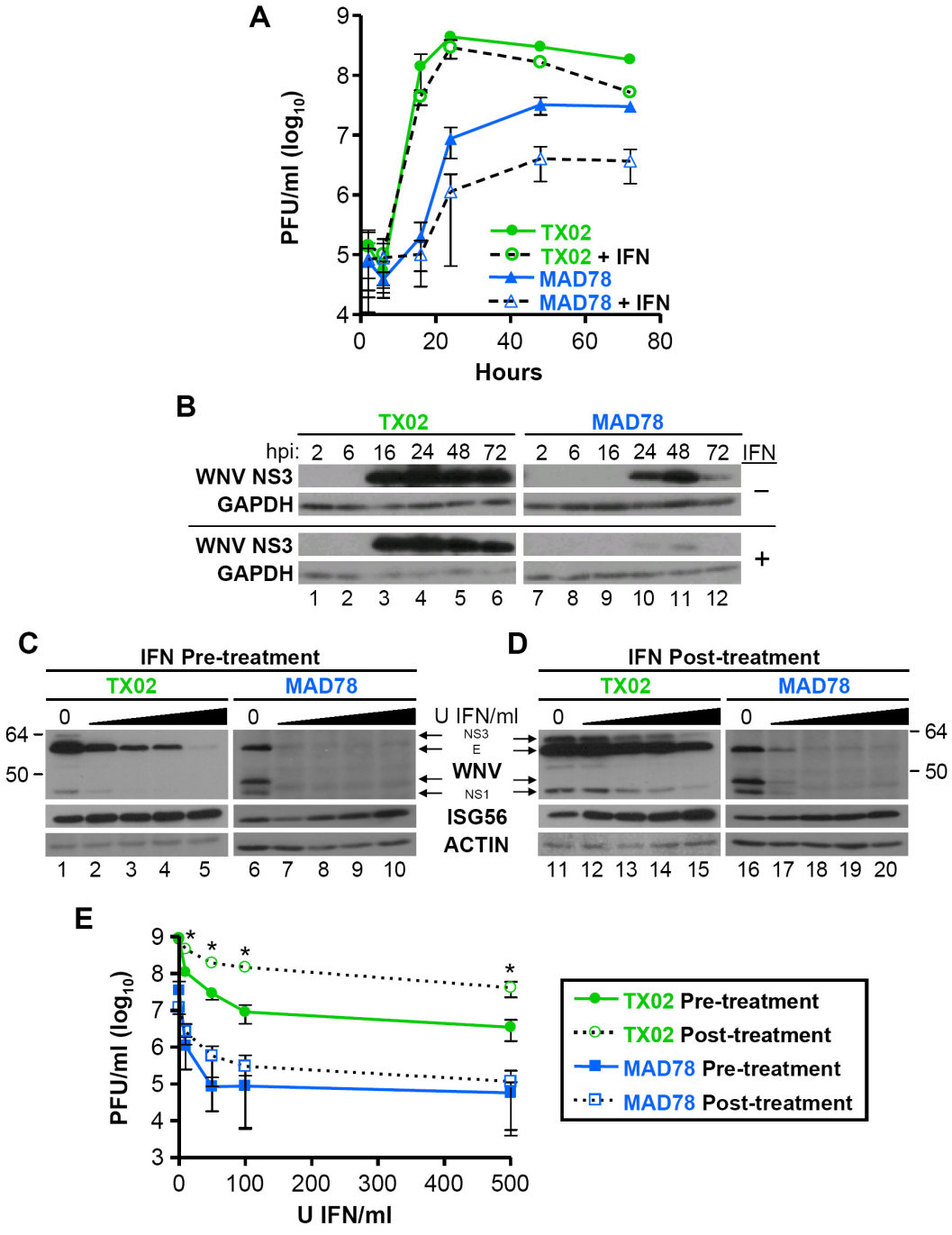

Figure 3-3. IFNα differentially controls growth of MAD78 and TX02.

processes induced by relevant doses of IFNα-2a, while TX02 is strongly resistant to IFN-induced antiviral actions.

To further analyze the differential responses of MAD78 and TX02 to the antiviral effects of IFN, A549 cells were left untreated or were treated with increasing doses of IFNα-2a for 24 hours to induce an intracellular antiviral state. Cells were then infected in the presence of IFNα-2a and maintained under these conditions for the duration of the experiment (IFN pre-treatment; Figure 3-3 C). Alternatively, cell cultures were infected with MAD78 or TX02, and increasing doses of IFNα-2a were added to the growth medium following a 1 hour virus adsorption (IFN post-treatment; Figure 3-3 D). In the absence of exogenous IFN, WNV infection triggered the accumulation of ISG56 consistent with virus-

---

Figure 3-3. IFNα differentially controls growth of MAD78 and TX02.
(A) A549 cells were infected (MOI = 1) with TX02 or MAD78 for 1 hour. Following infection, media containing 0 or 10 U IFNα/ml was added to the cells. At 2, 6, 16, 24, 48 and 72 hours post-infection (hpi), culture supernatants were collected and viral titers were determined by plaque assay on Vero cells. Results are expressed as the mean ± SD. (B) Whole-cell lysates from samples in (A) were analyzed by immunoblot for WNV and GAPDH protein abundance. (C and D) A549 cells were treated with 0, 10, 50, 100, or 500 U IFNα. In (C), cells were pretreated with IFNα for 24 hours prior to WNV infection. In (D), cells were first infected with WNV and then treated with IFN directly after virus adsorption. Cell cultures were maintained in the presence of the respective IFNα dose for 24 hours before harvesting. Whole cell lysates were collected and analyzed by immunoblotting for the abundance of WNV proteins, ISG56 and actin. Cells were infected with TX02 or MAD78 at MOI = 5. WNV proteins were detected with an antibody raised against the lineage I Egypt 1951 strain (GenBank accession #AF260968) revealing strain-specific differences in epitopes on the E and NS1 proteins. (E) Culture supernatants from the samples in (C) and (D) were titered by plaque assay on Vero cells: TX02, IFNα pre-treatment (●); TX02, IFNα post-treatment (○); MAD78, IFNα pre-treatment (■); MAD78, IFNα post-treatment (□). Results are expressed as the mean ± SD. *, $P < 0.01$, unpaired t-test.

induced activation of an IRF-3 dependent host response (76) (Figures 3-3 C and 3-3 D, lanes 1, 6, 11, and 16). Treatment with as little as 10 U of IFN greatly reduced MAD78 protein abundance, whereas TX02 was refractory to this effect with viral protein levels only slightly affected at an 100 U IFN. Both IFN treatment regimens resulted in approximately 1000-fold decreases in infectious particle production in cells infected with MAD78, indicating that timing of IFN treatment is not an important determinant of antiviral effectiveness against an IFN-sensitive strain of WNV (Figure 3-3 E). However, resistance of TX02 to IFN antiviral actions was significantly enhanced when IFN was added following virus infection ($P < 0.01$, unpaired t-test) suggesting that products of TX02 are more effective than those of MAD78 at antagonizing IFN actions.

Differential regulation of JAK-STAT signaling by WNV.

WNV has previously been shown to antagonize IFN signaling (93,164), but the conservation of this regulation among strains of divergent virulence features has not been assessed. We therefore examined the effects of MAD78 and TX02 on IFN signaling processes. A549 cells were infected with MAD78 or TX02 for 24 hours, treated with a high dose (1000 U) of IFNα-2a and analyzed by confocal microscopy. In uninfected and MAD78 infected cells STAT2 translocated to the nucleus following IFN treatment. However, the IFN-induced nuclear translocation of STAT2 was blocked in cells infected with TX02 (Figure 3-4 A). WNV infection triggers IFN production after infection (76), and in the absence of exogenous IFN treatment we found that STAT2 accumulated in the nucleus of

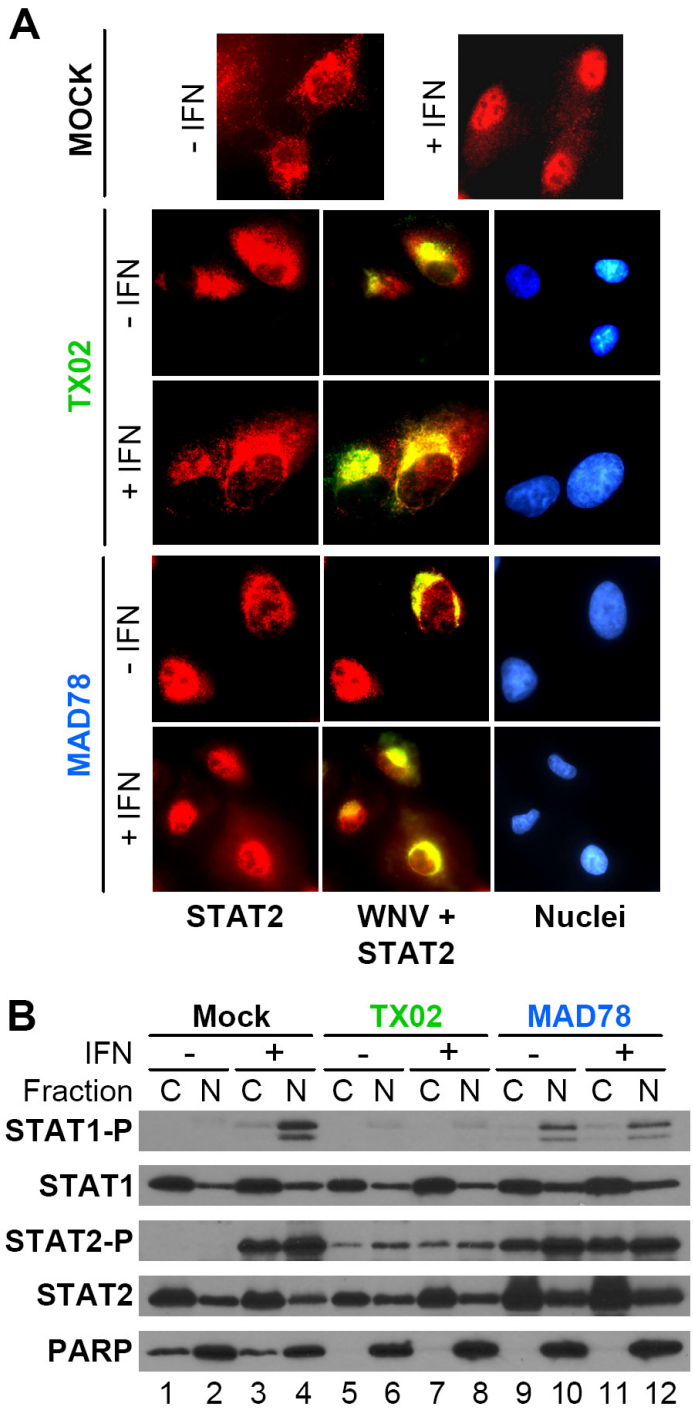

Figure 3-4. TX02 prevents IFNα-induced STAT1 and STAT2 nuclear translocation.

cells infected with MAD78 but not TX02, suggesting that MAD78 is incapable of blocking even endogenous JAK-STAT signaling. Cellular fractionation further revealed the differential control of IFN signaling between WNV strains. Cultures of A549 cells infected with MAD78 or TX02 for 24 hours were treated with high dose IFNα-2a for 1 hour, after which cytoplasmic and nuclear extracts were prepared and subjected to immunoblot analysis to measure the abundance of the active, tyrosine-phosphorylated isoforms of STAT1 and STAT2 (Figure 3-4 B). In resting cells, STAT1 and STAT2 are expressed at a low level and shuttle between cytoplasmic and nuclear compartments (14,182). Their levels increase through IFN-induced positive feedback signaling concomitant with the nuclear accumulation of their active, phosphotyrosine isoforms (232). Consistent with this, IFN treatment stimulated the accumulation of phospho-STAT1 and phospho-STAT2 in extracts of mock-infected control cells, with high levels present in the nuclear fraction (Figure 3-4 B, lanes 1-4). MAD78 infection stimulated the expression and nuclear accumulation of phospho-STAT isoforms both in the absence and presence of IFN. In contrast, STAT protein accumulation

---

Figure 3-4. TX02 prevents IFNα-induced STAT1 and STAT2 nuclear translocation. (A) A549 cells were infected (MOI = 2) with TX02 or MAD78 or were left uninfected (Mock). 24 hours post-infection, cells were treated with 1000 U IFNα for 1 hour and then stained using primary antibodies directed against WNV or STAT2. Nuclei were stained with DAPI. Panels show representative confocal micrographs of images obtained at 40X magnification. Top panels show STAT2 in mock-infected control cells. Images from infected cells show STAT2 (left column), STAT and WNV merged (middle column) or nuclei (right column). (B) A549 cells were infected (MOI = 5) with TX02 or MAD78. 24 hours post-infection cells were left untreated or were treated with 1000 U IFNα for 1 hour. Whole-cell lysates were fractionated into cytoplasmic and nuclear extracts and analyzed by immunoblot using STAT or phospho-STAT specific antibodies. The fractionation of poly (ADP-ribose) polymerase (PARP) was monitored as a nuclear control protein. This shows that lanes 1 and 3 contained a residual level of nuclear material not present in lanes 4-12.

was suppressed and only occurred at very low levels regardless of IFN treatment in cells infected with TX02 (Figure 3-4 B, compare lanes 9-12 with lanes 5-8, respectively). Taken together, these results confirm that WNV has the capacity to induce a host response that includes STAT1 and STAT2 activation, and that compared to pathogenic WNV strains, the ability to suppress STAT activation is attenuated in MAD78.

To determine the level at which MAD78 was defective in blocking IFN-induced STAT phosphorylation, we examined the IFN-induced activation state of JAK-STAT components in cells infected with MAD78 or TX02 and treated with high dose IFNα-2a for 15 or 30 minutes. IFN treatment of uninfected cells induced the accumulation of the active, phosphotyrosine isoforms of Tyk2, STAT1 and STAT2 (Figure 3-5 A, lanes 1-3). TX02 prevented the IFN-induced tyrosine phosphorylation of Tyk2 and the downstream phosphorylation of STAT1 and STAT2. MAD78 infection resulted in a very low level accumulation of the active, phosphotyrosine isoform of Tyk2 and a low level accumulation of phospho-STAT2 in the absence or presence of exogenous IFN, whereas phospho-STAT1 was only detected after IFN treatment. In contrast to Tyk2, JAK1 tyrosine phosphorylation was detected in lysates of cells infected with TX02 or MAD78 even in the absence of exogenous IFN treatment (Figure 3-5 B). A basal level of phospho-JAK1 was found in all cells, while IFN treatment or WNV infection caused an accumulation of slower migrating isoforms of phospho-JAK1 consistent with its activation (Figure 3-5 C). These results indicate that TX02 directs a blockade of Tyk2 but not JAK1 activation induced by IFN, and that this prevents the downstream phosphorylation and activation of STAT1 and STAT2, but

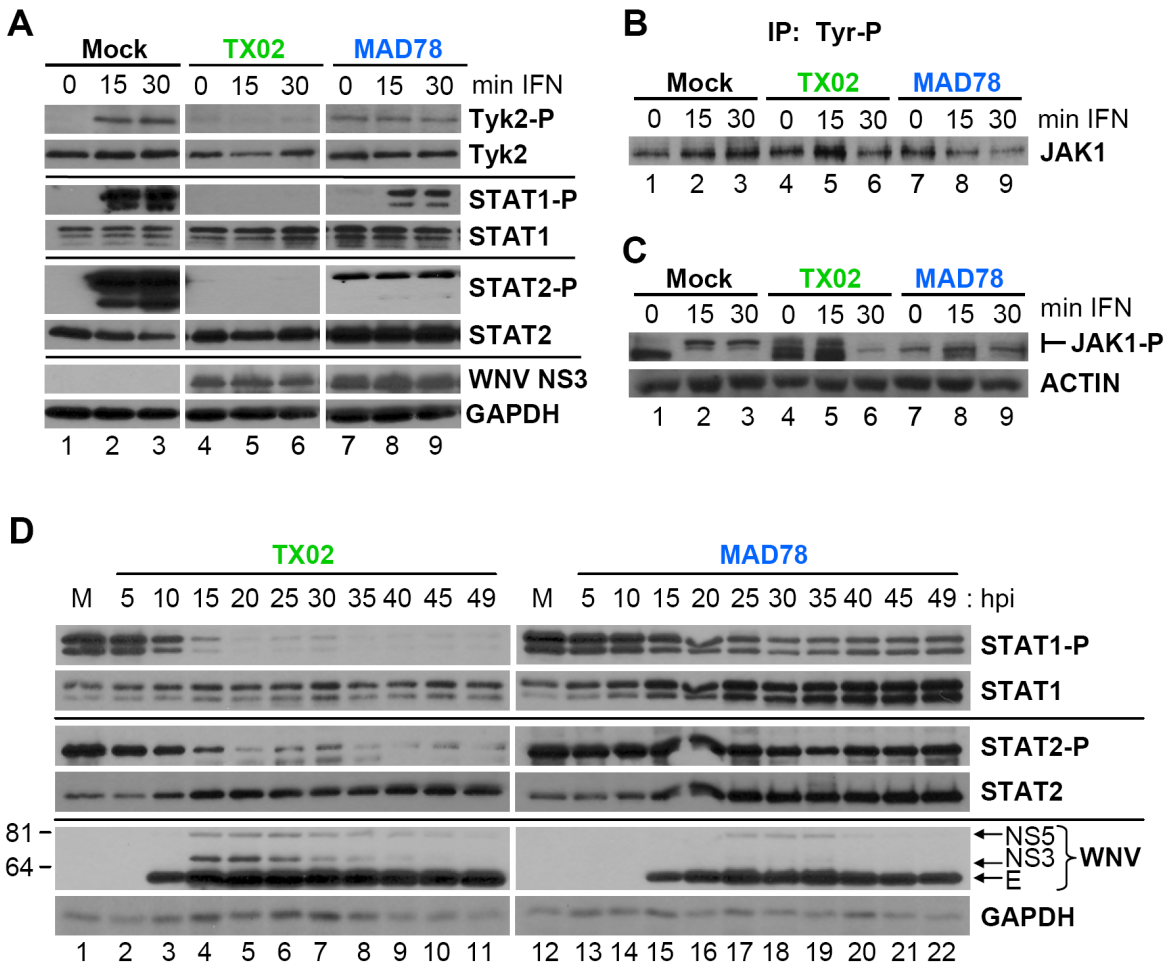

Figure 3-5. MAD78 regulation of JAK-STAT signaling is attenuated.
(A) A549 cells were mock-infected (lanes 1-3) or infected (MOI = 5) with WNV (TX02, lanes 4-6; MAD78, lanes 7-9). 24 hours post-infection cells were pulse-treated with 1000 U IFNα for 0, 15, or 30 minutes, and whole-cell lysates were collected and analyzed by immunoblot to determine WNV protein (NS3) abundance or the abundance of the active, tyrosine phosphorylated isoforms of Tyk2, STAT1 and STAT2. (B) A549 cells were mock-infected or infected with TX02 or MAD78. Cells were then treated with 1000 U IFNα for the times indicated. Proteins were immunoprecipitated from whole cell lysates using an anti-phosphotyrosine antibody followed by JAK1 immunoblot analysis. (C) A549 cells were infected with TX02 or MAD78 and treated with IFN as described for (A). Whole-cell lysates were analyzed for the presence of phospho-JAK1. (D) A549 cells were mock-infected (M; lanes 1 and 12) or infected (MOI = 5) with TX02 (lanes 2-11) or MAD78 (lanes 13-22). In 5 hour increments, cells were pulse-treated with 1000 U IFNα for 30 minutes, and whole-cell lysates were collected and analyzed by immunoblot to detect GAPDH, WNV, phosphotyrosine STAT isoforms and total STAT1 or STAT2 abundance. Bars at left indicate the positions of molecular mass (kilodalton) standards. Arrows at right denote the positions of the indicated WNV proteins.

MAD78 is attenuated in this function. To define the kinetics of this regulation, A549 cells were infected with TX02 or MAD78 and, at 5 hour increments, were treated with IFNα-2a for 30 minutes. Cell lysates were then collected and analyzed for abundance of phosphorylated isoforms of STAT1 and STAT2. IFN treatment of mock-infected control cells induced high level accumulation of the phosphotyrosine isoforms of STAT1 and STAT2 (Figure 3-5 D**,** lanes 1 & 12). In cells infected with MAD78, IFN responsiveness and the induction of STAT phosphorylation were preserved throughout the time course, though we did observe a partial suppression of phospho-STAT1 abundance that occurred in parallel with the accumulation of viral proteins. On the other hand, IFN treatment efficiently induced STAT phosphorylation during the first 5 hrs of infection with TX02, but this response was completely suppressed by 20 hours concomitant with the accumulation of viral proteins. This suggests that one or more viral proteins may influence IFN-induced JAK-STAT signaling during WNV infection, and that these regulatory properties are defective in MAD78.

Control of IFN α/β signaling is a determinant of WNV replication fitness in vitro and of virulence in vivo.

Since MAD78 is attenuated in its ability to inhibit JAK-STAT signaling, we sought to determine the relative fitness of MAD78 and TX02 and whether or not WNV growth is enhanced in the absence of functional IFN α/β signaling. Wild-type and congenic IFN α/β receptor null (IFNAR-/-) mouse embryo fibroblasts (MEFs) were infected with MAD78 or TX02 and viral growth was analyzed by Vero cell plaque assay of the resulting culture

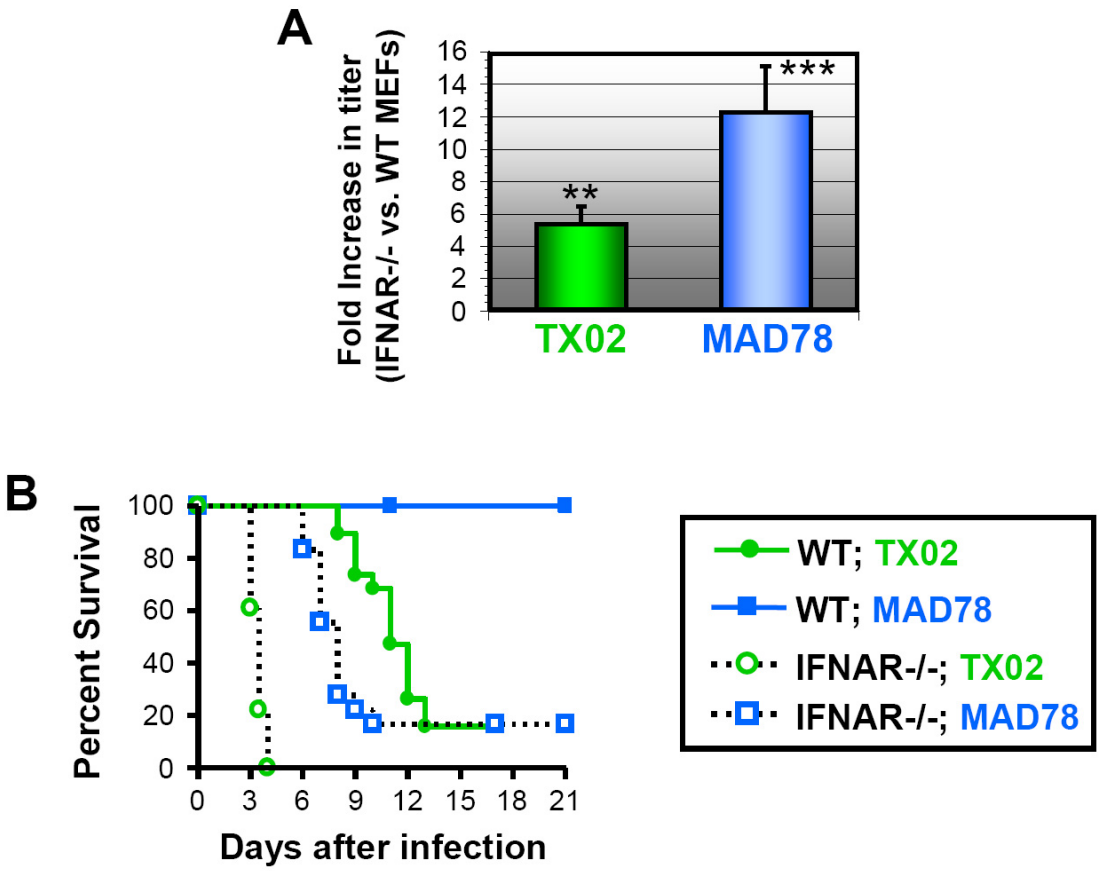

Figure 3-6. JAK-STAT signaling controls WNV replication and virulence.
(A) Wild-type and IFNAR-/- MEFs were infected with TX02 or MAD78, and viral supernatants were titered by plaque assay on Vero cells. Columns represent the fold increase in titer of viral supernatant from IFNAR-/- MEFs compared to WT MEFs. ** $P<0.01$, *** $P<0.0001$. (B) Groups of wild-type and congenic IFNAR-/- C57BL/6 mice were inoculated subcutaneously with 10^2 PFU of TX02 or MAD78 and monitored for survival. Results are plotted as percent survival for each group: WT, TX02 (●); WT, MAD78 (■); IFNAR-/-, TX02 (○); IFNAR-/-, MAD78 (□).

supernatants. MAD78 yields were significantly enhanced ($P < 0.0001$, t-test) 12-fold (Figure 3-6 A) in IFNAR-/- MEFs relative to infected wild-type MEFs. Interestingly, the yield of TX02 increased 5 fold ($P < 0.01$, t-test) in IFNAR-/- MEFs. This is not unexpected since the block to JAK-STAT activation is most likely not absolute as indicated by the very low level accumulation of phosphorylated STAT2 in the nuclear fraction of TX02-infected cells treated with high dose IFN (see Figure 3-4 B, lane 8). Similar results were obtained from WNV infection of IFNAR-deficient U5A cells, STAT2-deficient U6A cells and STAT1-deficient U3A cells (154,168,179) (B. Keller and M. Gale Jr., unpublished observations). These results define JAK-STAT signaling and IFN actions as important determinants of viral fitness, and they indicate that viral regulation of these processes can enhance WNV replication in vitro.

To determine if the differential control of IFN signaling associated with differential virulence of WNV, lethality studies of MAD78 or TX02 infection of wild-type and congenic IFNAR-/- C57BL/6 mice were performed (Figure 3-6 B). Subcutaneous infection of wild-type mice with 10^2 PFU of TX02 or MAD78 resulted in 86% and 0% lethality, respectively ($n = 19$, $P < 0.0001$), confirming the attenuated nature of the MAD78 strain. Importantly, virulence of MAD78 was unmasked in animals lacking IFNAR where an 84% mortality rate ($n = 18$; median time to death, 8 days) was observed. In parallel studies of TX02 infection, we observed a 100% mortality in the IFNAR-/- mice ($n = 18$, $P < 0.0001$, median time to death, 3.5 days). Because its virulence in vivo is largely restored in mice that lack responsiveness to IFN α/β, the relative absence of IFN antagonism by the MAD78 strain

explains, in part, its attenuated phenotype. Nonetheless, because the virulence of MAD78 was not completely restored, additional as yet uncharacterized genetic variations must also contribute to the pathogenicity of WNV.

DISCUSSION

This study examined the relationship between IFN, virus replication, and viral pathogenesis of distinct WNV isolates that differ widely in their distribution pattern, pathogenesis and epidemic behavior. Whereas MAD78 is a non-pathogenic lineage II strain with endemic transmission behavior (18,188), TX02 is a virulent strain of the current epidemic expansion of WNV lineage I in the Western Hemisphere. Our results provide evidence linking WNV virulence to control of the host cell JAK-STAT signaling pathway and overall resistance to the antiviral actions of IFN.

Sequence comparison of the complete open reading frames of MAD78 and TX02 to published complete WNV genomes confirmed the placement of MAD78 in lineage II (17,18,147,148). Compared to epidemic lineage I WNV strains, MAD78 exhibited slower growth in vitro and an avirulent phenotype in vivo when inoculated peripherally into inbred C57BL/6 mice. TX02 clustered with emergent lineage I strains currently circulating in North America, and more specifically, with a subgroup of strains localized to the southwestern U.S. In addition to sharing genotypic traits with other lineage I strains, TX02 also exhibited similar phenotypic growth profiles and protein expression in multiple human and mouse cell

lines. Furthermore, when inoculated intraperitoneally into outbred Swiss-Webster mice, TX02 was nearly identical to NY 385-99 in its lethality. In agreement with others (16,67), our data suggests very little genetic and phenotypic divergence has occurred among WNV strains circulating in North America. Thus, control of JAK-STAT signaling is likely a shared phenotype that confers virulence among emerging WNV strains while supporting virus replication and spread.

IFN α/β plays an integral role in intracellular innate immunity as well as in linking the innate immune response to cell-mediated defenses against virus infection. In order to replicate and spread, viruses direct processes to attenuate the initiation of IFN production and/or to antagonize the antiviral actions of IFN inside the host cell (127). The processes by which members of the *Flaviviridae* regulate host defense and IFN actions vary widely. For example, hepatitis C virus (HCV) and certain pestiviruses direct a blockade to IRF-3 activation, thus regulating the production of IFN by the infected cell (74,107,146,166). WNV avoids activating IRF-3 early in infection but triggers its activation and IFN production during the late stages of infection when viral proteins are abundant (75,76). Consistent with this, infection of cells with TX02 or MAD78 conferred IRF-3 activation and its triggering of the host response (B. Fredericksen, B. Keller, and M. Gale Jr., unpublished observations). In terms of TX02 infection, our results show that JAK-STAT activation by IFN becomes compromised in the host cell concomitant with viral protein accumulation. In contrast, JAK-STAT signaling and IFN responsiveness remained largely intact in cells infected with MAD78, suggesting that the ability of this virus to regulate IFN signaling

actions is defective. This held true even late in infection when MAD78 protein expression was at its maximum. The observations that 1) IFN treatment of cells prior to TX02 infection significantly reduced levels of virus production relative to IFN treatment after infection, and 2) the block in JAK-STAT signaling by TX02 occurred with the onset of viral protein expression, suggest that one or more WNV proteins may block IFN-induced signaling through the JAK-STAT pathway.

Results from several recent studies now indicate that flaviviruses, including WNV, direct processes to regulate JAK-STAT signaling and IFN actions in the infected cell. Studies of WNV and Kunjin virus replicons provide evidence that viral protein(s) can direct a blockade of JAK-STAT signaling (93,164,230)**,** and it is noteworthy that these replicons were derived from WNV strains that are virulent in vivo (17,131). Others have identified various flavivirus nonstructural (NS) proteins as possible regulators of JAK-STAT signaling. The NS2A through NS4B proteins of Kunjin virus have been shown to regulate STAT phosphorylation (164), while the NS5 protein of Langat virus (a tick-borne flavivirus) and the NS2A, NS4A and NS4B proteins from WNV and dengue virus can antagonize IFN action and regulate STAT1 phosphorylation when expressed alone or in trans during infection (24,118,193,194). While these results may highlight distinct mechanisms by which different strains of flaviviruses control IFN actions, they collectively demonstrate that pathogenic strains of WNV can evade IFN through properties of JAK-STAT regulation. Tyk2 is essential for STAT1 and STAT2 phosphorylation in response to IFN α/β receptor stimulation (232), and we found that infection of cells with TX02 resulted in a block of IFN-

induced Tyk2 tyrosine phosphorylation and abrogation of downstream STAT1 and STAT2 phosphorylation and nuclear translocation. Our data provide further support for a model in which one or more WNV NS proteins direct a blockade of IFN-induced Tyk2 activation and downstream STAT phosphorylation to attenuate the expression of ISGs that would otherwise control infection (93), thus allowing unimpeded virus replication and spread.

We have characterized MAD78, the first WNV strain shown to be incapable of regulating IFN-induced JAK-STAT signaling in infected cells. Absence of JAK-STAT regulation associated with a lack of virulence during MAD78 infection of wild-type animals. MAD78 also exhibited lower overall fitness when compared to TX02. This attenuated MAD78 replication was augmented in vitro in cells lacking a functional IFN α/β receptor, and a virulent phenotype was unmasked in vivo upon infection of IFNAR-/- mice. Taken together, these results imply that the normally avirulent phenotype of MAD78 (3, 23, 35) is due to overall reduced replication fitness and an inability of viral proteins to direct an effective JAK-STAT signaling blockade within the host cell. The reduced replication fitness of MAD78 may play a part in the IFN sensitivity of this strain early in infection, but no significant differences in infectious particle production were observed until late in infection (see Figure 3-3 A). Furthermore, when MAD78 protein expression was at its maximum, JAK-STAT signaling remained largely intact (Figure 3-5 C) in contrast to that seen with TX02. Lineage II WNV strains, including MAD78, differ from the emergent lineage I strains by approximately 22% at the nucleotide level but only by 7% at the amino acid level of encoded proteins (B. Keller and M. Gale Jr., unpublished observations and (23,148), and

these variations are scattered throughout the polyprotein. Of note is a Ser→Pro substitution at residue 156 of the MAD78 E protein that abolishes the *N*-linked glycosylation motif (N-Y-T/S). Recently, Hanna et al. reported that WNV subviral particles lacking the E glycosylation site had 10-fold lower viral particle release compared to strains with an intact N-Y-T/S motif (96). Expanding on this theme, a report by Borisevich et al. demonstrated that WNV strains containing a functional E glycosylation motif exhibited approximately 1.5 log increases in peak viral titers, irrespective of the origin of the NS genes (lineage I vs. lineage II) (30). However, the effect of E glycosylation on virulence in vivo was minimal compared to the effect conferred by NS genes from different WNV strains. Results from these reports may explain the attenuated growth of MAD78 in vitro compared to strains that have an intact E glycosylation motif. Additionally, these studies further support our hypothesis that viral regulation of JAK-STAT signaling is a major determinant of WNV virulence in vivo. Since MAD78 appears to be attenuated at both the level of viral fitness and JAK-STAT regulation, it is likely that amino acid changes at multiple sites within the NS proteins account for its attenuated properties. Importantly, IFN imparts control of WNV virulence by limiting tissue tropism and the systemic dissemination of the virus while enhancing neuronal survival (222). Though the molecular mechanisms of these actions are not known, they underscore the importance of the IFN response as the body's first line of defense against WNV infection and serve to define the processes and viral factors that determine WNV virulence and infection outcome.

Viral phenotypic traits that induce IFN and host defense processes could serve as a basis for attenuated vaccine approaches to confer protection against WNV infection in naïve populations. Hall et al. showed an attenuated strain of Kunjin virus was able to protect mice against lethal challenge with WNV (94). In this case the attenuated viral phenotype was attributed to a single point mutation in the NS1 protein, and it is possible that attenuation could be mediated through loss of JAK-STAT signaling control. Such an approach could yield vaccine strains that replicate at levels controlled by IFN α/β host defenses but that stimulate protective immunity against the virulence and neuroinvasiveness typical of current emergent WNV strains. The viral and host determinants that have allowed certain WNV strains to cause human epidemics in the recent past are largely unknown. It was reported that Toll-like receptor 3 and subsequent tumor necrosis factor-α production is required for WNV entry into the brain (269). Additionally, several groups have reported on the role of envelope (E) protein glycosylation in the neuroinvasiveness of WNV (19,236). As mentioned earlier, MAD78 contains a Ser→Pro substitution in the E protein *N*-linked glycosylation motif. However, MAD78 retains a neuroinvasive phenotype but only in the absence of intact IFN α/β signaling. While E glycosylation may play a role in particle assembly and infectivity (96), epitope masking, changing affinities for certain cellular receptors, or some other undefined mechanism, other viral and/or host determinants, including the ability to control the IFN system, likely contribute to the enhanced virulence of epidemic WNV. The attenuated phenotype of MAD78 may provide a starting point for exploiting the link between viral stimulation of innate host defenses and immunity to infection.

CHAPTER FOUR
Viral and cellular regulation of cytokine signaling during WNV infection

INTRODUCTION

It is now well established that the *Flaviviridae* regulate IFN signaling through JAK-STAT (24,93,106,118,130,160,161,164,193,194). The mechanisms underlying this regulation, however, are still not understood, and there remains considerable debate as to the role specific viral proteins play in this antagonism. Flavivirus proteins implicated in attenuating IFN signaling include NS2A, NS2B3, NS4A and NS4B from WNV (164,193); NS2A, NS4A and NS4B from DENV (194); NS5 from JEV (160); and NS5 from LGTV (24). Clearly, more work is needed to decipher the various roles of flaviviral proteins in this process.

In studies of related flaviviruses, researchers have suggested potential mechanisms for the observed IFN signaling block that could be due to viral and/or cellular processes. In JEV-infected mosquito cell lines, tyrosine phosphatase activity was shown to be important for the block in phosphorylation of newly identified mosquito STATs during JEV infection (159). A more recent study of JEV correlated this tyrosine phosphatase activity with the ability of NS5 to antagonize IFN signaling (160). In contrast to JEV NS5, LGTV NS5 was shown to bind IFNAR leading to a block to IFN signaling (24). Whether the NS5 signal block is due to steric interference by NS5 itself, NS5 enzymatic activity, recruitment of other factors by NS5 to the receptor complex, or a combination thereof remains to be determined. Also, it is currently not clear why NS5, a viral RNA-dependent RNA polymerase, would

localize to the cell membrane since flavivirus replication occurs on perinuclear membrane-bound vesicles near the endoplasmic reticulum/Golgi complex (170,171,272,273). Another proposed mechanism for the inhibition of IFN signaling by flaviviruses involves the degradation of STAT2 during DENV infection (118), although it is unclear what degradation pathway(s) are involved. The processes described here could be due cellular mechanisms since flaviviruses are not currently thought to possess activities leading to dephosphorylation or degradation of proteins.

As indicated by the studies described above, cellular processes, in addition to viral protein expression, may be important in regulating JAK-STAT signaling during flaviviral infection. IFN signaling is critical for inducing an antiviral and proinflammatory response in infected cells and neighboring tissue. As such, this signaling cascade must be tightly regulated by the cell to prevent excessive activation and subsequent immunopathogenesis. Several mechanisms are encoded by the cell to regulate JAK-STAT signaling at different steps in the pathway. In the nucleus, STAT transcriptional activity is regulated by the protein inhibitor of activated STAT (PIAS) family of proteins. PIAS proteins are thought to block STAT activity by preventing DNA binding, recruiting corepressors such as histone deacetylases, promoting sumoylation of STATs through the SUMO-E3 ligase activity of PIAS, or sequestering activated STATs in specialized nuclear compartments (239).

Cytoplasmic regulators of IFN signaling include the SH2-containing protein tyrosine phosphatases, SHP1 and SHP2. The SH2 domains of these proteins bind phospho-tyrosines

on activated receptors, JAKs and STATs resulting in the activation of phosphatase activity and subsequent dephosphorylation of signaling components (264). Dephosphorylation of receptors and JAKs not only blocks their activity but also blocks recruitment of STAT proteins to the receptor complex.

Another family of cytoplasmic regulators includes the suppressors of cytokine signaling (SOCS) proteins which are, as their name suggests, negative regulators of JAK-STAT signaling in response to a wide array of cytokines (4,111,141). Important for IFN signaling are SOCS1 and SOCS3, two closely related members of the SOCS family of proteins. SOCS1 binds to activated JAKs via its central SH2 domain (280). Such binding allows for the insertion of the SOCS1 kinase inhibitory region (KIR) into the JAK activation loop, precluding downstream phosphorylation events (197,280). SOCS3, on the other hand, binds activated receptors thereby bringing its KIR domain into close proximity to the JAK proteins (196). Similar to SOCS1, the SOCS3 KIR occludes the JAK catalytic pocket preventing recruitment and activation of STAT proteins (141). Both SOCS1 and SOCS3 also contain C-terminal SOCS box (103) motifs that have been shown to interact with the elongin BC complex (283). Elongin BC is known to bind to cullin-2 resulting in the formation of an E3 ubiquitin ligase. Therefore, it is postulated that SOCS proteins may target signaling components to the proteasome for degradation in addition to directly inhibiting JAK catalytic activity.

In this chapter we demonstrate that, although WNV proteins play a role in attenuating IFN signaling, expression of individual WNV proteins is not sufficient to explain the IFN resistance phenotype observed during active WNV infection. Through functional genomics, qRT-PCR and immunoblot studies we show that SOCS1 and SOCS3 are upregulated during WNV infection, and levels of induced SOCS expression correlate with a stronger or weaker antagonism of JAK-STAT signaling by viruses of different virulence phenotypes. We further demonstrate that regulation of WNV-induced SOCS expression is complex and occurs through multiple pathways including the IFN, mitogen activated protein kinase (MAPK) and phosphatidylinositol 3-kinase (PI3K) signaling networks. The expression of SOCS proteins during WNV infection suggested that other JAK-STAT pathways, in addition to IFN, may also be inhibited. Consistent with this hypothesis we found that signaling by IFNβ, multiple subtypes of IFNα, IFNγ and IL-6 was inhibited by WNV infection. We propose a model in which viral proteins act in concert with cellular inhibitors to globally regulate cytokine signaling through JAK-STAT. Results of this regulation could potentially affect not only the establishment of an intracellular antiviral response but also the development of a proper adaptive immune response as both IFN and IL-6 are critical to the immunological switch from innate immunity to an adaptive response (119,150-152,261).

RESULTS

Differential activation of IFN signaling between virulent and avirulent WNV strains

We previously reported that a virulent WNV strain (TX02) was more effective at blocking JAK-STAT than the avirulent MAD78 strain. To quantitate the relative amount of IFN signaling between pathogenic and nonpathogenic WNV strains, Huh7 cells were transfected with an ISRE promoter reporter plasmid driving the expression of a firefly luciferase gene and a transfection control plasmid encoding Renilla luciferase under the control of a CMV promoter 24 h prior to infection with TX02 or MAD78 (MOI = 1). Twenty-four h after infection, cells were treated with IFNα (1000 U/ml) or media alone for 6 h at which time lysates were collected and analyzed for luciferase activity. In the absence of exogenous IFN treatment, the virulent TX02 strain induced a much lower (43 relative

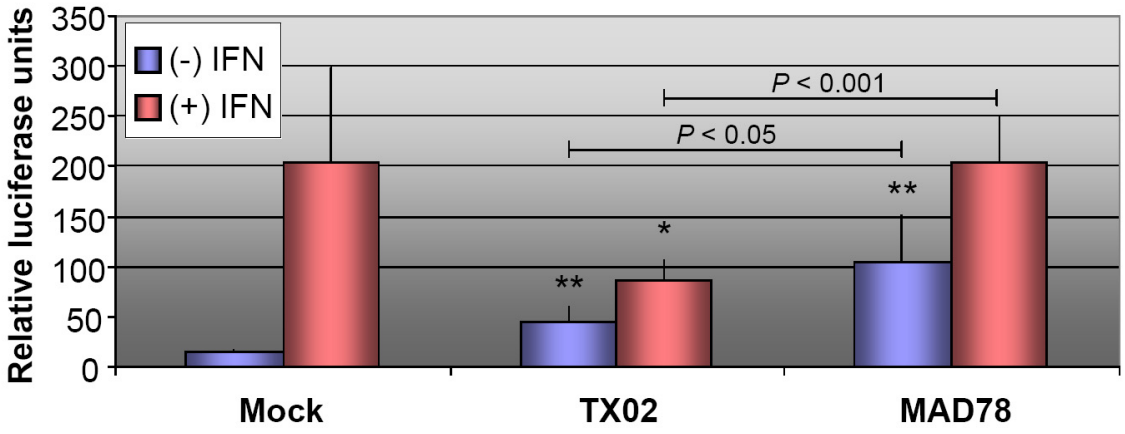

Figure 4-1. Differential activation of an ISRE reporter in response to TX02 or MAD78. Huh7 cells transfected with pISRE-TA-luc and pRL-CMV were infected with TX02 or MAD78 for 24 h at which time luciferase activity was measured. TX02 infection resulted in a 3-fold activation of the ISRE compared to a 7-fold increase with MAD78. IFN treatment of mock-infected or MAD78-infected cells resulted in nearly identical stimulation of the ISRE reporter whereas TX02 infection inhibited activation of the ISRE by 57%. Asterisks indicate significance relative to Mock-infected controls. *, $P \leq 0.05$; **, $P \leq 0.001$.

luciferase units [RLU]) activation of the ISRE promoter than did MAD78 (103 RLU) when compared to uninfected controls (14 RLU; Figure 4-1). The addition of IFNα for 6 h induced ISRE activation in the MAD78-infected cells to nearly identical levels as uninfected controls (203 RLU), whereas ISRE activation in TX02-infected cells was only 40% (87 RLU) of that seen in controls. Interestingly, in infected cells when ISRE activation in response to IFN was normalized to ISRE activation in the absence of exogenous IFN, induction was increased only 2-fold for both TX02 (43 to 87 arbitrary units) and MAD78 (103 to 203 arbitrary units). Thus, although each virus limits exogenous IFN signaling to 2-fold more than basal, MAD78 faces a greater absolute IFN response than does TX02.

Antagonism of JAK-STAT signaling by WNV gene products

Since there were clear differences in the absolute activation of the ISRE promoter in response to IFN signaling between TX02 and MAD78 but no difference in the relative fold activation between strains, we decided to compare individual viral proteins for their ability to attenuate JAK-STAT signaling. All predicted genes from TX02 and MAD78 were cloned into the mammalian expression vector pCAGGS-HA-COOH (194), yielding C-terminal Hemagglutinin-tagged viral proteins. Additionally, genomic elements encoding precursors to mature viral proteins (e.g. the C-terminal membrane anchor of C, N-terminal part of prM and the NS2B3 polyprotein) were also included in the expression plasmid library. Plasmids were tested for their ability to block IFNα signaling to an ISRE promoter (Figure 4-2). Using a previously described DENV NS4B construct (194) as the cutoff point for minimum regulatory activity (28% reduction, $P \leq 0.05$), our results demonstrate that

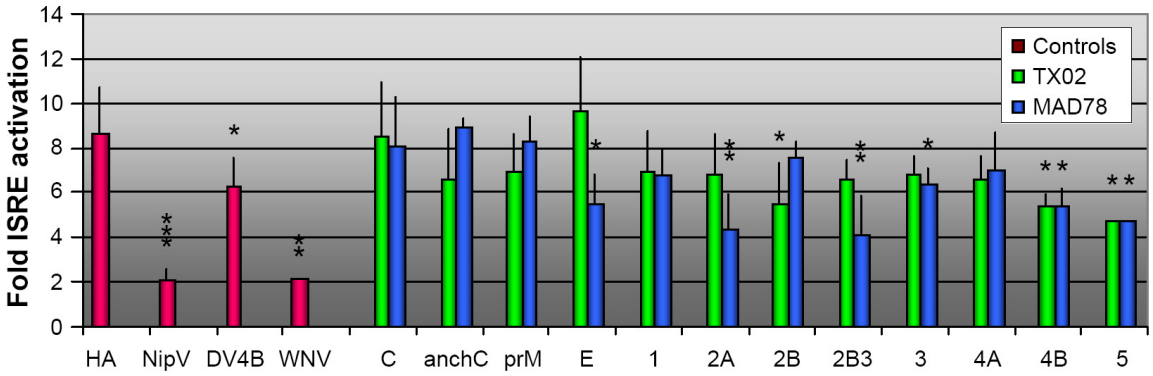

Figure 4-2. WNV proteins partially suppress IFN signaling.
Huh7 cells were transfected with pISRE-TA-luc and the indicated control plasmid or pCAGGS WNV expression plasmid for 24 h. Cells were then stimulated with IFNα for 6 h, and luciferase acitivity was measured. Bars represent fold activation in response to IFN treatment compared to untreated transfected controls. DENV NS4B was previously reported to block IFN signaling and was therefore used as the minimal inhibitory setpoint in this assay. WNV represents TX02 infection in the presence of the pISRE-TA-luc reporter followed by 6 h IFN treatment. *, $P \leq 0.05$; **, $P \leq 0.001$; ***, $P \leq 0.0001$.

NS4B from both TX02 and MAD78 functions equally (38% reduction, $P \leq 0.05$) to block IFN signaling. This data is consistent with other reports on WNV and DENV (164,193). NS5 from both strains also blocked signaling in our assay (TX02 NS5, 44% reduction, $P \leq 0.01$; MAD78 NS5, 46% reduction, $P \leq 0.01$) as was previously reported for NS5 of JEV and LGTV (24,160). NS4A from both TX02 (24% reduction) and MAD78 (20% reduction) exhibited a trend toward inhibiting signaling, but this was not significant. Since TX02 is more efficient at antagonizing the IFN response in infected cells (130), we predicted that perhaps a TX02 gene product would be clearly more effective than its MAD78 counterpart. This was not the case, with only the anchored form of C (anchC) (24% reduction, $P \leq 0.05$), prM (21% reduction, $P = 0.06$) and NS2B (37% reduction, $P \leq 0.01$) from TX02 exhibiting a stronger inhibitory effect than the respective MAD78 proteins. Surprisingly, NS2B3 (53% reduction, $P \leq 0.001$), NS2A (49% reduction, $P \leq 0.001$) and E (38% reduction, $P \leq 0.01$)

from MAD78 were much better at antagonizing JAK-STAT signaling than the respective TX02 proteins. This effect was not due to differential protein expression between the MAD78 and TX02 constructs as the corresponding plasmids were expressed at similar levels (data now shown). NS2B3 (from Kunjin) and NS2A (from Kunjin and DENV) were previously shown to exhibit functional activity in other types of reporter assays (164,194), but we cannot at this time explain why the TX02 versions of these proteins did not block signaling to the same extent as the MAD78 proteins. Although multiple WNV proteins are capable of attenuating JAK-STAT signaling to some degree, there does not appear to be a single viral protein responsible for the dramatic signaling shut off seen during WNV infection, especially when compared to the effects seen with our positive control, the V protein from Nipah virus. However, WNV infection blocks ISRE reporter activity (76% reduction, $P \leq 0.001$) in response to IFNα to the same degree as transfection of Nipah V (76% reduction, $P \leq 0.0001$) (Figure 4-2) indicating that mechanisms other than individual WNV protein expression may be involved in shutting down the IFN response.

Suppressors of cytokine signaling are upregulated during WNV infection

The IFN system is critical for inducing a broad array of ISGs leading to the establishment of an antiviral state within the infected cell and a proinflammatory environment in the surrounding tissue (39,127). As such, the IFN system is subject to regulation at multiple steps by the host cell to prevent hyperactivation of the response and subsequent autoinflammatory conditions. To understand whether host regulatory mechanisms are involved in the resistance of WNV to IFN signaling we performed a

functional genomics analysis of A549 cells infected with TX02 or MAD78 compared to uninfected control cells. TX02 upregulated 1473 and 1630 genes more than 2-fold ($P \leq 0.01$) at 24 and 48 hpi, respectively. MAD78, in contrast, upregulated only 501 and 564 genes at these same time points. Of the genes upregulated at 24 hpi, 365 were common to both strains, and this number increased to 401 commonly regulated genes by 48 hpi. Of interest to our current study, we noted that TX02 induced SOCS1 (2.69 fold at 24 h; 2.94 fold at 48 h; $P \leq 0.01$) and SOCS3 (19.59 fold at 24 h; 8.21 fold at 48 h; $P \leq 0.01$) (Figure 4-3 A). Expression of these same genes was only increased 2.09 and 2.42 fold (SOCS1) and 5.18 and 2.95 fold (SOCS3) at 24 and 48 h, respectively, by MAD78 infection. We confirmed the microarray results with qRT-PCR and Western blot analysis (Figure 4-3 B and C). A549 cells (Figure 4-3 B) were infected with TX02 or MAD78 and total RNA was collected at the indicated times. At 24 hpi, TX02 induced an approximate 5-fold increase in SOCS1 and SOCS3 mRNA levels. In contrast, accumulation of MAD78-induced SOCS1 and SOCS3 mRNA was not observed until 48 hpi. The discrepancies detected between the microarray analysis and the qRT-PCR are most likely due to the different sensitivities of each method. To detect SOCS protein expression, A549 cells were infected with TX02 for 48 h. Because SOCS proteins have an extremely short half-life due to their targeting to the proteasome, A549 cells were treated with the proteasome inhibitor MG132 for 8 h prior to collection of TX02-infected cell lysates. This allowed us to confirm that expression of SOCS proteins was indeed enhanced during WNV infection (Figure 4-3 C). We next tested whether expression of individual viral proteins could induce SOCS expression. Huh7 cells were transfected with

A

	Fold change in expression of each gene in response to TX02 or MAD78 at the indicated times post-infection			
	24 hpi		48 hpi	
	TX02	MAD78	TX02	MAD78
SOCS1	2.69	2.09	2.94	2.42
SOCS3	19.59	5.18	8.21	2.95

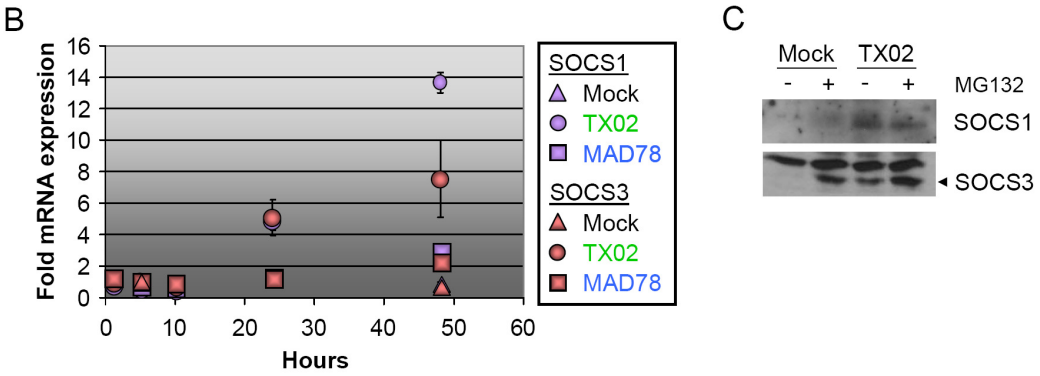

Figure 4-3. WNV infection induces SOCS1 and SOCS3 expression.
(A) Microarray analysis was performed on A549 cells infected with TX02 or MAD78 for 24 or 48 h. SOCS1 and SOCS3 were identified as being upregulated at least 2-fold ($P \leq 0.01$) in response to both strains. SOCS1 expression continues to rise over the time-course of infection, whereas SOCS3 expression is more transient. (B) Microarray results were confirmed by qRT-PCR analysis of SOCS1 and SOCS3 mRNA expression in A549 cells infected with TX02 or MAD78. Results are plotted as fold increase in mRNA compared to uninfected control at 1 hpi. (C) Levels of SOCS1 and SOCS3 protein expression A549 cells infected with TX02 was determined. Forty-eight h after infection, cells were left untreated or were treated with MG132 for 8 h. Lysates were analyzed by SDS-PAGE and immunoblotting for SOCS1 and SOCS3. Levels of a nonspecific band detected just above SOCS3 indicated equal loading in all lanes.

TX02 expression plasmids and assayed for the induction of SOCS mRNA 24 h later by qRT-PCR (Figure 4-4). Expression of individual TX02 proteins failed to significantly upregulate SOCS mRNA suggesting that some other aspect of the viral life cycle may be responsible for the induction of SOCS genes expression.

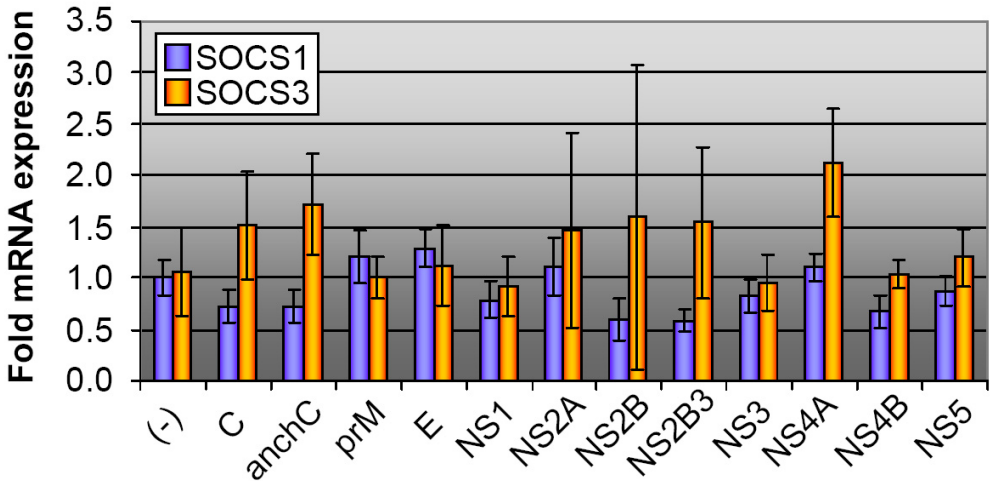

Figure 4-4. WNV proteins do not increase SOCS1 or SOCS3 expression. Huh7 cells were transfected with pISRE-TA-luc, pRL-CMV, and pCAGGS-TX02 or pCAGGS-MAD78 expression plasmids for 24 h followed by a 6 h IFN treatment and measurement of luciferase activity. Bars indicate fold induction of ISRE-luc activity normalized to the *Renilla* luciferase transfection control. None of the results were statistically significant by the t-test.

SOCS1 and SOCS3 promoters possess a variety of putative transcription factor binding sites

Many different cellular signaling pathways are capable of inducing SOCS proteins in response to various stimuli (4,29). We therefore sought to determine which pathways were responsible for SOCS induction during WNV infection. Using a transcription factor binding site predictor program, TFSEARCH (http://www.cbrc.jp/research/db/ TFSEARCH.html), the genomic region encompassing 1000 nucleotides upstream from the predicted TATA box of SOCS1 or SOCS3 was analyzed for potential transcription factor binding sites

GGAGCAGTAGGAGGGGGAAATCTATGAGGAAGGGGTCGGGGGAGAGGAGGGCTAGGAAA

CCAGGTTTGGGGATTCATCACGTCTGAGAATGCACCATTTTTTCACTGGGCTCCAATTTGAT

GTCGTCCAGCTGCACCTCTCCCCAAAATGAAGACGGGGAAGGCGAGATCCAGGTCCAGAG

CTCCCAATCTGCAAGCCATTGCAAATCCCAGCCCCTCCCCAGCCTCAGTTTCTTCCGCAGC

CGGGTAGTGGGAGCGCAGGGAGGGCAGTCGAGGCCACCAGGGACCTTGCCCGGCCCCG

CCCAGTTTCCGAGGAACTGGGCCGGGGTGGAGGCGCCCGCGCCGCCAGGGGTTCCTCTG

AAGCCTGTGGTCAGGCCGCCGCTTCCCGGGAAGCCCGAGCCAAGACCAGAGACCGCGGC

CGGCCGGGGCTTCGGGACAGCAGGGCGGGCGACTGAGGGCGTCGACGGCGGGTGGAGC

AGGGGCTAGGAGGGGGTCTACGGGTGGGGTCAGGCTCAGGGTTGGGGACACCTTCTGTG

GCCTCCTAGGGGGATCTGGCTGCAGGGGAGGAGAGGACAGGGCTCTGCCCCCGGCGGGT

GTGGAGACAGCTGGGGCGGAGGAGGGTGTGTCAGGGCGCGTCCCAAGAGGGCCTGGCG

GCAGAAAGTGGAACCCGAGGTAGCGGGGCAAAATCGGGGTCGCCAAGTCCGAAGGAGGG

GTCCGAGAAGTGGCCGGAAGGCGCAGGGTCGGGGCCAGAGCCCCTCGAGAGGCGGGTG

CTGGGGCAGGTGCGAACAGGCGGGCAGAGGGCCCCGCGGGAGGGTCCAGAAGAGAGGG

AAACAGGGCCGAAGCGGTCCTCGCCGGACGCCACCGCGGAAAGAGAAACCAAAAGTGGA

GCTGGGGGCGGGGCCGGCAGGGGGCGGGGCCTCCCGCCGTCGCCAGCCCCGCCTCCGA

GCCGGTTTAAAAGACTGGCGCAGGGGCGGGCGCCGAACAGAGCGAGCTGCGGCCGTGGC

AGCTGCACGGCT. . .

Figure 4-5. SOCS1 promoter analysis.
Genomic sequence encompassing 1000 nucleotides upstream of the putative SOCS1 TATA box was analyzed for putative transcription factor binding sites with TFSEARCH using a threshold value of 85.0. Potential binding sites for transcription factors activated in response to various signaling pathways are indicated by colored underlining (green, IFN; orange, p38 MAPK; blue, MKK1/2-ERK; purple, PI3K). The putative TATA sequence is boxed, and the arrow indicates the start of the SOCS1 gene.

(SOCS1, Figure 4-5; SOCS3, data not shown). Over 90 putative binding sites were identified with a threshold score of 85.0 or higher. Many of these putative binding sites were predicted to be targeted by transcription factors activated downstream of the IFN, p38 MAPK, MKK1/2-ERK and PI3K signaling pathways.

WNV induces SOCS expression through multiple signaling pathways

To begin to address which of the implicated signaling pathways were responsible for activating SOCS1 and SOCS3 during WNV infection, U5A (IFNAR2 mutant, (168)) and U3A (STAT1 mutant, (179)) cells were infected with TX02 (MOI = 5), and SOCS1 and SOCS3 expression were determined by qRT-PCR at the indicated times post-infection. In these cells, both genes were activated in response to WNV infection in the absence of functional IFN signaling (Figure 4-6). These results indicate that although IFN appears to

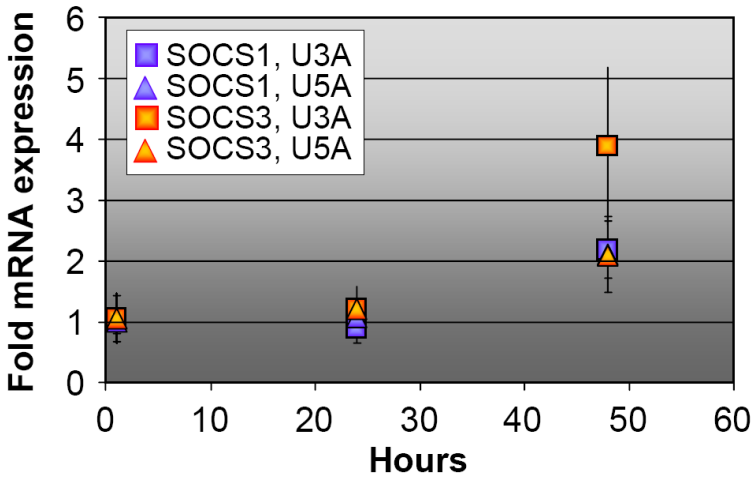

Figure 4-6. WNV induces SOCS1 and SOCS3 expression in the absence of functional IFN signaling. U3A and U5A cells were infected with TX02 (MOI=5) and levels of SOCS1 and SOCS3 mRNA were measured at the indicated times post-infection by qRT-PCR. Values were normalized to GAPDH and are graphed relative to the 1 hpi timepoint.

play a critical role in SOCS expression, other IFN-independent and STAT1-independent pathways also activate the SOCS promoter during WNV infection.

To confirm the results observed with the U3A and U5A cells, A549 cells were infected with TX02 for 1 h. Following infection, the virus was replaced with complete DMEM or with complete DMEM containing anti-IFNAR neutralizing antibodies for 23 h, after which SOCS1 and SOCS3 mRNA levels were determined by qRT-PCR (Figure 4-7 A). Treatment of WNV-infected A549 cells with neutralizing antibodies against IFNAR reduced virus induction of SOCS1 and SOCS3 expression.

To examine STAT1-independent (and therefore IFN-independent) induction of SOCS1 and SOCS3, U3A cells were infected with TX02 (MOI = 1) for 24 h at which time chemical inhibitors (10 μM) or DMSO were added for another 8 h. The inhibitors included SB203580 which selectively blocks p38 MAPK activity by competing with ATP for binding; PD98059 which inhibits the phosphorylation of inactive MKK1 by Raf but does not block downstream MKK1 activity; U0126 which inhibits both the active and inactive forms of MKK1 and MKK2; and LY249002 which is a selective inhibitor of PI3K. Total RNA was collected, and SOCS1 and SOCS3 expression were determined by qRT-PCR (Figure 4-7 B). All of the inhibitors tested were able to significantly block WNV-induced expression of SOCS3 (SB203580, 53%, $P < 0.05$; PD98059, 72%, $P < 0.01$; U0126, 79%, $P < 0.01$; LY294002, 56%, $P < 0.05$). SOCS1 expression was inhibited by PD98059 (56%, $P < 0.01$), LY294002 (33%, $P < 0.01$) and, to a lesser extent, U0126 (21%, $P = 0.08$) during WNV

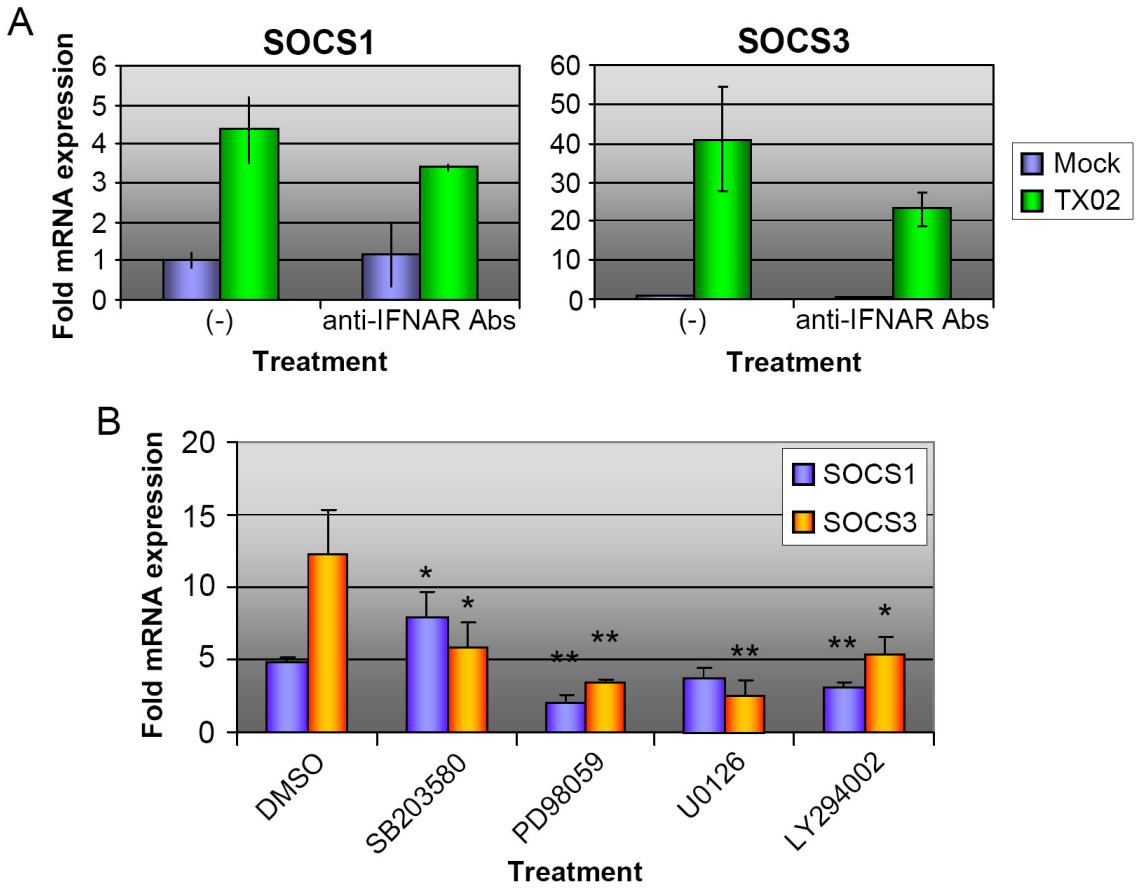

Figure 4-7. Multiple signaling pathways contribute to WNV-induced SOCS expression. (A) A549 cells were infected with TX02. Virus was replaced after 1 h with complete DMEM alone or with complete DMEM containing anti-IFNAR neutralizing antibodies for 23 h. Relative levels of SOCS1 and SOCS3 mRNA were determined by qRT-PCR. Values were normalized to GAPDH and plotted as fold increase over untreated, mock-infected samples. (B) U3A cells were infected with TX02 for 46 h and treated with 10 μM of the indicated inhibitors for an additional 8 h. SOCS1 and SOCS3 mRNA expression was determined by qRT-PCR. Values for each infected, treated sample were normalized to the respective uninfected, treated control and plotted as fold mRNA increase. *, $P \leq 0.05$; **, $P \leq 0.01$.

infection. Taken together, these results indicate that the MKK1/2 and PI3K pathways are involved in upregulation of SOCS expression independently of STAT1 in WNV-infected cells. In contrast to SOCS3, SB203580 treatment of WNV-infected U3A cells enhanced SOCS1 expression (65% increase, $P < 0.05$) suggesting that p38 may negatively regulate SOCS1 expression but positively regulate transcription of SOCS3 during WNV infection.

Inhibition of SOCS activity partially relieves the WNV IFN block

SOCS1 and SOCS3 inhibit JAK-STAT signaling in response to various stimuli including IFNα/β. The induction of SOCS1 and SOCS3 expression during WNV infection suggested that one or both of these proteins may be involved in virus-induced attenuation of IFN signaling. To test this idea, Huh7 cells were transfected with an ISRE-luciferase reporter construct along with plasmids encoding dominant negative (DN) forms of SOCS1 (SOCS1 DN, (95)), SOCS3 (SOCS3 DN, (225)) or both. The next day, cells were infected with TX02 for 24 h, treated with IFN for 6 h and analyzed for luciferase activity (Figure 4-8). Expression of SOCS1 DN partially restored IFN signaling in the context of WNV infection. This included not only JAK-STAT signaling in response to exogenously added IFN, but also basal signaling by endogenously produced IFN. The SOCS3 DN construct as well as a combination of the SOCS1 DN and SOCS3 DN constructs did not have an effect on the WNV-induced IFN signaling block. In data not shown, the SOCS3 DN construct did not completely restore IFN signaling in mock-infected cells treated with IFN indicating that this construct may not be fully DN. These results are consistent with a report from Sasaki and colleagues who first described the SOCS3 DN construct used in these studies (225). These

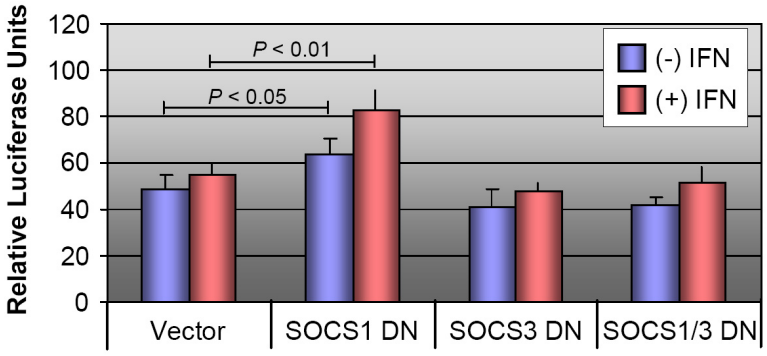

Figure 4-8. A dominant negative form of SOCS1 partially relieves the WNV JAK-STAT block. Huh7 cells transfected with pISRE-TA-luc, pRL-CMV and DN forms of SOCS1, SOCS3 or both were infected with TX02 for 24 h. Cells were then treated with IFNα for 6 h and assayed for luciferase activity. Bars indicate relative luciferase units (RLU) of untreated and IFN-treated samples. SOCS1 restored IFN signaling to the ISRE promoter both basally and in the context of exogenous IFN treatment.

results may also explain why the combination of SOCS1 DN and SOCS3 DN failed to restore signaling to the same degree as SOCS1 DN alone. Studies are currently underway to identify and test other DN forms of SOCS3 for their ability to restore signaling.

To begin to understand the importance of SOCS proteins in the WNV block to IFN signaling, siRNA-mediated knockdown of SOCS1 and SOCS3 expression was undertaken. It was hypothesized that reduction of SOCS 1 and SOCS3 levels might restore host innate antiviral signaling resulting in lower viral levels. A549 cells were transfected with a cocktail containing siRNA directed against SOCS1 and SOCS3 and then infected with TX02 or MAD78. Forty-eight h after infection viral supernatants and total cellular RNA and protein were collected and analyzed for effects on viral replication. Efficient reduction in SOCS1 and SOCS3 levels were confirmed by qRT-PCR (Figure 4-9 A). siRNA knockdown of SOCS1 and SOCS3 resulted in drastic reductions in TX02 and MAD78 protein levels by

immunoblot (Figure 4-9 B). Furthermore, TX02 titers on cells treated with SOCS1/3 siRNA were nearly 3-fold lower than sham-treated cells (Figure 4-9 C). MAD78 titers were below the level of detection (data not shown). These results suggest that reduction of SOCS1 and SOCS3 levels partially restores the cell's innate ability to respond to WNV infection.

WNV regulates other cytokine signaling pathways

SOCS proteins are involved in the negative regulation of a number of cellular signaling pathways involving JAKs and STATs (4,102,111,141). Since SOCS protein expression was increased during WNV infection, we sought to determine whether signaling by cytokines other than IFNα-2a was also being attenuated. A549 cells were infected with TX02 (MOI = 1 or 5) for 24 hours. The cells were then stimulated with IFNβ (1000 U/ml), IFNγ (6000 pg/ml), pegylated IFNα-2b (PEG-INTRON; 500 U/ml), consensus IFN (CIFN, IFN alfacon-1; 1600 U/ml), or IL-6 (50 ng/ml) for 30 min and cell lysates were analyzed for phosphorylated JAK-STAT components by immunoblot (Figure 4-10). For the IFNs, the amounts used were 20 times greater than their respective serum maximum concentrations. WNV prevented activation of JAK-STAT in response to all IFNs tested (Figure 4-10 A) as well as IL-6 activation of STAT3 (Figure 4-10 B). Regulation of cytokine signaling was not specific to human cells as identical regulation in MEFs was also observed (data not shown). These results demonstrate that WNV regulates multiple cytokine signaling networks that utilize JAK-STAT in human and murine systems. The consequence of such regulation is currently an area of active investigation.

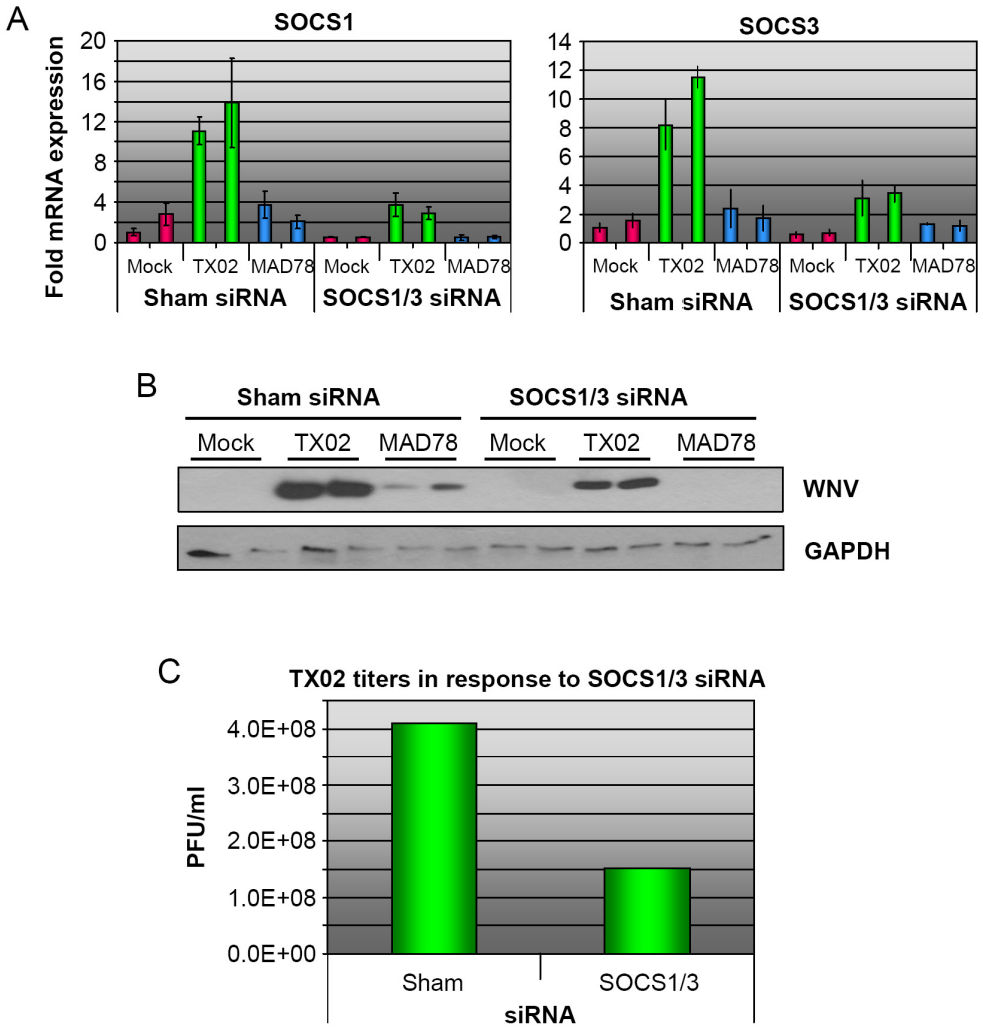

Figure 4-9. Reduction of SOCS1/3 partially restores the host response against WNV. (A) siRNA knockdown of SOCS1/3 reduces basal and virus-induced SOCS1 and SOCS3 mRNA levels. A549 cells transfected with siRNA against SOCS1 and SOCS3 or sham-treated were infected with TX02 or MAD78 for 48 h. Following infection, RNA was collected and analyzed by qRT-PCR. Values were normalized to GAPDH. Experiment was performed in duplicate. (B) Immunoblot analysis of cells transfected with SOCS1/3 siRNA or sham-treated. (C) Cell supernatants from TX02 infected cells in (A) were titered on Vero cells. MAD78 titers were below detection in this experiment.

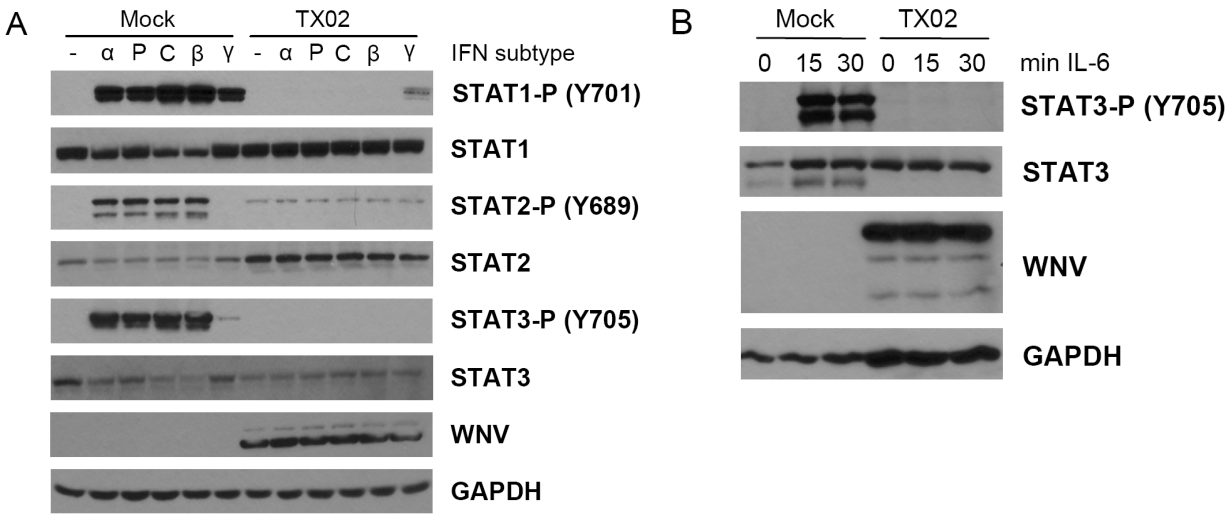

Figure 4-10. WNV inhibits JAK-STAT signaling in response to multiple cytokines. (A) A549 cells were infected with TX02 for 24 h. Cells were then treated for 30 min with IFNα-2a (α), PEG-Intron (P), CIFN (C), IFNβ (β) or IFNγ (γ) and cell lysates were analyzed by immunoblotting for tyrosine-phosphorylated STAT1, STAT2 and STAT3. TX02 blocked activation of all three STATs in response to all cytokines tested without affected total STAT levels. (B) The effect of TX02 on IL-6 induced STAT3 activation was determined in A549 cells. Cells were treated with IL-6 for 15 or 30 min after a 24 h infection with TX02. Tyrosine phosphorylation of STAT3 in response to IL-6 was absent in cells infected with TX02 but not in uninfected controls. Loading was controlled with GAPDH.

DISCUSSION

WNV antagonizes IFN signaling (93,164,193), and this regulation contributes to the pathogenesis seen with epidemic forms of the virus (130). The mechanism whereby WNV blocks signaling through JAK-STAT is currently unknown, although several viral proteins have been reported to play a role (164,193). Here we provide evidence that WNV attenuation of host signaling networks is a complex, multifactorial event involving viral and host regulatory proteins.

WNV regulation of JAK-STAT is not absolute. Rather, it is an attenuation of signaling resulting in just enough of an effect to give the virus a replicative advantage. Different pathological responses arise in vivo because some WNV strains are more effective at dampening the IFN response than others (130). In addition to differences in their ability to antagonize signaling, other factors likely also contribute to the divergent phenotypes between the virulent TX02 and avirulent MAD78 strains. For example, MAD78 induces a much stronger basal IFN response in infected cells (Figure 4-1) that, coupled with exogenous IFN, negatively regulates viral replication kinetics (130). It is still unclear at this time whether MAD78 activates a stronger host response resulting in reduced replication fitness or whether the replication fitness of MAD78 is naturally weak thereby delaying production of MAD78 gene products capable of effectively blocking downstream IFN signaling. In either case, the final outcome is reduced ability of MAD78 to block JAK-STAT. In contrast, when MAD78 viral proteins were overexpressed, several (E, NS2A, NS2B3, NS4B and NS5) exhibited equal or greater ability to block IFN signaling than the corresponding TX02

proteins. On the other hand, some TX02 proteins were clearly more efficient blockers than the respective MAD78 proteins, yet no single viral protein was capable of antagonizing JAK-STAT signaling to the same degree as active viral infection.

To our knowledge this is the first report describing the effects of WNV structural proteins on IFN signaling. The anchC and prM proteins from TX02 exhibited a trend toward blocking signaling. It appears that membrane localization is a prerequisite for the IFN antagonism seen with anchC since the mature C protein lacking the C-terminal membrane anchor failed to affect signaling (Figure 4-2). Of the structural proteins tested MAD78 E was the most effective IFN blocker. The mechanism of antagonism by the E protein is not known, but the obvious difference between the E proteins from the two viral strains is the lack of a N-linked glycosylation site in MAD78 E (130). Future studies are aimed at identifying the role subcellular localization and posttranslational modifications play in the function of these proteins in blocking JAK-STAT.

Of the nonstructural constructs tested, NS4B and NS5 were the only proteins from both TX02 and MAD78 that were able to block IFN signaling. Other nonstructural proteins demonstrated some degree of inhibition, but this was not conserved across WNV strains. NS2A and NS4B are small hydrophobic proteins predicted to each contain several transmembrane domains (B. Keller, unpublished data). As with the anchC protein, there appears to be a general correlation between membrane-associated WNV proteins and the ability to antagonize IFN signaling (this study and (164,193)), but the potential role of

membrane localization in signal inhibition is still not understood. NS2B3 and NS5 are obvious exceptions to this rule. While MAD78 NS2B3 was shown to block JAK-STAT, it is not known whether its protease activity is required for this effect. In data not shown, MAD78 NS3 began to exhibit greater inhibitory activity at higher input levels, and this activity was greatly enhanced when NS3 was expressed in cis with NS2B in the NS2B3 polygene construct. Future experiments will more closely define the genetic elements responsible for the enhanced IFN antagonism observed with NS2B3 compared to NS3 alone. Finally, NS5 from LGTV has been reported to associate with IFNAR to inhibit signaling, but it remains to be determined if WNV NS5 also interacts with the receptor complex. The C-terminal HA epitope tags on each WNV expression construct will allow for the analysis of putative binding partners. In summary, although several viral proteins attenuated IFN signaling to different degrees in vitro, expression of a single WNV protein was not sufficient to completely account for the dramatic phenotype seen during viral infection. Preliminary studies using combinations of viral proteins also failed to produce any significant signaling inhibition (data not shown).

The failure of individual WNV proteins to recapitulate the dramatic JAK-STAT block observed with viral infection suggested that other regulatory mechanisms may be contributing to the WNV-induced signaling inhibition. SOCS proteins are negative regulators of many cellular signaling networks. Functional genomics and qRT-PCR analyses demonstrated that SOCS1 and SOCS3 were upregulated during WNV infection, and the levels of expression during TX02 and MAD78 infection correlated with the relative JAK-

STAT block seen with each virus. The IFN-JAK-STAT axis is functional early during WNV infection (130) and therefore probably contributes to SOCS induction during WNV infection (247). This hypothesis is supported by the finding of potential binding sites for transcription factors downstream of IFN. The SOCS1 and SOCS3 promoter analyses also suggested that other signaling pathways including the MKK1/2-ERK, p38 MAPK and PI3K pathways, may contribute to the overall SOCS levels during WNV infection. Inhibitor studies implicated the MKK1/2, p38 MAPK and PI3K pathways in the induction of SOCS3 during WNV infection, while SOCS1 expression appeared to be increased by MKK1/2 and PI3K but negatively regulated by p38 MAPK. There is extensive cross-talk between cellular signaling networks, and much work remains to be done to identify the upstream components resulting in SOCS induction. Interestingly, components of two of these pathways are known to associate with the IFNα/β receptor complex and become activated when IFNα/β binds IFNAR (126,128). Although canonical IFN-JAK-STAT signaling may be blocked either directly or indirectly by WNV, it is not known if these alternative signaling networks are similarly affected. We postulate that WNV induces IFNβ production, and subsequent IFN binding to IFNAR may activate these alternative pathways, leading to upregulation of SOCS and potentially other host regulatory machinery. Because the IFN signaling inhibition is not absolute there may also likely be some direct induction of SOCS gene expression by the IFN-JAK-STAT pathway.

Although SOCS1 and SOCS3 levels were increased during WNV infection and their expression was thought to contribute to the observed IFN signaling block, the exact

physiological benefit expression of these proteins provided the virus was not well defined. Through the use of dominant negative SOCS expression plasmids and siRNA-mediated knockdown of SOCS1/3 expression, the host's innate antiviral signaling machinery could be partially restored resulting in restrictions on viral growth. It therefore appears that upregulation of these proteins during WNV infection benefits the virus by allowing for enhanced viral growth due to reduced antiviral signaling. Studies are currently underway to measure the extent of signaling restoration when SOCS1/3 expression and activity are suppressed.

The expression of host regulatory proteins in combination with WNV proteins provides a potent inhibitory force on JAK-STAT signaling networks, which has potentially significant ramifications for the development not only of an intracellular antiviral response, but also for the priming of an effective adaptive immune response required to clear the virus. Our results provide the first evidence that regulation of cytokine signaling by WNV is not restricted to canonical IFN signaling but also involves IFN and IL-6 activation of STAT3. Regulation of STAT3 activation is important since it has been shown that STAT3 supports the induction of an antiviral state by STAT1 and STAT2 (105). Furthermore, we demonstrated that WNV was capable of efficiently blocking multiple types of IFN signaling (α subtypes, β, and γ). Finally, this is the first report implicating the p38 MAPK, MKK1/2-ERK and PI3K pathways in the induction of SOCS expression during viral infection. It is therefore possible that WNV-induced SOCS expression may lead to a global regulation of cytokine signaling with dire consequences for the host cell.

CHAPTER FIVE
Studies on other WNV-host interactions

INTRODUCTION

Viruses are obligate intracellular pathogens and as such require extensive and intimate interactions with various components of the infected host cell. Chapter 3 demonstrated the importance of the IFN system in controlling virus replication and virulence, while Chapter 4 detailed mechanisms employed by WNV to antagonize cytokine signaling through JAK-STAT. This chapter describes smaller studies undertaken to examine the interaction of WNV with other host factors and their effects on the viral life cycle.

RESULTS

Reduced basal expression of RIG-I/MDA5 correlates with enhanced WNV permissiveness in cortical neurons

Studies of knockout mice have begun to reveal the tropism of WNV in vivo and to identify factors that restrict viral replication in vivo and in vitro. For example, IFNAR and PKR/RNaseL were shown to be critical in restricting WNV replication in peripheral tissues and spread to the CNS (222,223). IRF-3 is important in controlling cell-to-cell spread in vitro (76), and WNV replicates to higher titers in MEFs lacking RIG-I (75). The in vivo significance of these two molecules in WNV infection is currently areas of active investigation by a number of labs. In collaboration with Michael Diamond, we demonstrated

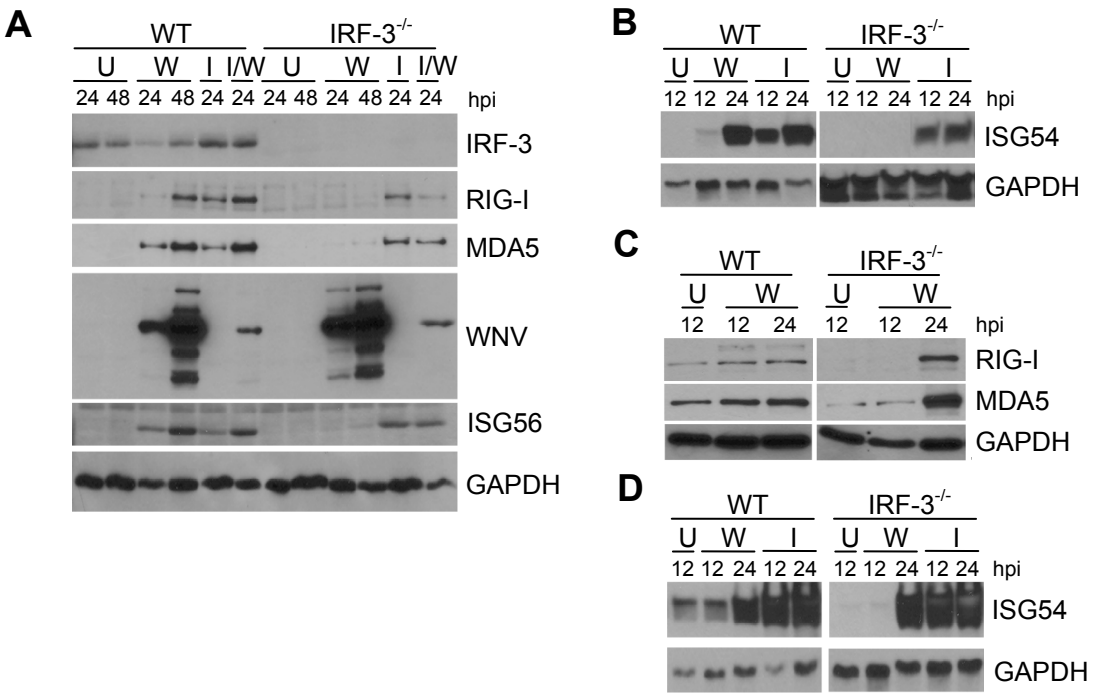

Figure 5-1. Cell-type specific basal expression of RIG-I and MDA5 correlates with susceptibility to WNV . (A) WT or IRF3$^{-/-}$ cortical neurons were infected ex vivo with WNV strain for 24 or 48 h, treated with IFN for 24 h, or pre-treated with IFN and infected with WNV. Cell extracts were immunoblotted for the presence of IRF-3, RIG-I, MDA5, WNV and ISG56. Loading was controlled with GAPDH. (B) WNV induces the expression of ISG54 in WT cortical neurons but not in neurons deficient in IRF-3. IFN treatment induces ISG54 expression independently of IRF-3. (C) WT or IRF3$^{-/-}$ MΦ were infected with WNV and analyzed for the expression of RIG-I and MDA5. In MΦs IRF-3 appears to control basal expression of RIG-I and MDA5, yet MΦs were still able to induce their expression in response to WNV independent of IRF-3. (D) Basal expression of ISG54 is controlled by IRF-3 in MΦ, but virus-induced ISG54 expression is IRF-3 independent. U = uninfected, W = WNV infected, I = interferon pretreatment, I/W = interferon pretreatment, WNV infected.

the importance of IRF-3 in controlling virulence and dissemination of WNV in vivo (56). It was also noted that certain cell types were more susceptible to WNV ex vivo. Cortical neurons, for example, were highly susceptible to WNV infection compared to bone-marrow derived macrophages (MΦ) (56). The susceptibility of neurons correlated with a reduced basal expression of the cytoplasmic sensors RIG-I and MDA5 compared to that observed in MΦ (Figure 5-1 A, C). Likewise, cortical neurons also exhibited reduced activation of ISG54 and ISG56 in response to virus but not exogenous IFN treatment confirming that the defect was due to lack of IRF-3 (Figure 5-1 B, D). These results suggest that IRF-3 is important for maintaining basal levels of RIG-I/MDA5 but that expression of these sensors is independent of IRF-3 in MΦ. Therefore, it appears that higher basal expression of RIG-I and/or MDA5 is critical for cells to resist infection with WNV and this may explain why some cells are more permissive to infection than others. Future studies in mice lacking RIG-I will more closely examine the role of RIG-I in controlling permissiveness to WNV in MΦ and other resistant cell types.

IPS-1 is required to initiate host defenses against WNV

RIG-I and IRF-3 were shown to be critical for controlling cellular permissiveness to WNV and virulence in vivo (56). RIG-I signals to IRF-3 via the mitochondrially localized IPS-1 molecule. The importance of IPS-1 during WNV infection is not known, but is believed to be critical based on results from other RNA viruses (144). In collaboration with Brenda Fredericksen, studies were initiated to determine the role that IPS-1 plays in the antiviral response to WNV. WT C57BL/6 or IPS-$1^{-/-}$ MEFs were infected with WNV (strain

NY3356) at a high MOI (Figure 5-2). At the indicated times post-infection, cell lysates were collected and analyzed by immunoblot for the activation of ISG54 and ISG56, known IRF-3 target genes (91). In WT MEF, ISGs are induced concomitant with WNV protein expression, peaking at 40-48 h post-infection. In contrast, there is a complete lack of ISG expression in cells deficient in IPS-1 despite strong WNV protein expression at 48 h. These

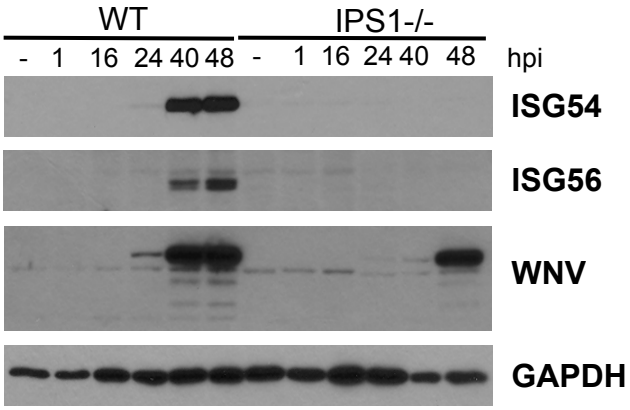

Figure 5-2. IPS-1 is required for the initiation of the host antiviral response.
WT or IPS1-/- MEFs were infected with NY3356 (MOI = 10) for the indicated times and analyzed for the presence of ISG54 and ISG56 proteins, IRF-3 targets downstream of IPS-1.

results demonstrate that IPS-1 plays a critical and non-redundant role in signaling to IRF-3 and inducing expression of certain ISGs. Since IRF-3 activation is a prerequisite for IFNβ transcription, a lack of IPS-1 should have global effects on WNV-induced ISG expression. Studies are currently underway to further clarify the exact role of IPS-1 in WNV infection.

Identification of potential anti-WNV effector proteins

WNV strains of divergent virulence exhibit differential resistance to IFN signaling (130). It is possible, therefore, that replication of less virulent strains whose ability to block signaling is attenuated may be controlled by ISGs or other virus-induced gene products. To begin to elucidate potential effector proteins responsible for controlling WNV infection in vitro, a functional genomics approach was taken. A549 cells were mock infected or infected with TX02 or MAD78 for 24 or 48 h. At each time point, cells were either treated with IFN (100 U/ml) or left untreated for 6 h. Total RNA was isolated and subjected to mRNA oligonucleotide microarray analysis. Experimentally-derived ISGs were determined from the mock-infected samples as genes exhibiting at least a 2-fold upregulation ($P \leq 0.01$) in response to IFN compared to untreated controls. At 24 and 48 h, 151 and 105 ISGs were identified, respectively. The response of these genes after 24 h of infection with TX02 or MAD78 in the absence of exogenous IFN treatment was then compared (Figure 5-3). The majority of the ISGs were upregulated by infection with both WNV strains. There was a subset of ISGs that were highly expressed during MAD78 infection but whose expression did not significantly change or was downregulated during TX02 infection. It is possible that this subset of genes includes antiviral effectors important for controlling MAD78 infection, but whose expression during TX02 infection is not sufficiently high enough to confer antiviral activity. Future studies utilizing expression cloning will seek to identify any antiviral functions of these genes during WNV infection. Additional work is also needed to identify other differentially expressed genes that are independent of IFN but

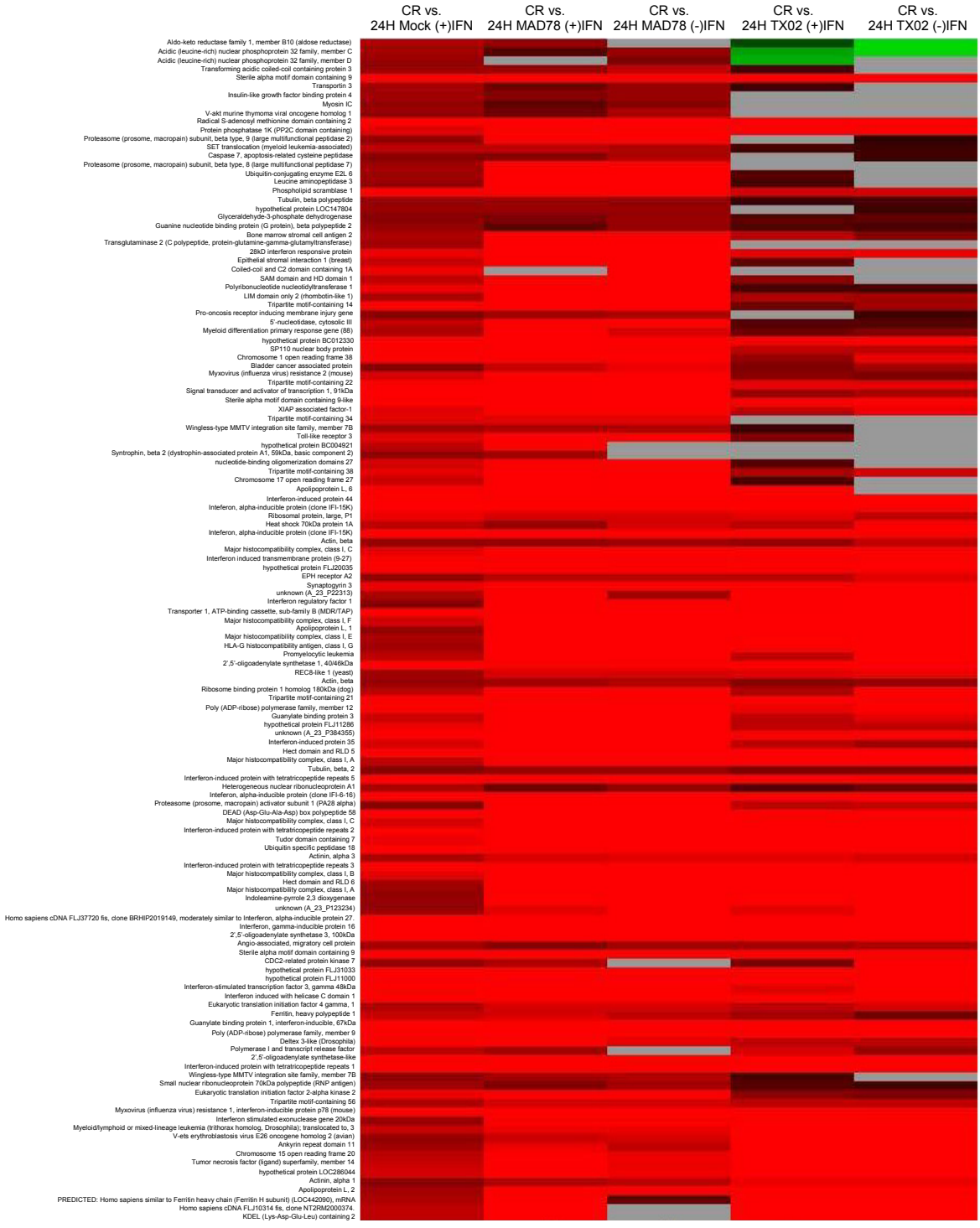

Figure 5-3. Expression of experimentally-derived ISGs during infection with TX02 or MAD78.

which might still have antiviral properties against WNV. Finally, in-depth data analysis of the WNV-infected, IFN-treated samples should provide novel insights into the differential regulation of IFN signaling by TX02 and MAD78.

IFN reduces WNV RNA levels and translation efficiency

As mentioned previously, it is well known that WNV blocks IFN signaling. The block, however, is not absolute resulting in the leak-through of some signaling. This is evidenced by the detection of a dose-dependent increase in ISG expression with a concomitant decrease in WNV protein levels in response to IFN treatment (Figure 3-3 C and D). This data suggests that IFN and its downstream effectors have some antiviral activity against WNV. To understand at what level ISGs were exerting their activity, studies were initiated to examine the translation efficiency of WNV RNA. Huh7 cells harboring the WNV 1.1 replicon (218) were treated with 100 U/ml IFNα for 24 h or left untreated. Cell lysates were centrifuged through a sucrose gradient to separate RNA-ribosome complexes. Gradient fractions were collected based on optical density readings (Figure 5-4 A), and total RNA was isolated from each fraction. RT-PCR analysis of WNV RNA using primers directed to the 3'NTR of the viral genome was performed, and the distribution of WNV RNA among the collected fractions was compared to the distribution of β-actin RNA (Figure 5-4

Figure 5-3. Expression of experimentally-derived ISGs during infection with TX02 or MAD78. A549 cells were infected with TX02 or MAD78 for 24 or 48 h followed by treatment with IFN or media alone for 6 h. Total RNA was collected and analyzed by Agilent oligonucleotide expression array. Shown are ISGs from the 24 h timepoint whose expression increased ≥ 2 fold ($P < 0.01$) in response to IFN treatment of uninfected control cells. Gray bars indicated genes whose expression was not significantly changed.

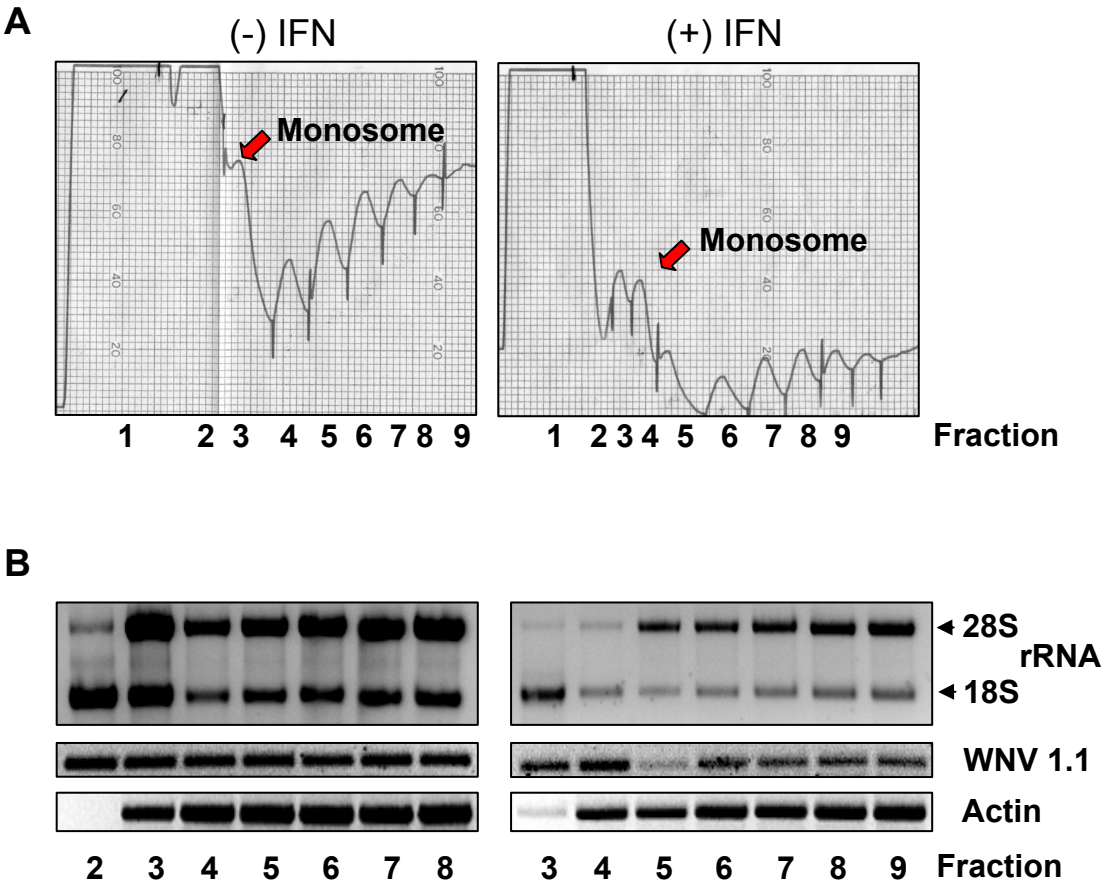

Figure 5-4. IFN blocks WNV translation efficiency by reducing polyribosome binding to viral RNA. (A) WNV 1.1 replicon cells were left untreated or were treated with IFN for 24 h at which time cell lysates were collected, sedimented through a sucrose gradient, and ribosomal fractions were collected. The monosome fraction is indicated by the red arrow. (B) Gradient fractions were analyzed for the presence of WNV and β-actin RNA by RT-PCR. Total RNA from each fraction was also separated on an agarose gel to identify the monosome fraction which contains nearly equal levels of 28S and 18S rRNA, corresponding to the 40S and 60S ribosomal subunits, respectively.

B). Determination of the monosome fraction was accomplished by separating total RNA from each fraction on an agarose gel and comparing the relative levels of 18S and 28S ribosomal RNA bands (Figure 5-4 B). WNV RNA in untreated WNV 1.1 cells was evenly distributed among ribosome fractions from monosome to hexasome. In contrast, IFN treatment shifted WNV RNA disproportionately to the monosome fraction with striking reductions in the amount of polyribosome-associated viral RNA. Control β-actin RNA was not affected by IFN treatment and remained evenly distributed throughout the ribosomal fractions. These results suggest that IFN treatment affects WNV translation efficiency by preventing the association of viral RNA with multimeric ribosomal complexes.

It was also noted from the polyribosome distribution analysis that total WNV RNA levels appeared to be reduced in response to IFN treatment. To better define the effect of IFN on viral RNA, Huh7 cells were treated with different doses of IFN, infected with TX02 and maintained in IFN (IFN pre-treatment) or were left untreated, infected with TX02 and treated with IFN after WNV infection (IFN post-treatment). Total RNA was harvested and analyzed by Northern Blot with probes specific for WNV, GAPDH and various ISGs, including 2',5'-OAS, ISG6-16, ISG15 and ISG56 (Figure 5-5). Levels of WNV RNA were reduced in a dose-dependent manner following IFN treatment with treatment initiated prior to infection having a greater effect than IFN added after infection. Concomitant with the decrease in viral RNA was an IFN dose-dependent increase in ISG RNA levels, including the levels of 2',5'-OAS. 2',5'-OAS is an enzyme that, upon dsRNA binding, activates downstream proteins including RNaseL leading to the degradation of viral and cellular

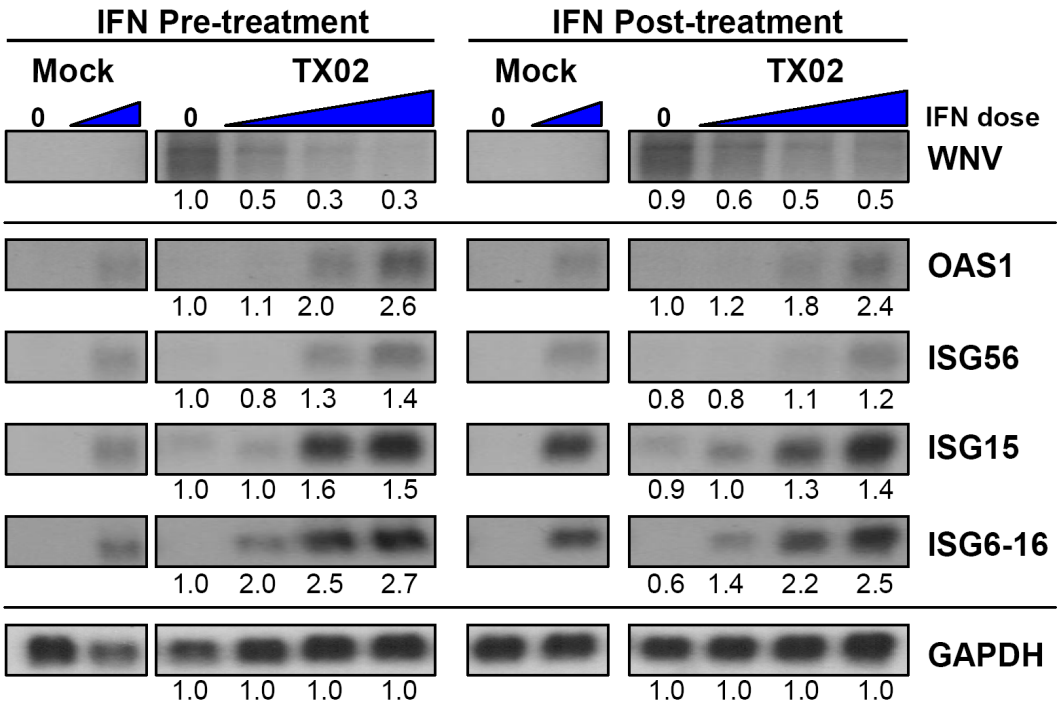

Figure 5-5. IFN reduces WNV RNA abundance.
Huh7 cells were treated with 10, 50, or 100 U IFN for 24 h ,infected with TX02 and maintained in IFN for 24 h more (pre-treatment). Alternatively, cells were left untreated, infected with TX02 and then treated with IFN (post-treatment). RNA was analyzed by Northern blotting for the presence of WNV, GAPDH, 2',5'-OAS, ISG6-16, ISG15 and ISG56. The relative intensities of each band were normalized to the respective GAPDH band using the histogram function in Adobe Photoshop and are expressed as fold increase.

mRNAs. Induction of RNaseL activity in response to WNV infection has been previously documented (B. Keller and B. Fredericksen, unpublished data), and this could contribute to the decline in viral RNA levels. On the other hand, reductions in viral RNA levels may simply be secondary to IFN-dependent decreases in viral protein expression including the NS5 RNA-dependent RNA polymerase. Further work is needed to more clearly define the cellular mechanisms responsible for restricting WNV RNA and protein expression during infection.

WNV induces a partial host translational shut-off

In addition to antagonizing cytokine signaling pathways, many viruses direct mechanisms to block host protein synthesis (53), yet it is not known whether WNV also affects host translation control programs. To address this issue, A549 or Huh7 cells were infected with TX02 (MOI = 4.62), radiolabeled with ^{35}S-Methionine at various times post infection and analyzed by SDS-PAGE (Figure 5-6). Total protein loading was equal in all lanes as determined by Coomassie staining (data not shown). By autoradiography, it was determined that beginning at 16 hpi and continuing throughout the infection newly synthesized protein was predominantly viral in nature. Compared to uninfected controls, the smear of cellular proteins in TX02-infected cells was gradually reduced over the course of the infection, indicating a switch from cellular protein synthesis to production of viral proteins. These results suggest that WNV induces a partial shut-off of host translation. It remains to be determined how exactly this shut-off occurs, but potential mechanisms include inhibition of protein synthesis through the activation of PKR and eIF2α or the degradation of

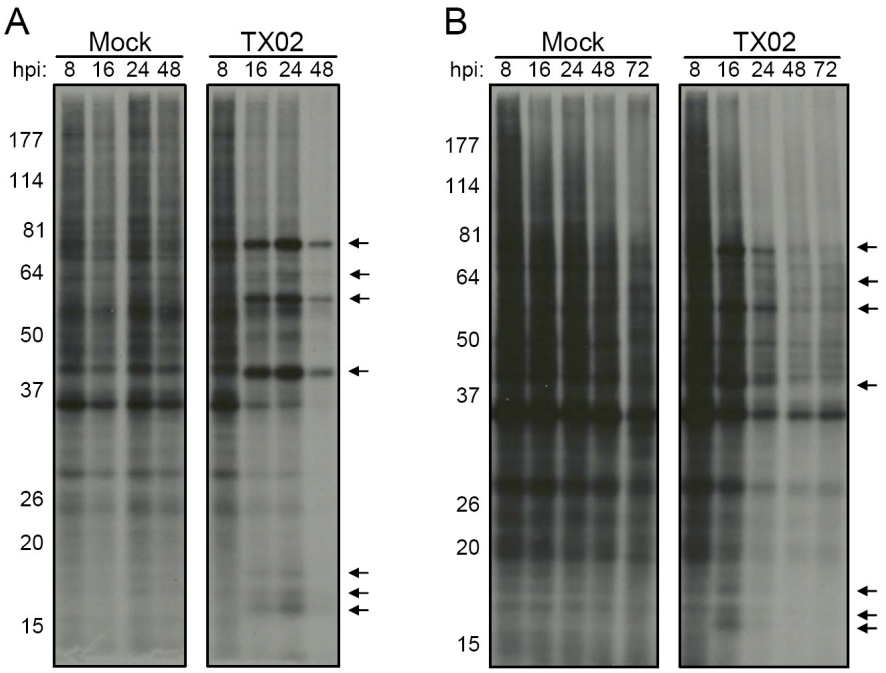

Figure 5-6. WNV induces a partial host translational shutoff.
Huh7 (A) or A549 (B) cells were mock-infected infected with TX02. Prior to the indicated times, cells were starved of methionine for 2 h followed by a 30 min labeling with ^{35}S-methionine. Cell extracts were separated by SDS-PAGE and equal loading was confirmed by Coomassie staining (data not shown). Arrows indicate viral proteins.

mRNA through the actions of RNaseL. WNV induces PKR activation and the subsequent phosphorylation of eIF2α (223). The phosphorylation of eIF2α prevents its recycling, limiting the available pool of eIF2α and shutting down translation. It is also known that WNV activates the 2',5'-oligoadenylate synthetase (2',5'-OAS)/RNaseL system (B. Keller, unpublished observations and (228)) which leads to the cleavage of cellular and viral mRNAs. Future studies are needed to determine the relative contribution of the PKR-eIF2α and 2',5'-OAS/RNaseL pathways to the observed host shut-off.

Discussion

The interactions between an invading virus and the host cell occur on an intimate level beginning with engagement of the cellular receptor, continuing throughout the intracellular lifecycle of the virus and ending with egress of mature virions from the infected cell. Critical to the health of the host are the interactions of intracellular antiviral detection and defense molecules with the invading pathogen. Flaviviruses are detected by the cytoplasmic sensor RIG-I (281). In collaboration with Michael Diamond, we recently demonstrated that variations in cell-type specific expression of RIG-I and MDA5 correlate with susceptibility to WNV infection. In particular, cortical neurons basally express almost no detectable RIG-I/MDA5 and are especially sensitive to infection with WNV. Macrophages, in contrast, contain higher levels of these important sensors and are more resistant to WNV infection. These results could help to explain the proclivity of WNV to

target the CNS. Future studies are aimed at delineating tissue-specific expression of RIG-I and MDA5 to identify other potential sites of viral amplification within an infected host.

RIG-I and MDA5 are critical to the antiviral response to many RNA viruses because they initiate a signaling cascade that results in the production of IFNβ. The focal point of both of these signaling pathways, as well as some of the TLR pathways, is the mitochondrially localized IPS-1 protein. In collaboration with Brenda Fredericksen, we demonstrated the importance of this signaling molecule in the host response to WNV. In cells lacking IPS-1, induction of ISG54 and ISG56 was completely absent by immunoblot analysis supporting the role of IPS-1 as a central figure in the innate antiviral response to WNV.

WNV infection results in IFNβ production and activation of downstream ISGs, the antiviral effector proteins of the cell. These ISGs act to repress viral replication through many different mechanisms. Unfortunately, the data concerning ISGs effective at controlling WNV is extremely limited. The functional genomics analysis presented here should advance this area of research by allowing comparison of genes induced by pathogenic and nonpathogenic WNV strains. Genes that are highly upregulated during infection with the avirulent MAD78 strain but not the virulent TX02 strain may be critical in controlling infection as witnessed by the phenotypic outcomes of each infection in vivo. Identification of these potential anti-WNV effectors will narrow the spectrum of candidate genes allowing for a directed study of possible antiviral functions. Our previous studies and the ones

presented here provide some clues as to the identification of anti-WNV proteins. IFN treatment results in a reduction in WNV translational efficiency and a reduction in viral RNA (Figures 5-4 and 5-5). Translational effects could be due to the activation of PKR and ISG56 in response to WNV infection ((223) and Figure 3-2). Both of these proteins are known to direct mechanism to disrupt protein synthesis (77,253) and could be involved in the translational effects observed during WNV infection. We and others have also demonstrated that the 2',5'-OAS/RNaseL system is active during WNV infection, and this could be involved in reducing viral RNA levels (B. Keller, unpublished data and (223,228).

Finally, WNV encodes mechanisms to counter host antiviral defenses. In addition to antagonizing cytokine signaling, it now appears that WNV also directs a partial shutoff of host translation. Metabolic labeling experiments demonstrated a shift from cellular protein synthesis to viral protein synthesis over the course of infection. These results are consistent with the host shutoff observed with other viruses (31). Further studies are needed to identify the mechanism by which host protein synthesis is attenuated during infection with WNV.

As mentioned above, viruses interact with their infected host on many levels. The studies in this chapter are only snapshots of the full story. They do, however, provide evidence of new mechanisms at work (WNV regulation of host protein synthesis) as well as contribute to the identification of host factors important in recognizing and responding to WNV infection (RIG-I, IPS-1). Results from these studies should allow for the development

of many testable hypotheses that can be used to increase our understanding of this very complex system, the virus-host interaction.

CHAPTER SIX
Final Thoughts and Future Directions

PUTTING IT ALL TOGETHER

IFN controls WNV pathogenicity

The innate intracellular antiviral response is the first line of defense an organism possesses in the war against invading pathogens. Critical to this initial barrier is the production and subsequent signaling of IFNα/β. The recent emergence of highly pathogenic strains of WNV and their association with severe neurological disease in avians and humans suggests that WNV has acquired the ability to effectively evade host defenses. To better understand the interactions of WNV with host defenses, studies were undertaken to examine the role IFN plays in controlling WNV infection.

Consistent with a report from Beasley and colleagues (16), characterization of a new pathogenic WNV isolate (TX02) revealed very few changes in the viral genome as the virus spread throughout the United States. This new WNV isolate exhibited high sequence homology and similar growth kinetics to a strain isolated early in the epidemic (NY3356). In contrast, a nonpathogenic strain from Madagascar (MAD78) was quite divergent from the recent epidemic isolates and exhibited delayed growth kinetics and reduced peak viral titers. In vitro, MAD78 was highly susceptible to the antiviral effects of IFN, while TX02 was resistant. The resistance of TX02 was greater if IFN was applied after virus infection suggesting that the virus encoded mechanisms to antagonize IFN signaling. It was

demonstrated that activation of STAT1, STAT2 and STAT3 as well as the upstream activation of TYK2 and JAK1 were blocked by infection with TX02, yet the nonpathogenic MAD78 was attenuated in this ability. Infection of cells deficient in IFNAR rescued MAD78 replication, and the virulence of MAD78 was unmasked in mice lacking a functional IFNα/β signaling cascade. These results indicate that IFNα/β controls WNV replication and virulence in vivo (130). Additionally, IFN was also shown to control the tropism of the virus in vivo (222) highlighting the critical role played by this initial line of defense.

A complex model of viral and host regulation of cytokine signaling

Although several groups reported that WNV blocked JAK-STAT signaling in response to IFN (93,130,164,193), the mechanism of such regulation was not clear. Overexpression of WNV gene products implicated several viral proteins from both TX02 and MAD78 in the JAK-STAT block. However, none of these proteins could fully attenuate signaling to the levels observed during viral infection. These results suggested that other regulatory mechanisms must also be at work, and studies were undertaken to identify other components involved in blocking IFN signaling. Functional genomics combined with quantitative RT-PCR revealed that SOCS1 and SOCS3 were differentially upregulated during infection with TX02 and MAD78, and this differential expression correlated with the relative JAK-STAT block observed with each strain. Expression of a dominant negative form of SOCS1 as well as siRNA-mediated knockdown of SOCS1 and SOCS3 levels partially restored IFN signaling confirming the role of SOCS in the WNV-induced JAK-STAT block.

The question remained as to how SOCS proteins were being upregulated since both SOCS1 and SOCS3 are ISGs (4,247). Overexpression of individual viral proteins was not sufficient to induce SOCS expression indicating that some other aspect of the viral life cycle may be responsible for activating cellular pathways leading to SOCS upregulation. Alternatively, a combination of viral proteins may be required for induction of SOCS expression. Infection of cells deficient in STAT1 demonstrated that SOCS induction could occur in the absence of canonical IFN signaling. These results were confirmed in cells with a functional IFN signaling pathway. In these cells, treatment with anti-IFNAR neutralizing antibodies reduced WNV-induced SOCS1 and SOCS3 expression. To identify the IFN-independent, STAT1-independent signaling pathways through which SOCS induction was occurring, chemical inhibitor studies were initiated. The results of these studies indicated that the PI3K and MAPK pathways promoted SOCS expression during WNV infection.

Interestingly, the PI3K and MAPK pathways intersect the IFN-JAK-STAT axis at the level of the IFNAR, independent of STAT binding and activation. Various adaptor molecules bind the IFNAR and become phosphorylated in response to IFN binding. Insulin receptor substrate-1 (IRS-1) and IRS-2 are two such molecules that, upon phosphorylation by JAK1, recruit the p85 regulatory subunit of phosphatidylinositol 3-kinase (PI3K) leading to the activation of the constitutively bound p110 catalytic subunit (128). PI3K phosphorylation results in the downstream activation of multiple signaling molecules including 3-phosphoinositide-dependent protein kinase (PDK1), Akt and the mammalian target of rapamycin (mTOR) (128). It was recently shown that IFNα-induced transcription

of SOCS3 is dependent on the activation of PI3K since treatment with LY294002 blocked IFNα-induced SOCS3 expression by microarray analysis (104).

The p38 MAPK pathway is also activated in response to IFN, presumably through the activation of Rac1 by one or more guanine exchange factors (GEFs) (126) that interact with the IFNAR complex. Rac1 activation in turns stimulates MAPK kinases 3 and 6 (MKK3/6) leading to the phosphorylation of p38. The role of MKK6 and p38 in the induction of SOCS expression was confirmed in studies using the p38 MAPK-specific inhibitor SB202190 and dominant negative forms of p38 and MKK6 (29). Inhibition of p38 MAPK, either chemically or by transfection of dominant negative constructs, amplified IL-6 signaling in HepG2 cells. Furthermore, expression of a constitutively active form of MKK6 activated the SOCS3 promoter and upregulated SOCS3 mRNA expression confirming the ability of p38 to positively regulate SOCS3 and potentially SOCS1 (29). p38 MAPK is also thought to be activated via PKR phosphorylation of MKK6 in response to dsRNA (240). We previously demonstrated that PKR is stimulated in response to WNV infection (223), so this provides another potential means of p38 activation and subsequent SOCS expression.

Finally, it is possible that ERK1/2 may also be activated in response to IFNα stimulation. The adaptor protein GRB2, in complex with the GEF SOS1, is recruited to activated receptor tyrosine kinases via its SH2 domain (198). Whether GRB2 interacts with the IFNAR complex is currently not known, but GRB2 has been shown to bind IRS-1 (244), an adaptor found in complex with the IFNAR. GRB2 facilitates the GEF activity of SOS1

which activates the Ras-Raf-MEK-ERK pathway (59). ERK is known to activate members of the AP-1 family of transcription factors, and potential AP-1 transcription factor binding sites were detected in the SOCS3 promoter (B. Keller, unpublished data). The involvement of ERK in SOCS induction was suggested by the reduction of SOCS mRNA expression observed in WNV-infected cells treated with MEK1/2 inhibitors (Figure 4-6). Further studies are needed to definitively connect the IFNAR to ERK signaling and SOCS induction in the context of WNV infection.

In summary, the literature and the work presented in this dissertation support a complex model of cytokine signaling regulation by WNV and cellular proteins (Figure 6-1). Early in WNV infection, IFN and other cytokines signal freely. When viral proteins (and/or viral RNA) reach a critical level, they begin to attenuate canonical JAK-STAT signaling, essentially shunting IFN signaling to alternative signaling pathways including PI3K and MAPK. This signal diversion affects the global transcriptome of the cell to a state favoring WNV. In particular, signaling through the PI3K and MAPK pathways leads to the induction of SOCS1 and SOCS3 which act in concert with viral proteins to further shut down IFN (and other cytokine) signaling. It must also be noted that the JAK-STAT block is not absolute, but rather an attenuation such that some signaling still occurs as evidenced by the detection of ISGs throughout WNV infection. The IFN-JAK-STAT axis, therefore, likely contributes to the induction and negative feedback of the SOCS proteins as well. The combination of SOCS and WNV protein expression results in a broad and potent blockade to cytokine

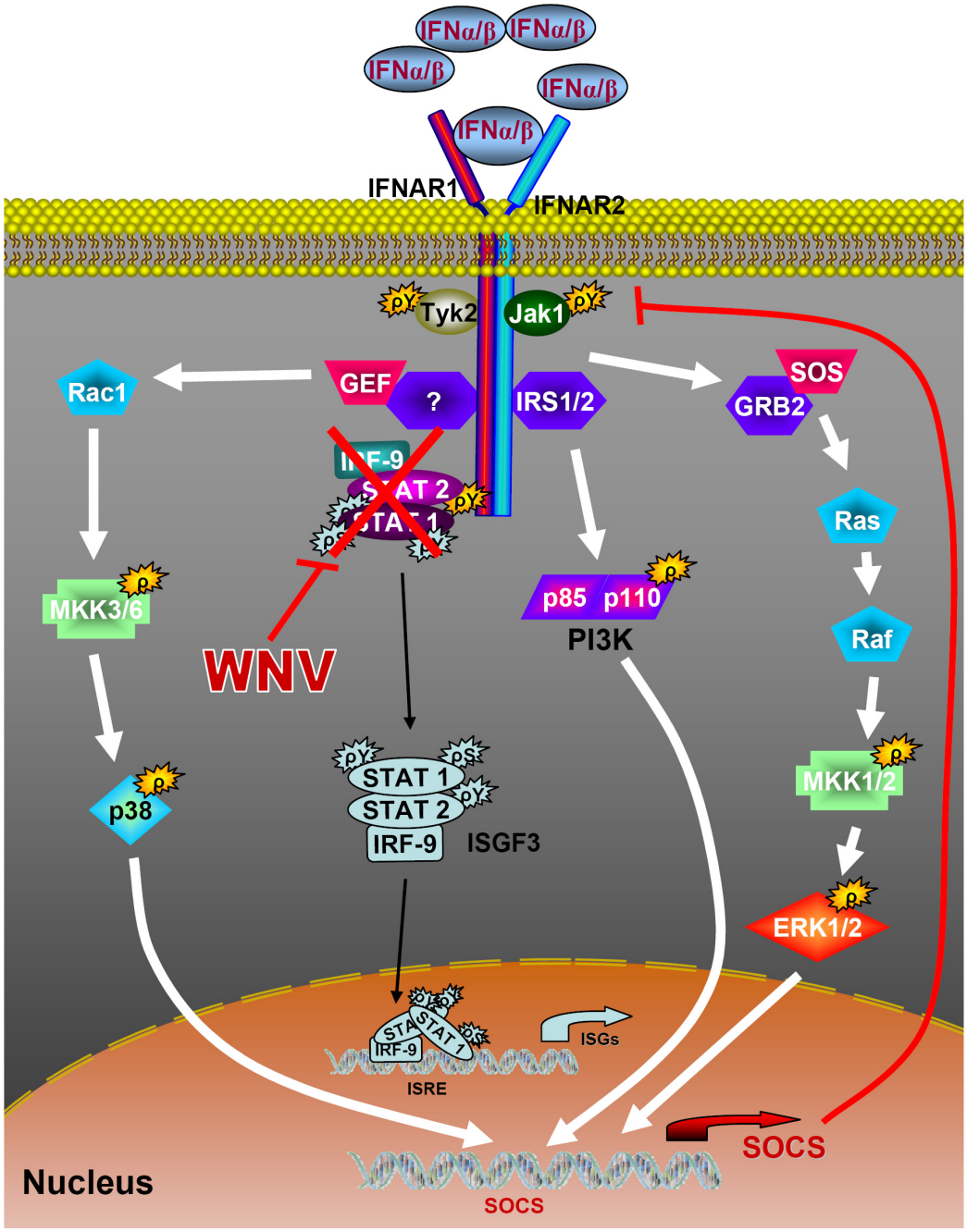

Figure 6-1. Model: Viral and cellular regulation of cytokine signaling.
Initially, WNV proteins act to suppress JAK-STAT signaling. Attenuation of the canonical JAK-STAT pathway shunts signaling into alternative pathways including the PI3K and MAPK cascades. These pathways converge at the SOCS promoter, driving transcription of SOCS1 and SOCS3 which feedback to further regulate cytokine signaling. The combination of viral and host regulatory proteins results in a potent signaling blockade.

signaling through JAK-STAT. Further studies, such as those outlined below, are essential to determine if the model proposed here persists.

WHERE TO GO FROM HERE?

MAD cloning

The studies in Chapter 3 clearly illustrate the phenotypic differences between the ability of TX02 and MAD78 to antagonize IFN signaling. The creation of TX02 and MAD78 gene expression plasmids will greatly aid in identifying the molecular mechanisms by which TX02 directly blocks JAK-STAT. Although no single viral protein could attenuate signaling to the same degree as viral infection, some proteins did exhibit antagonistic properties. This data, coupled with recent data from other flaviviruses, suggests that direct inhibition of IFN signaling by WNV is a component of the overall JAK-STAT block. Future studies will address whether individual WNV proteins directly interact with components of the JAK-STAT signaling cascade. Mutagenesis studies will allow for the identification of the protein domain or domains responsible for the signal block. Results from these studies may also provide insights into the reasons why MAD78 is attenuated in this ability. However, the best way to identify key elements preventing MAD78 from blocking IFN signaling is through the creation of a MAD78 infectious clone. Infectious clones, historically, have been very useful in studies of WNV pathogenesis and the role of E protein glycosylation in maturation and egress of viral particles from infected cells (30,96,235,274,279). Our lab currently possesses an infectious clone of the WNV NY strain

that is nearly identical to TX02. Through site-directed mutagenesis, the NY clone could very easily be converted to TX02. Additionally, a new postdoctoral researcher in our lab is undertaking the task of creating a MAD78 clone.

Having infectious clones of both TX02 and MAD78 will allow for the swapping of viral genetic elements between the two strains. Phenotypic alterations can then be examined to identify genes or genomic regions responsible for antagonizing JAK-STAT in the context of a productive viral infection.

Currently, there are three major hypotheses concerning the discrepancy observed between TX02 and MAD78: 1) differences in viral protein activity, 2) differences in viral replication/translation, and 3) differences in the induction of cellular cytokine regulatory machinery. The first hypothesis suggests that perhaps a TX02 gene product(s) is simply better at antagonizing signaling than the corresponding MAD78 protein. If this was true, we would expect to see a difference using the TX02 and MAD78 expression plasmids. The results (Figure 4-2) were surprisingly almost the exact opposite of what we predicted. NS4B and NS5 from both strains equally blocked IFN signaling, while only anchC, prM and NS2B from TX02 were more effective at blocking IFNα signaling than the respective MAD78 proteins. However, TX02 anchC, prM and NS2B were still no more effective than NS4B or NS5. On the other hand, MAD78 NS2A and NS2B3 were extremely efficient at antagonizing JAK-STAT (~50% reduction in activation of ISRE reporter), while TX02 NS2A and NS2B3 exhibited no significant effect. These results suggest that MAD78

products are just as capable, in not more so, than TX02 at blocking JAK-STAT when overexpressed. Even though overexpressed MAD78 proteins are able to block JAK-STAT, it is possible that they are not expressed at high enough levels during active viral infection. This would indicate a defect in MAD78 replication relative to TX02. Formation of membrane-enclosed replication complexes and efficiency of the NS5 RNA-dependent RNA polymerase are both critical steps in the viral life-cycle that could affect the rate at which viral proteins are produced. Additionally, the NTRs of the WNV genome are involved in viral replication, translation of the viral proteins and interaction with various cellular proteins (27,28,35,156,233). Alignment of the TX02 and MAD78 genomic sequences reveals potentially important differences in the NTRs of the viruses, including a deletion of approximately nucleotides in the MAD78 3'-NTR. Because the viral NTRs are intimately involved in numerous aspects of the viral replication cycle, these NTR sequence changes could have a significant impact on viral replication, translation and recruitment of cellular factors, all of which could contribute to the phenotypic differences observed between TX02 and MAD78. The MAD78 infectious clone will be critical in determining the role of viral replication kinetics in attenuating JAK-STAT signaling. Finally, microarray and qRT-PCR studies suggest that TX02 induces higher levels of negative regulators of cytokine signaling (including SOCS1, SOCS3 and CIS) than does MAD78. Infectious studies also demonstrate that this appears to be dependent on the intracellular viral load. Perhaps then, TX02 is better able to counteract IFN signaling because it receives greater assistance from the cell's own negative feedback machinery. None of these hypotheses is mutually exclusive and, most likely, all three aspects play at least some role in WNV's antagonism of cytokine signaling

networks. Creation of a MAD78 infectious clone will allow us to begin to tease apart the relative contributions of viral proteins, viral replication kinetics and host regulatory proteins.

How exactly do WNV proteins block IFN signaling?

Even with all the recent activity describing flaviviral proteins that have regulatory effects on IFN signaling, we are still no closer to understanding mechanisms for regulation directly attributable to viral proteins. The TX02 and MAD78 HA-tagged expression constructs I created should be a valuable tool to begin to dissect these questions. Initial experiments will detail localization of viral proteins within the cell. Protein-protein interactions could then be analyzed using co-immunoprecipitation studies to look for potential targets within the JAK-STAT cascade. Mutational analysis of conserved regions may yield insight into the functional domains of each protein required for its regulation. Initial results from studies on LGTV NS5 look promising for identifying NS5 residues important in regulating JAK-STAT (S. Best personal communication). Finally, creation of the MAD78 infectious clone will allow gene swapping with TX02. This could provide insight into the relative contribution of each viral protein in regulating cytokine signaling during infection.

Is the secret in the ends?

One aspect of the WNV genome that has been overlooked in studies analyzing the role of viral proteins in signal regulation is the role of the 5'- and 3'-NTRs. These highly structured stretches of RNA have already been shown to interact with cellular proteins

resulting in effects on viral replication and translation (28,155,156). It is also possible that they could interact with components of the JAK-STAT pathway or regulators thereof. The 5'- and 3'-NTR sequences are very highly conserved among all WNV isolates sequenced to date (B. Keller, data not shown). The 3'-NTR, however, retains some variation that might account for phenotypic differences between isolates in terms of replication kinetics, interactions with cellular proteins and other, yet to be identified, functions. In particular, the 3'-NTR of MAD78 is missing a stretch of approximately 70 nucleotides or 10% of the 3'-NTR of TX02. Loss of this amount of genetic data could have drastic effects on the viral life cycle since the NTRs play such a critical role in viral replication and translation (156,176,259). RNA-protein interaction studies could identify potential interacting partners, while mutational analyses would determine the critical nucleotides for such interactions. These studies will provide novel insights into an aspect of the WNV life cycle not yet examined.

Overloading the system: Viral load effects on JAK-STAT signaling

A question that arose over the course of the TX02 IFN resistance studies was whether initial viral load played a significant role in the ability of the virus to efficiently shut down IFN signaling. The simplest means of determining this would be to examine the JAK-STAT block during TX02 infection with decreasing MOIs. Most likely, though, the antagonism would be similar but with slightly delayed kinetics since IRF-3 is not activated until late in infection. An alternative way to address this issue is to "prime" the antiviral response prior to infection with WNV and look for changes in the ability of the virus to block JAK-STAT.

Priming could be accomplished by transfection of a constitutively active form of RIG-I (282), the cytoplasmic sensor of WNV or similarly, by transfection of poly(I:C), a synthetic dsRNA known to activate host defenses. Priming would then be followed by infection with TX02 and subsequent IFN treatment. The readout for this assay would be phosphorylation status of JAKs and STATs as determined by immunoblot analysis. Alternatively, an ISRE-luciferase promoter construct could also be transfected along with the priming agent. The ability of WNV to block activation of the ISRE promoter in response to exogenous IFN could then be measured by luciferase assay. These experiments will provide much needed insight into the role early cellular events play in affecting later events during the viral life cycle. They may also provide a reason why MAD78 is less fit at inhibiting JAK-STAT than TX02.

A tale of two SOCS

In Chapter 4, I showed that SOCS1 and SOCS3 are upregulated during WNV infection, and the induced expression of these proteins acts synergistically with WNV proteins to antagonize cytokine signaling. Evidence was also presented demonstrating that expression of SOCS appears to be driven by multiple signaling pathways converging at the SOCS promoter. Chemical inhibitor studies implicated the PI3K, MEK2 and, to a lesser extent, the p38 MAPK pathways in the upregulation of SOCS mRNA expression during WNV infection. The IFN-JAK-STAT axis most likely also plays a role in SOCS induction since it is known that SOCS are IFN-induced negative feedback regulators of this pathway (4,81). Much work remains, though, to identify the mechanism whereby WNV induces each

of these pathways, their exact contribution to SOCS expression and other functional consequences of their activation.

Chromatin immunoprecipitation studies should identify the transcription factors involved in WNV-induced SOCS expression. From there, one could work backwards up the pathway to identify other key signaling proteins. Alternatively, more detailed chemical inhibitor studies or the use of dominant negative constructs would allow for the dissection of this complex signaling web. Finally, gene knockout mice lacking functional components of the implicated pathways could be used to determine the effect of each pathway on in vivo pathogenesis of WNV. To date, WNV infections of knockout mice have focused mainly on classical immunomodulatory components like IFNAR (130,222), IFNγ (238), TLR3 (269), T cells (242), B cells and antibodies (62), granzyme/perforin (237), PKR/RNaseL (223), IRF-3 (Daffis et al., in press) and IRF-7 (Gale and Diamond, unpublished results). Data examining the effect of the PI3K pathway and other proinflammatory or stress signaling pathways (p38 MAPK, JNK and ERK) on WNV infection are lacking. In vivo and ex vivo experiments from knockout mice should provide a wealth of new data on the functional significance of these and other signaling pathways on the outcome of WNV infection.

Emergence of WNV (Part I): Avian IFN studies

One of the most critical points to understanding the recent epidemics of WNV neuroinvasive disease in both humans and birds is to identify the mechanisms that have resulted in significantly enhanced virulence of the virus in avian populations. Like

mammals, birds possess a complex immune system consisting of innate and adaptive arms. Likewise, the IFN system is conserved in avians (231), however, there is no data concerning the interplay between WNV and avian IFN. It is possible that recent WNV epidemics are the result of an adaptation acquired by certain isolates that allows the virus to attenuate avian IFN responses, thereby resulting in increased viral loads and enhanced transmission to arthropod vectors. On the other hand, the ability to antagonize JAK-STAT signaling may be a conserved feature among all WNV isolates, and some other aspect of the viral life cycle may be responsible for the increased pathogenesis in avian species, particularly passerine birds. In order to fully understand the dynamics of WNV infection in humans, we must also understand the virus-host interactions that occur in amplifying hosts and transmission vectors (see below). A paucity of reagents required for the analysis of avian innate immune defenses has historically been the primary barrier to examination of this important issue. With the recent WNV epidemics as well as global concerns regarding avian influenza, new and improved avian antibodies, reagents and cell lines should be coming on line soon. Already, there are enough reagents to determine at least preliminarily whether WNV can attenuate JAK-STAT signaling in an avian host cell. It is also possible that antibodies raised against mammalian JAK and STAT proteins may cross-react with their avian counterparts, further increasing the effective tools available. These analyses are simple, straightforward experiments that will yield critical information as to the manner in which WNV interacts with its native host. They may also provide insight into treatment strategies, not only for the protection of avian species, but perhaps for pan-species protection against WNV infection.

Emergence of WNV (Part II): Insect antiviral studies

While little is known about how WNV interacts with its avian host, even less is known about the type of antiviral response it encounters in its arthropod vector. Very little genetic drift has occurred as WNV has spread throughout North America (16), suggesting a lack of a selective pressure on the virus. Still, to be successful, the virus must evade host immune defenses in three very different hosts (insect, bird and mammal). While there appears to be conservation of STAT proteins in all three of these families (2,34,157,159), it is currently not known what role insect STATs play, if any, in controlling viral infections. One of the initial studies identifying the insect STAT proteins also looked at whether JEV could prevent phosphorylation of these proteins in vitro ((159)). Protein phosphatase activity seemed to be responsible for preventing phosphorylation of mosquito STAT since this could be overcome by treatment with orthovanadate, a tyrosine and alkaline phosphatase inhibitor. In humans, tyrosine phosphatases do not appear to play a significant role in antagonizing JAK-STAT since orthovanadate treatment has little effect on restoring signaling (B. Keller, unpublished observations). It is possible, though, that WNV may use different mechanisms in different animal species to evade innate host defenses. There are several well-characterized mosquito cell lines and an increasing number of reagents that make studies of WNV-host interactions in its native vector a real possibility. Like the avian IFN studies mentioned above, experiments detailing WNV's evasion of insect antiviral defenses should provide a greater understanding of the viral life cycle.

Cellular control of WNV: TRIMming the virus??

Despite the recent explosion of research on WNV and related flaviviruses there has been a glaring absence of work analyzing the specific ISG effector proteins responsible for restricting WNV replication. As mentioned above, several studies have utilized gene knockout mice to identify immune components involved in recognizing WNV and controlling its pathogenesis in vivo, but detailed mechanisms by which these components exert their effects remain unknown. To fully understand the interplay between WNV and the infected cell, it is not enough to simply study the effects of viral proteins on the cell. The multitude of defenses employed by the cell to fight off viral infection must also be examined, as this response is tailored to the specific invading virus. Results from the functional genomics experiment presented here should form the basis for future studies identifying the antiviral effector molecules and their mechanisms of action against WNV.

The functional genomics analysis we conducted was designed to not only compare the ability of TX02 and MAD78 to antagonize induction of ISGs in response to IFN, but also to detect differentially regulated genes during infection with these divergent strains (Figure 5-3). Focusing on the experimentally-derived ISGs as a preliminary subset of potential anti-WNV effector proteins, we demonstrated that several classical ISGs (including ISG54, ISG56, RIG-I, 2',5'-oligoadenylate synthetase, IRF-9, IRF-1 and various members of the Major Histocompatibility Complex class I among others) were upregulated equally by both viruses. Interestingly, we also identified several genes that were highly upregulated during MAD78 infection but whose expression was downregulated or not significantly changed

during infection with TX02. Included in this subset were members of the tripartite motif (TRIM) family of proteins, TRIM14, TRIM34 and TRIM38. The TRIM family of proteins includes 68 human genes with homologues in many other species, even nematodes (200). Nearly all TRIM proteins contain a RING domain in their N-terminus that has been shown to possess ubiquitin E3 ligase activity. The central portion of the protein includes one or two B-boxes whose function is unknown. This is followed by a coiled-coil domain that is thought to play a role in homo-oligomerization, resulting in high molecular weight complexes that may compartmentalize the cell. Finally, a variable domain in the C-terminus differentiates the members of the family from each other. For example TRIM14, TRIM 34 and TRIM38 all contain a SPRY domain in their C-termini (200). SPRY domains have been shown to mediate RNA binding and protein-protein interactions, yet the exact function is still not known.

The TRIM proteins are of note to our studies because other members of the family have been shown to play roles in restricting replication of both DNA and RNA viruses. TRIM5α has been extensively studied for its role in restricting HIV replication ((200)). Like the three TRIMs mentioned above, TRIM5α also possess a C-terminal SPRY domain, and it is this domain that is responsible for the retroviral restriction. Another extremely well characterized member is TRIM19, also known as promyelocytic leukemia (PML). PML is involved in controlling replication of a wide array of viruses (Lassa virus, influenza, vesicular stomatitis virus, rabies virus, ebola, HIV and HSV-1), yet the exact function it plays in each infection remains to be determined (200). Although not as well studied, TRIM22 is

thought to downregulate HIV transcription (200), and TRIM22 is one of the genes upregulated by both TX02 and MAD78. It is possible that TRIM22 may have some role in limiting WNV infection, but it is probably not responsible for the differences observed between the two strains. Rather, TRIM14, TRIM34 and TRIM38 appear to be better candidates for antiviral effectors controlling MAD78 but not TX02. These proteins are highly expressed during MAD78 infection. However, upregulation of TRIM14 and TRIM38 is lower during TX02 infection, and the expression of TRIM34 is not significantly changed at all. These proteins provide a wonderful starting point for identifying antiviral effector molecules responsible for controlling WNV infection. Perhaps these TRIMs would also be effective against TX02 if their expression was enhanced to levels seen during MAD78 infection. These issues can be readily addressed through overexpression studies and gene knockdown experiments.

Currently, WNV blocks the signaling action of the only treatment approved for use in humans that has any demonstrated efficacy (IFN). Therefore, the identification of cellular antiviral effector molecules effective in controlling WNV is critical to the development of better WNV therapeutics. Future therapies could target the antiviral effectors, increasing their expression and aiding the infected cell in clearing the virus itself. A minimal reduction in viral load may be enough to tip the balance in favor of host immune defenses, restoring IFN signaling and priming of an effective adaptive immune response. The studies presented in this dissertation provide novel insights into the complex virus-host interactions that occur

during WNV infection and could lead to the development of improved antiviral therapy or vaccine strategies.

APPENDIX A
Bird species naturally infected with WNV

Common name	Scientific name	Reference
	Antichromas minutus	(226)
Anhinga	*Anhinga anhinga*	(26)
Bananaquit	*Coereba flaveola*	(66)
Bishop, Red	*Euplectes orix*	(122)
Bittern, Least	*Ixobrychus exilis*	(47)
Blackbird	*Turdus merula*	(36)
Blackbird, Brewer's	*Euphagus cyanocephalus*	(47)
Blackbird, Red-winged	*Agelaius phoeniceus*	(136)
Blackbird, Rusty	*Euphagus carolinus*	(47)
Bluebird, Eastern	*Sialia sialis*	(22)
Bluebird, Mountain	*Sialia currucoides*	(47)
Bluebird, Western	*Sialia mexicana*	(47)
Bobolink	*Dolichonyx oryzivorus*	(47)
Bobwhite, Northern	*Colinus virginianus*	(47)
Budgerigar	*Melopsittacus undulatus*	(47)
Bufflehead	*Bucephala albeola*	(47)
Bulbul, Red-eyed	*Pycnostictus nigricans*	(122)
Bunting, Black-faced	*Emberiza spodocephala*	(255)
Bunting, Blue	*Cyanocompsa parellina*	(70)
Bunting, Indigo	*Passerina cyanea*	(70)
Bunting, Reed	*Emberiza schoeniclus*	(36)
Buzzard	*Buteo buteo*	(36)
Canary, Common	*Serinus canaria*	(47)
Canvasback	*Aythya valisineria*	(47)
Cardinal, Northern	*Cardinalis cardinalis*	(137)
Cardinal, Red Crested	*Paroaria coronata*	(167)
Catbird, Gray	*Dumatella carlinensis*	(250)
Chaffinch	*Fringilla coelebs*	(36)
Chat, Yellow-breasted	*Icteria virens*	(84)
Chickadee, Black-capped	*Poecile atricapilla*	(47)
Chickadee, Carolina	*Parus carolinensis*	(47)
Chickadee, Mountain	*Poecile gambeli*	(47)
Chicken, Greater Prairie	*Tympanuchus cupido*	(47)
Chiffchaff	*Phylloscopus collybita*	(40)
Chukar	*Alectoris chukar*	(47)
Cockatiel	*Nymphicus hollandicus*	(47)
Cockatoo	*Cacatua* spp.	(47)
Conure, Blue-crowned	*Thectocercus acuticaudata*	(47)
Coot	*Fulica atra*	(10)
Coot	*Fulica* spp.	(3)
Coot, American	*Fulica americana*	(47)
Coot, Red-knobbed	*Fulica eristata*	(122)
Cormorant	*Phalacrocorax* spp.	(3)

Common name	Scientific name	Reference
Cormorant, Great	*Phalacrocorax carbo*	(145)
Cormorant, Guanay	*Phalacrocorax bougainvillei*	(167)
Cowbird, Brown-headed	*Molothrus ater*	(250)
Crane, Black-necked	*Grus nigricollis*	(262)
Crane, Demoiselle	*Antrhopoides virgo*	(262)
Crane, Hooded	*Grus monacha*	(167)
Crane, Mississippi sandhill	*Grus canadaensis pulla*	(262)
Crane, Red-crowned (Manchurian)	*Grus japonensis*	(167)
Crane, Sandhill	*Grus canadensis*	(47)
Crane, Siberian	*Grus leucogeranus*	(262)
Crane, Wattled	*Bugeranus carunculatus*	(262)
Crane, West African crowned	*Balearica pavonina pavonina*	(262)
Crane, White Naped	*Grus vipio*	(167)
Crane, Whooping	*Grus americana*	(262)
Crombec, Long-billed	*Sylvietta rufescens*	(37)
Crossbill, Red	*Loxia curvirostra*	(47)
Crow, American	*Corvus brachyrhynchos*	(250)
Crow, Carrion	*Corvus corone*	(36)
Crow, Fish	*Corvus ossifragus*	(250)
Crow, Hooded	*Corvus cornix*	(276)
Crow, Large-billed	*Corvus macrorhynchos*	(255)
Cuckoo	*Cuculus canorus*	(26)
Cuckoo, Hispaniolan lizard	*Saurothera longirostris*	(138)
Cuckoo, Mangrove	*Coccyzus minor*	(138)
Cuckoo, Yellow-billed	*Coccyzus americanus*	(47)
Dickcissel	*Spiza americana*	(47)
Dipper, American	*Cinclus mexicanus*	(47)
Diver, Black-throated	*Gavia arctica*	(10)
Dove, Caribbean	*Leptotila jamaicensis*	(66)
Dove, Common Ground	*Columbina passerina*	(87)
Dove, Eurasian Collared turtle	*Streptopelia decaocto*	(40)
Dove, European turtle	*Streptopelia turtur*	(13)
Dove, Inca	*Columbina inca*	(47)
Dove, Laughing	*Streptopelia senegalensis*	(122)
Dove, Mourning	*Zenaida macroura*	(250)
Dove, Turtle	*Streptopelia capicola*	(122)
Dove, White-winged	*Zenaida asiatica*	(47)
Dove, Zenaida	*Zenaida aurita*	(47)
Drongo, Black (Fork-tailed)	*Dicrurus adsimilis*	(260)
Duck, Bronze-winged	*Anas specularis*	(248)
Duck, Mallard	*Anas platyrhynchos*	(250)
Duck, Mottled	*Anas fulvigula*	(47)
Duck, Muscovy	*Cairina moschata*	(47)
Duck, Roseybill	*Netta peposaca*	(262)
Duck, Ruddy	*Oxyura jamaicensis*	(47)
Duck, Wood	*Aix sponsa*	(47)

Common name	Scientific name	Reference
Duck, Yellow-billed	*Anas undulata*	(47)
Dunnock	*Prunella modularis*	(36)
Eagle, Bald	*Haliaeetus leucocephalus*	(250)
Eagle, Golden	*Aquila chrysaetos*	(47)
Eagle, Tawny	*Aquila rapax*	(217)
Eagle, Wedge-tail	*Aquila audax*	(47)
Egret, Cattle	*Bubulcus ibis*	(84)
Egret, Great	*Ardea alba*	(47)
Egret, Little	*Egretta garzetta*	(210)
Egret, Snowy	*Egretta thula*	(262)
Elaenia, Jamaican	*Myiopagis cotta*	(66)
Emu	*Dromaius novaehollandiae*	(47)
Falcon, Peregrine	*Falco peregrinus*	(78)
Falcon, Prairie	*Falco mexicanus*	(47)
Finch, Cassin's	*Carpodacus cassinii*	(47)
Finch, Gouldian	*Chloebia gouldiae*	(47)
Finch, House	*Carpodacus mexicanus*	(250)
Finch, Purple	*Carpodacus purpureus*	(47)
Finch, Society	*Lonchura domestica*	(47)
Finch, Zebra	*Taeniophygia guttata*	(47)
Flamingo, Chilean	*Phoenicopterus chilensis*	(167)
Flamingo, Greater (American)	*Phoenicopterus ruber ruber*	(47)
Flicker, Northern	*Colaptes auratus*	(47)
Flycatcher, Brown-crested	*Myiarchus tyrranulus*	(70)
Flycatcher, Great-crested	*Myiarchus crinitus*	(257)
Flycatcher, Hammond's	*Empidonax hammondii*	(47)
Flycatcher, Olive-sided	*Contopus cooperi*	(47)
Flycatcher, Pacific-slope	*Empidonax difficilis*	(47)
Flycatcher, Scissor-tailed	*Tyrannus forficatus*	(47)
Flycatcher, Spotted	*Muscicapa striata*	(40)
Flycatcher, Traill's	*Empidonax traillii/alnorum*	(47)
Gallinule, Purple	*Porphyrula martinica*	(47)
Garganey	*Anas querquedula*	(256)
Goldeneye, Common	*Bucephala, clangula*	(47)
Goldfinch, American	*Carduelis tristis*	(257)
Goldfinch, European	*Carduelis carduelis*	(40)
Goldfinch, Lesser	*Carduelis psaltria*	(47)
Goose, Abyssinian blue-winged	*Cyanochen cyanopterus*	(167)
Goose, Barnacle	*Branta leucopsis*	(262)
Goose, Canada	*Branta canadensis*	(136)
Goose, Chinese	*Anser cygnoides*	(47)
Goose, Domestic	*Anser anser domesticus*	(11)
Goose, Emperor	*Chen canagica*	(47)
Goose, Graylag	*Anser anser*	(86)
Goose, Greater Magellan (Andean)	*Chloephagapicta leucoptera*	(262)
Goose, Greater White-fronted	*Anser albifons*	(47)

Common name	Scientific name	Reference
Goose, Hawaiian	*Branta sandvicensis*	(47)
Goose, Red-breasted	*Branta ruficollis*	(47)
Goshawk, Northern	*Accipiter gentilis*	(250)
Grackle, Boat-tailed	*Quiscalus major*	(47)
Grackle, Common	*Quiscalus quiscula*	(250)
Grackle, Great-tailed	*Quiscalus mexicanus*	(47)
Grassquit, Black-faced	*Tiaris bicolor*	(66)
Grebe, Clark's	*Aechmophorus clarkii*	(47)
Grebe, Great	*Podiceps major*	(21)
Grebe, Pied-billed	*Podilymbus podiceps*	(47)
Grosbeak, Black-headed	*Pheucticus melanocephalus*	(47)
Grosbeak, Blue	*Guiraca caerulea*	(262)
Grosbeak, Evening	*Coccothraustes vespertinus*	(47)
Grosbeak, Rose-breasted	*Pheucticus leudovicianus*	(47)
Grouse, Greater Sage	*Centrocercus urophasianus ssp. Phaios*	(47)
Grouse, Ruffed	*Bonasa umbellus*	(47)
Guineafowl, Kenya Crested	*Guttera pucherani*	(167)
Gull, Black headed	*Larus ridibundus*	(40)
Gull, Black-tailed	*Larus crassirostris*	(255)
Gull, California	*Larus californicus*	(47)
Gull, Great black-backed	*Larus marinus*	(250)
Gull, Grey	*Larus modestus*	(167)
Gull, Herring	*Larus argentatus*	(250)
Gull, Laughing	*Larus atricilla*	(167)
Gull, Ring-billed	*Larus delawarensis*	(136)
Gull, Thayer's	*Larus thayeri*	(262)
Gull, White-eyed	*Larus leucophthalmus*	(26)
Gyrfalcon	*Falco rusticolus*	(47)
Harrier, Northern	*Circus cyaneus*	(47)
Hawk, Broad-winged	*Buteo playpterus*	(250)
Hawk, Cooper's	*Accipiter cooperii*	(250)
Hawk, Ferruginous	*Buteo regalis*	(47)
Hawk, Harris'	*Parabuteo unicinctus*	(47)
Hawk, Red-shouldered	*Buteo lineatus*	(47)
Hawk, Red-tailed	*Buteo jamaicensis*	(79)
Hawk, Rough-legged	*Buteo lagopus*	(47)
Hawk, Sharp-shinned	*Accipiter striatus*	(79)
Hawk, Swainson's	*Buteo swainsoni*	(47)
Heron, Black-crowned Night	*Nycticorax nycticorax*	(167)
Heron, Gray	*Ardea cinerea*	(10)
Heron, Great blue	*Ardea herodias*	(250)
Heron, Green	*Butorides virescens*	(22)
Heron, Squacco	*Ardeola ralloides*	(40)
Heron, Yellow-crowned night	*Nyctanassa violacea*	(47)
Hornbill, Abyssinian Ground	*Bucorvus abyssinicus*	(47)
Hummingbird, Anna's	*Calypte anna*	(47)

Common name	Scientific name	Reference
Hummingbird, Ruby-throated	*Archilochus colubris*	(47)
Hummingbird, Rufous	*Selasphorus rufus*	(47)
Ibis, Glossy	*Plegadis falcinellus*	(10)
Ibis, Sacred	*Threskiornis aethiopicus*	(122)
Ibis, Scarlet	*Eudocimus ruber*	(47)
Ibis, Waldrapp	*Geronticus eremita*	(167)
Jay, Blue	*Cyanocitta cristata*	(137)
Jay, Eurasian	*Garrulus glandarius*	(36)
Jay, Mexican	*Aphelocoma ultramarina*	(47)
Jay, Pinyon	*Gymnorhinus cyanocephalus*	(47)
Jay, Steller's	*Cyanocitta stelleri*	(47)
Jay, Western Scrub	*Aphelocoma californica*	(47)
Junco, Dark-eyed	*Junco hyemalis*	(47)
Junglefowl, Green	*Gallus varius*	(167)
Junglefowl, Red (Chicken)	*Gallus gallus*	(87)
Kestrel, American	*Falco sparverius*	(250)
Kestrel, Common	*Falco tinnunculus*	(12)
Kestrel, Lesser	*Falco naumanni*	(12)
Killdeer	*Charadrius vociferus*	(136)
Kingbird, Eastern	*Tyrannus tyrannus*	(47)
Kingbird, Loggerhead	*Tyrannus caudifasciatus*	(66)
Kingbird, Western	*Tyrannus verticalis*	(47)
Kingfisher, Belted	*Ceryle alcyon*	(47)
Kingfisher, Micronesian	*Halcyon cinnamomina*	(47)
Kite, Mississippi	*Ictinia mississippiensis*	(47)
Kite, Swallow-tailed	*Elanoides forficatus*	(47)
Kite, White-tailed	*Elanus leucrus*	(47)
Lapwing, Northern	*Vanellus vanellus*	(92)
Laughingthrush, White-crested	*Garrulax leucolophus*	(262)
Limpkin	*Aramus guarauna*	(47)
Loon, Common	*Gavia immer*	(47)
Lorikeet, Violet-necked	*Eos beckstein*	(47)
Lorkeet, Rainbow	*Trichoglossus haematodus*	(47)
Lory, Black-capped	*Lorius lory*	(47)
Lory, Blue-streaked	*Eos reticulata*	(47)
Lory, Dusky	*Pseudos fuscata*	(47)
Lory, Red	*Eos bornea*	(47)
Macaw	*Ara* spp.	(47)
Magpie, Black-billed	*Pica hudsonia*	(163)
Magpie, Black-billed	*Pica pica*	(255)
Magpie, Yellow-billed	*Pica nuttalli*	(47)
Mannikin, Nutmeg	*Lonchura punctulata*	(262)
Martin, House	*Delichon urbica*	(36)
Martin, Purple	*Progne subis*	(47)
Meadowlark, Eastern	*Sturnella magna*	(84)
Meadowlark, Western	*Sturnella neglecta*	(47)

Common name	Scientific name	Reference
Merganser, Common	*Mergus merganser*	(47)
Merganser, Hooded	*Lophodytes cucullatus*	(47)
Merlin	*Falco columbarius*	(250)
Mockingbird, Northern	*Mimus polyglottos*	(137)
Moorhen, Common	*Gallinula chloropus*	(47)
Nighthawk, Common	*Chordeiles minor*	(47)
Nighthawk, Lesser	*Chordeiles acutipennis*	(47)
Nightingale	*Luscinia megarhynchos*	(40)
Nutcracker, Clark's	*Nucifraga columbiana*	(47)
Nuthatch, Pygmy	*Sitta pygmaea*	(47)
Nuthatch, White-breasted	*Sitta carolinensis*	(47)
Oriole, Baltimore	*Icterus galbula*	(47)
Oriole, Hooded	*Icterus cucullatus*	(47)
Oriole, Jamaican	*Icterus leucopteryx*	(66)
Oriole, Orchard	*Icterus spurius*	(257)
Osprey	*Pandion haliaetus*	(47)
Ostrich	*Struthio camelis*	(262)
Ovenbird	*Seiurus aurocapillus*	(47)
Owl, Barn	*Tyto alba*	(47)
Owl, Barred	*Strix varia*	(78)
Owl, Boreal	*Aegolius funereus*	(79)
Owl, Burrowing	*Athene cunicularia*	(47)
Owl, Eastern screech	*Megascops asio*	(47)
Owl, Elf	*Micrathene whitneyi*	(47)
Owl, Flammulated	*Otus flammeolus*	(79)
Owl, Great gray	*Strix nebulosa*	(79)
Owl, Great horned	*Bubo virginianus*	(251)
Owl, Long-eared	*Asio otus*	(79)
Owl, Milky Eagle	*Bubo lacteus*	(167)
Owl, Northern hawk	*Surnia ulula*	(79)
Owl, Northern pygmy	*Glaucidium gnoma*	(79)
Owl, Northern saw-whet	*Aegolius acadicus*	(79)
Owl, Short-eared	*Asio flammeus*	(79)
Owl, Snowy	*Nyctea scandiaca*	(167)
Owl, Spotted	*Strix oocidentalis*	(47)
Owl, Tawny	*Strix aluco*	(79)
Owl, Typical		(26)
Owl, Western screech	*Otus kennicottii*	(47)
Parakeet		(22)
Parakeet, Canary-winged	*Brotogeris versicolurus*	(47)
Parakeet, Monk	*Myiopsitta monachus*	(136)
Parrot, African Gray	*Psittacus erythacus*	(47)
Parrot, Greater vasa	*Coracopsis vasa*	(37)
Parrot, Red-crowned	*Amazona viridigenalis*	(47)
Parrot, Thick-billed	*Rhynchopsitta pachyrhyncha*	(47)
Parrotlet, Pacific	*Forpus coelestis*	(47)

Common name	Scientific name	Reference
Partridge, Crested Wood	*Rollulus roulroul*	(167)
Parula, Northern	*Parula americana*	(47)
Peafowl, Common	*Pavo cristatus*	(47)
Pelican, American White	*Pelecanus erythrorhynchos*	(47)
Pelican, Brown	*Pelecanus occidentalis*	(167)
Penguin, Humboldt	*Spheniscus humboldti*	(47)
Penguin, Magellan	*Spheniscus magellanicus*	(167)
Penquin, Black-footed (Jackass)	*Spheniscus demersus*	(47)
Pheasant, Blue-eared	*Crossoptilan aurifum*	(47)
Pheasant, Bulwar's Wattled	*Lophura bulweri*	(167)
Pheasant, Impeyan	*Lophophorus impeyanus*	(250)
Pheasant, Monal	*Lophophorus ihuysii*	(47)
Pheasant, Mount Peacock	*Polyplectron inopinatum*	(167)
Pheasant, Ring-necked	*Phasianus colchicus*	(136)
Phoebe, Black	*Sayornis nigricans*	(47)
Phoebe, Eastern	*Sayornis phoebe*	(47)
Pigeon, Bleeding Heart	*Gallicolumba luzonica*	(167)
Pigeon, Domestic	*Columba livia*	(5)
Pigeon, Mauritius Pink	*Columba mayeri*	(167)
Pigeon, White-crowned	*Columba leucocephala*	(47)
Pipit	*Anthus* spp.	(26)
Pipit, Meadow	*Anthus pratensus*	(36)
Plaintain-eater, Lady Ross'	*Musophaga rossae*	(167)
Plover, Piping	*Charadrius melodus*	(47)
Quail	*Coturnix coturnix*	(97)
Quail, California	*Callipepla californica*	(47)
Quail, Japanese	*Coturnix japonicus*	(136)
Quail, Mountain	*Oreortyx pictus*	(47)
Quail-dove, Ruddy	*Geotrygon montana*	(138)
Quelea, Red-billed	*Quelea quelea*	(122)
Rail, Clapper	*Rallus longirostris*	(262)
Rail, Virginia	*Rallus limicola*	(47)
Raven, Chihuahuan	*Corvus cryptoleucus*	(47)
Raven, Common	*Corvus corax*	(250)
Redstart		(36)
Robin	*Erithacus rubecula*	(226)
Robin, American	*Turdus migratorius*	(250)
Rook	*Corvus frugilegus*	(256)
Rosella, Crimson	*Platycercus elegans*	(47)
Sandpiper, Green	*Tringa ochropus*	(92)
Sandpiper, Western	*Calidris mauri*	(47)
Sandpiper, Wood	*Tringa glareola*	(97)
Sapsucker, Red-breasted	*Sphyrapicus ruber*	(47)
Sapsucker, Yellow-bellied	*Sphyrapicus varius*	(47)
Scaup, Greater	*Aythya marila*	(47)
Scaup, Lesser	*Aythya affinis*	(47)

Common name	Scientific name	Reference
Shrike	*Lanius* spp.	(26)
Shrike, Loggerhead	*Lanius ludovicianus*	(257)
Shrike, Red backed	*Lanius collurio*	(40)
Siskin, Pine	*Carduelis pinus*	(47)
Skimmer, Black	*Rhynchops niger*	(47)
Smew	*Mergellus albellus*	(47)
Sparrow, Black-chinned	*Spizella atrogularis*	(47)
Sparrow, Field	*Spizella pusilla*	(47)
Sparrow, Fox	*Passerella iliaca*	(47)
Sparrow, Golden-crowned	*Zonotrichia atricapilla*	(262)
Sparrow, House	*Passer domesticus*	(137)
Sparrow, Lark	*Chondestes grammacus*	(47)
Sparrow, Savannah	*Passerculus sandwichensis*	(47)
Sparrow, Song	*Melospiza melodia*	(47)
Sparrow, Tree	*Passer montanus*	(40)
Sparrow, White-crowned	*Zonotrichia leucophrys*	(47)
Sparrow, White-throated	*Zonotrichia albicollis*	(84)
Starling, European	*Sturnus vulgaris*	(250)
Stint, Little	*Calidris minuta*	(97)
Stork, Lesser Adjutant	*Leptoptilos javanicus*	(167)
Stork, Marabou	*Leptopilos crumeniferus*	(262)
Stork, Sand-billed	*Ephippiorhynchos senegalensis*	(262)
Stork, White	*Ciconia ciconi*	(13)
Swallow, Bank	*Riparia riparia*	(47)
Swallow, Barn	*Hirundo rustica*	(47)
Swallow, Cliff	*Petrochelidon pyrrhonota*	(47)
Swallow, Tree	*Tachycineta bicolor*	(47)
Swan, Mute	*Cygnus olor*	(47)
Swan, Trumpeter	*Cygnus cygnus buccinator*	(262)
Swan, Tundra	*Cygnus columbianus*	(47)
Swift, Chimney	*Chaetura pelagica*	(47)
Tanager, Palm	*Thraupis palmarum*	(47)
Tanager, Scarlet	*Piranga olivacea*	(250)
Tanager, Summer	*Piranga rubra*	(262)
Tanager, Western	*Piranga ludoviciana*	(47)
Teal	*Anas crecca*	(256)
Teal, Cinnamon	*Anas cyanoptera*	(47)
Teal, Puna	*Anas puna*	(47)
Teal, Red-bill	*Anas erythrorhyncha*	(122)
Tern, Inca	*Larosterna inca*	(47)
Thrasher, Brown	*Toxostoma rufum*	(47)
Thrush, Gray-cheeked	*Catharus minimus*	(47)
Thrush, Hermit	*Catharus guttatus*	(47)
Thrush, Kukrichane	*Turdus libonyacus*	(260)
Thrush, Olive	*Turdus olivaceus*	(122)
Thrush, Red-legged	*Turdus plumbeus*	(138)

Common name	Scientific name	Reference
Thrush, Song	*Turdus philornelos*	(36)
Thrush, Swainson's	*Catharus ustulatus*	(47)
Thrush, Varied	*Ixoreus naevius*	(47)
Thrush, White-chinned	*Turdus aurantius*	(66)
Thrush, White-eyed	*Turdus jamaicensis*	(66)
Thrush, Wood	*Hylocichla mustelina*	(22)
Tinamou, Elegant Crested	*Eudromia elegans*	(47)
Tit, Blue	*Parus caeruleus*	(40)
Tit, Great	*Parus major*	(36)
Tit, Japanese	*Parus minor*	(255)
Tit, Penduline	*Remiz pendulinus*	(40)
Tit, Varied	*Parus varius*	(47)
Titmouse	*Parus* spp.	(26)
Titmouse, Tufted	*Baeolophus bicolor*	(257)
Towhee, California	*Pipilo crissalis*	(47)
Towhee, Eastern	*Pipilo erythrophthalmus*	(47)
Towhee, Spotted	*Pipilo maculatus*	(47)
Tragopan, Blyth's	*Tragopan blythii*	(167)
Tragopan, Satyr	*Tragopan satyr*	(47)
Troupial	*Icterus icterus*	(26)
Turkey, Wild & Domestic	*Meleagris gallopavo*	(167)
Turnstone, Ruddy	*Arenaria interpres*	(47)
Veery	*Catharus fuscescens*	(47)
Verdin	*Auriparus flaviceps*	(72)
Vireo	*Vireo* spp.	(26)
Vireo, Black-whiskered	*Vireo altiloquus*	(47)
Vireo, Jamaican	*Vireo modestus*	(66)
Vireo, Red-eyed	*Vireo olivaceus*	(47)
Vireo, Warbling	*Vireo gilvus*	(47)
Vulture, Black	*Coragyps atratus*	(47)
Vulture, Cinereus	*Aegypius monachus*	(47)
Vulture, King	*Sarcoramphus papa*	(167)
Vulture, Turkey	*Cathartes aura*	(47)
Waldrapp	*Geronticus eremita*	(262)
Warbler, Barred	*Sylvia risoria*	(199)
Warbler, Black and white	*Mniotilta varia*	(66)
Warbler, Blackpoll	*Dendroica striata*	(47)
Warbler, Black-throated Blue	*Dendroica caerulescens*	(47)
Warbler, Canada	*Wilsonia canadensis*	(47)
Warbler, Cape reed	*Acrocephalus gracilirostris*	(122)
Warbler, Garden	*Sylvia borin*	(36)
Warbler, Grasshopper	*Locustella naevia*	(40)
Warbler, Hooded	*Wilsonia citrina*	(47)
Warbler, Kentucky	*Oporornis formosus*	(47)
Warbler, Magnolia	*Dendroica magnolia*	(262)
Warbler, Marsh	*Acrocephalus palustris*	(40)

Common name	Scientific name	Reference
Warbler, Nashville	*Vermivora ruficapilla*	(47)
Warbler, Old world	Family SYLVIIDAE	(26)
Warbler, Orange-crowned	*Vermivora celata*	(47)
Warbler, Prairie	*Dendroica discolor*	(262)
Warbler, Reed	*Acrocephalus scirpaceus*	(36)
Warbler, Sedge	*Acrocephalus schoenobaenus*	(36)
Warbler, Tennessee	*Vermivora peregrina*	(262)
Warbler, Townsend's	*Dendroica townsendsi*	(47)
Warbler, Willow	*Phylloscopus trochilus*	(40)
Warbler, Wilson's	*Wilsonia pusilla*	(47)
Warbler, Yellow	*Dendroica petechia*	(66)
Warbler, Yellow-rumped	*Dendroica coronata*	(47)
Warbler, Yellow-throated	*Dendroica dominica*	(262)
Waterhen		(21)
Waterthrush, Northern	*Seiurus noveboracensis*	(47)
Waxwing, Cedar	*Bombycilla cedrorum*	(47)
Weaver, Masked	*Ploceus velatus*	(122)
Whitethroat	*Sylvia* spp.	(36)
Whitethroat, Lesser	*Sylvia curruca*	(36)
Wigeon, Eurasian	*Anas penelope*	(47)
Woodpecker, Acorn	*Melanerpes formicivorus*	(47)
Woodpecker, Downy	*Picoides pubescens*	(47)
Woodpecker, Gila	*Melanerpes uropygialis*	(47)
Woodpecker, Green	*Picus viridis*	(36)
Woodpecker, Hairy	*Picoides villosus*	(47)
Woodpecker, Lesser spotted	*Dendrocopos minor*	(40)
Woodpecker, Lewis'	*Melanerpes lewis*	(47)
Woodpecker, Pileated	*Dryocopus pileatus*	(84)
Woodpecker, Red-bellied	*Melanerpes carolinus*	(47)
Woodpecker, Red-headed	*Melanerpes erythrocephalus*	(47)
Woodpecker, Syrian	*Dendrocopos syriacus balcanicus*	(40)
Wren, Bewick's	*Thryomanes bewickii*	(72)
Wren, Cactus	*Campylorhynchus brunneicapillus*	(47)
Wren, Carolina	*Thryothaurus ludovicianus*	(47)
Wren, House	*Troglodytes aedon*	(47)
Wren, Winter	*Troglodytes troglodytes*	(47)
Yellow-throat, Common	*Geothlypis trichas*	(121)

APPENDIX B
Potential arthropod vectors for WNV transmission

Common name	Scientific name	Reference
Fly, Louse	*Icosta americana*	(69)
Midge, Biting	*Culicoides Latreille*	(220)
Mite, Poultry Red (Chicken)	*Dermanyssus gallinae*	(192)
Mite, Tropical Fowl	*Ornithonyssus sylviarum*	(192)
Mosquito	*Aedeomyia africana*	(109)
Mosquito	*Aedes aegypti*	(109)
Mosquito	*Aedes africanus*	(109)
Mosquito	*Aedes albocephalus*	(109)
Mosquito	*Aedes albopictus*	(41)
Mosquito	*Aedes albothorax*	(226)
Mosquito	*Aedes atlanticus/tormentor*	(41)
Mosquito	*Aedes atropalpus*	(41)
Mosquito	*Aedes caballus*	(37)
Mosquito	*Aedes canadensis*	(41)
Mosquito	*Aedes cantans*	(109)
Mosquito	*Aedes cantator*	(41)
Mosquito	*Aedes caspius*	(109)
Mosquito	*Aedes cinereus*	(8)
Mosquito	*Aedes circumluteolus*	(109)
Mosquito	*Aedes condolescens*	(41)
Mosquito	*Aedes dorsalis*	(41)
Mosquito	*Aedes dupreei*	(41)
Mosquito	*Aedes excrucians*	(109)
Mosquito	*Aedes fitchii*	(41)
Mosquito	*Aedes fulvus pallens*	(41)
Mosquito	*Aedes grossbecki*	(41)
Mosquito	*Aedes infirmatus*	(41)
Mosquito	*Aedes japonicus*	(41)
Mosquito	*Aedes madagascarensis*	(109)
Mosquito	*Aedes malanimon*	(41)
Mosquito	*Aedes nigromaculis*	(41)
Mosquito	*Aedes provocans*	(41)
Mosquito	*Aedes sollicitans*	(41)
Mosquito	*Aedes squamiger*	(41)
Mosquito	*Aedes sticticus*	(41)
Mosquito	*Aedes stimulans*	(41)
Mosquito	*Aedes taeniorhynchus*	(41)
Mosquito	*Aedes triseriatus*	(41)
Mosquito	*Aedes trivittatus*	(41)
Mosquito	*Aedes vexans*	(8)
Mosquito	*Anopheles atropos*	(26)
Mosquito	*Anopheles barberi*	(41)
Mosquito	*Anopheles bradleyi*	(41)

Common name	Scientific name	Reference
Mosquito	*Anopheles brunnipes*	(109)
Mosquito	*Anopheles coustani*	(109)
Mosquito	*Anopheles crucians*	(26)
Mosquito	*Anopheles franciscanus*	(41)
Mosquito	*Anopheles freeborni*	(41)
Mosquito	*Anopheles hermsi*	(41)
Mosquito	*Anopheles maculipalpis*	(109)
Mosquito	*Anopheles maculipennis*	(109)
Mosquito	*Anopheles punctipennis*	(8)
Mosquito	*Anopheles quadrimaculatus*	(41)
Mosquito	*Anopheles subpictus*	(109)
Mosquito	*Anopheles walkeri*	(8)
Mosquito	*Coquilletidia metallica*	(226)
Mosquito	*Coquilletidia microannulata*	(109)
Mosquito	*Coquilletidia richardii*	(109)
Mosquito	*Coquillettidia perturbans*	(88)
Mosquito	*Culex annulirostris*	(226)
Mosquito	*Culex antennatus*	(109)
Mosquito	*Culex barraudius*	(190)
Mosquito	*Culex bitaeniorhynchus*	WNV strain WNI80755Cb Genbank entry #AY639641
Mosquito	*Culex coronator*	(41)
Mosquito	*Culex decens*	(109)
Mosquito	*Culex erraticus*	(41)
Mosquito	*Culex erythrothorax*	(41)
Mosquito	*Culex ethiopicus*	(109)
Mosquito	*Culex fatigans*	(205)
Mosquito	*Culex guiarti*	(226)
Mosquito	*Culex modestus*	(109)
Mosquito	*Culex molestus*	(181)
Mosquito	*Culex neavei*	(226)
Mosquito	*Culex nigripalpus*	(192)
Mosquito	*Culex nigripes*	(109)
Mosquito	*Culex palpalis*	(265)
Mosquito	*Culex perexiguus*	(109)
Mosquito	*Culex perfuscus*	(109)
Mosquito	*Culex pipiens pipiens L*	(175)
Mosquito	*Culex poicilipes*	(109)
Mosquito	*Culex pruina*	(109)
Mosquito	*Culex quinquefasciatus*	(88)
Mosquito	*Culex restuans*	(8)
Mosquito	*Culex salinarius*	(88)
Mosquito	*Culex scottii*	(109)
Mosquito	*Culex stigmatosoma*	(41)
Mosquito	*Culex tarsalis*	(41)
Mosquito	*Culex territans*	(41)

Common name	Scientific name	Reference
Mosquito	*Culex theileri*	(109)
Mosquito	*Culex thriambus*	(41)
Mosquito	*Culex tritaeniorhynchus*	(109)
Mosquito	*Culex univitattus*	(226)
Mosquito	*Culex vishnui*	WNV strain WNI804987Cv Genbank entry #AY639642
Mosquito	*Culex weschei*	(109)
Mosquito	*Culex whitmorei*	WNV strain WNI80829Cw GenBank entry #AY639640
Mosquito	*Culiseta impatiens*	(41)
Mosquito	*Culiseta inornata*	(41)
Mosquito	*Culiseta melanura*	(8)
Mosquito	*Culiseta morsitans*	(41)
Mosquito	*Deinocerites cancer*	(26)
Mosquito	*Mansonia metallica*	(275)
Mosquito	*Mansonia tittilans*	(41)
Mosquito	*Mansonia uniformis*	(109)
Mosquito	*Mimomyia hispida*	(109)
Mosquito	*Mimomyia lacustris*	(109)
Mosquito	*Mimomyia splendens*	(109)
Mosquito	*Ocherotatus atlanticus*	(26)
Mosquito	*Ochlerotatus canadensis*	(8)
Mosquito	*Ochlerotatus cantator*	(8)
Mosquito	*Ochlerotatus japonicus*	(175)
Mosquito	*Ochlerotatus sollicitans*	(8)
Mosquito	*Ochlerotatus sticticus*	(8)
Mosquito	*Ochlerotatus taeniorhynchus*	(8)
Mosquito	*Ochlerotatus triseriatus*	(8)
Mosquito	*Ochlerotatus trivittatus*	(8)
Mosquito	*Orthopodomyia signifera*	(41)
Mosquito	*Psorophora ciliata*	(41)
Mosquito	*Psorophora columbiae*	(41)
Mosquito	*Psorophora ferox*	(8)
Mosquito	*Psorophora howardii*	(41)
Mosquito	*Uranotaenia sapphirina*	(8)
Tick	*Argas reflexus hermanii*	(229)
Tick	*Haemaphysalis leachii*	(25)
Tick	*Hyalomma detritum*	(169)
Tick	*Hyalomma marginatum*	(109)
Tick	*Rhipicephalus turanicus*	(192)
Tick, Cattle egret argas	*Argas arboreus*	(192)
Tick, Hard	*Amblyomma variegatum*	(109)
Tick, Hard	*Dermacentor marginatus*	(109)
Tick, Hard	*Hyalomma detritum*	(109)
Tick, Hard	*Rhipicephalus muhsamae*	(109)
Tick, Hard	*Rhipicephalus turanicus*	(109)
Tick, Soft	*Argas hermann*i	(109)

Common name	Scientific name	Reference
Tick, Soft	*Ornithodoros capensis*	(109)

APPENDIX C
WNV naturally infects a broad array of mammalian species

Common name	Scientific name	Reference
Alpaca, Suri	*Lama pacos*	(278)
Babirusa	*Babyrousa babyrousa*	(262)
Baboon, Olive	*Papio cynocephalus anubis*	(262)
Bat, Big brown	*Eptesicus fuscus*	(262)
Bat, Frugivorous	*Rousettus leschenaulti*	(204)
Bat, Fruit	*Pteropus rufus*	(73)
Bat, Little brown	*Myotis lucifugus*	(262)
Bat, Northern long-eared	*Myotis septentrionalis*	(262)
Bear, Black	*Ursus americanus*	(262)
Bear, European brown	*Ursus arctos*	(174)
Boar, Wild	*Sus scrofa*	(85)
Buffalo, Water	*Bubalus bubalis*	(110)
Bush baby, Lesser	*Galago senegalensis*	(37)
Camel	*Camelus* spp.	(110)
Cat, Domestic	*Felis catus*	(262)
Cattle, Domestic	*Bos taurus*	(262)
Chimpanzee	*Pan troglodytes*	(201)
Chipmunk, Eastern	*Tamias striatus*	(262)
Cow, Indian	*Bos indicus*	(99)
Coyote	*Canis latrans*	(185)
Deer, Fallow	*Dama dama*	(123)
Deer, Mule	*Odocoileus hemionus*	(262)
Deer, Red	*Capreolus capreolus*	(123)
Deer, Roe	*Cervus elaphus*	(123)
Deer, White-tailed	*Odocoileus virginianus*	(224)
Dog, Domestic	*Canis familiaris*	(132)
Donkey	*Equus asinus*	(262)
Elephant, Indian	*Elephas maximus indicus*	(262)
Fox, Red	*Vulpes vulpes*	(185)
Goat, Domestic	*Capra hircus*	(64)
Goat, Mountain	*Oreamnos americanus*	(262)
Hamster		(180)
Hare, Brown	*Lepus europaeus*	(123)
Hedgehog	*Erinaceus europaeus*	(243)
Horse, Domestic	*Equus equus przeqalski caballus*	(65)
Lemur	*Lemur fulvus*	(99)
Lemur, Ring-tail	*Lemur catta*	(262)
Leopard, Snow	*Panthera uncia*	(262)
Llama	*Lama glama*	(262)
Macaque, Barbary	*Macaca sylvanus*	(262)
Macaque, Pigtail	*Macaca nemestrina*	(212)
Macaque, Rhesus	*Macaca mulatta*	(262)
Mangabey, Sooty	*Cercocebus atys*	(54)

Common name	Scientific name	Reference
Mole, Roman	*Talpa romana*	(149)
Mouse, Western European house	*Mus musculus domesticus*	(149)
Mouse, Western wild	*Mus spretus*	(50)
Mouse, Yellow-necked	*Apodemus flavicollis*	(109)
Mule		(262)
Opossum, Virginia	*Didelphis virginiana*	(185)
Ox		(4)
Panda, Red	*Ailurus fulgens fulgens*	(262)
Pig	*Sus spp.*	(211)
Prairie Dog, Black-tailed	*Cynomys ludovicianus*	(262)
Rabbit, Domestic	*Oryctolagus cuniculus*	(262)
Raccoon	*Procyon lotor*	(185)
Rat, Black (House)	*Rattus rattus*	(63)
Rat, Hispid cotton	*Sigmodon hispidus*	(63)
Rat, Nile (African) Grass	*Arvicanthis niloticus*	(109)
Reindeer	*Rangifer tarandus*	(203)
Rhinoceros, Great Indian	*Rhinoceros unicornis*	(262)
Rousette, Leschenault's	*Rousettus leschenaulti*	(109)
Seal, Harbor	*Phoca vitulina*	(262)
Sheep, Domestic (Suffolk)	*Ovis aries*	(12)
Shrew, House	*Suncus murinus*	(215)
Shrew, White-toothed	*Crocidura russula*	(50)
Skunk, Striped	*Mephitis mephitis*	(262)
Squirrel, Fox	*Sciurus niger*	(101)
Squirrel, Gray	*Sciurus carolinensis*	(63)
Vole, Bank	*Clethrionomys glareolus*	(109)
Wolf, Arctic	*Canis lupus*	(158)
	Aethomys spp.	(122)

APPENDIX D
Reptiles and amphibians are susceptible hosts for WNV

Common name	Scientific name	Natural infection	Experimental infection	Reference
Alligator, American	*Alligator mississippiensis*	X		(115)
Bullfrog, North American	*Rana catesbeiana*		X	(135)
Crocodile	*Crocodylus niloticus*	X		(249)
Crocodile Monitor	*Varamus salvadori*	X		(262)
Frog, Lake	*Rana ridibunda*		X	(139)
Iguana, Green	*Iguana iguana*		X	(135)
Snake, Florida garter	*Thamnophis sirtalis sirtalis*		X	(135)

BIBLIOGRAPHY

1. **Adachi, J. and Hasegawa, M.** 1996**.** MOLPHY version 2.3: Programs for molecular phylogenetics based on maximum likelihood. Computer Science Monographs. Institute of Statistical Mathematics. Tokyo. **28:**1-150.

2. **Agaisse, H. and N. Perrimon**. 2004. The roles of JAK/STAT signaling in Drosophila immune responses. Immunol. Rev. **198**:72-82.

3. **Al'khovskii, S. V., D. N. L'vov, E. I. Samokhvalov, A. G. Prilipov, D. K. L'vov, V. A. Aristova, V. L. Gromashevskii, A. F. Dzharkenov, A. I. Kovtunov, P. G. Deriabin, E. I. Odolevskii, and R. M. Ibragimov**. 2003. [Screening of birds in the Volga delta (Astrakhan region, 2001) for the West Nile virus by reverse transcription-polymerase chain reaction]. Vopr. Virusol. **48**:14-17.

4. **Alexander, W. S.** 2002. Suppressors of cytokine signalling (SOCS) in the immune system. Nat. Rev. Immunol. **2**:410-416.

5. **Allison, A. B., D. G. Mead, S. E. Gibbs, D. M. Hoffman, and D. E. Stallknecht**. 2004. West Nile virus viremia in wild rock pigeons. Emerg. Infect. Dis. **10**:2252-2255.

6. **Alpert, S. G., J. Fergerson, and L. P. Noel**. 2003. Intrauterine West Nile virus: ocular and systemic findings. Am. J. Ophthalmol. **136**:733-735.

7. **Anderson, J. F. and J. J. Rahal**. 2002. Efficacy of interferon alpha-2b and ribavirin against West Nile virus in vitro. Emerg. Infect. Dis. **8**:107-108.

8. **Andreadis, T. G., J. F. Anderson, C. R. Vossbrinck, and A. J. Main**. 2004. Epidemiology of West Nile virus in Connecticut: a five-year analysis of mosquito data 1999-2003. Vector Borne Zoonotic. Dis. **4**:360-378.

9. **Ank, N., H. West, and S. R. Paludan**. 2006. IFN-lambda: novel antiviral cytokines. J. Interferon Cytokine Res. **26**:373-379.

10. **Antipa, C., E. Girjabu, R. Iftimovici, and N. Draganescu**. 1984. Serological investigations concerning the presence of antibodies to arboviruses in wild birds. Virologie. **35**:5-9.

11. **Austin, R. J., T. L. Whiting, R. A. Anderson, and M. A. Drebot**. 2004. An outbreak of West Nile virus-associated disease in domestic geese (Anser anser domesticus) upon initial introduction to a geographic region, with evidence of bird to bird transmission. Can. Vet. J. **45**:117-123.

12. **Banet-Noach, C., A. Y. Gancz, A. Lublin, and M. Malkinson**. 2004. A twelve-month study of West Nile virus antibodies in a resident and a migrant species of kestrels in Israel. Vector Borne Zoonotic. Dis. **4**:15-22.

13. **Banet-Noach, C., M. Malkinson, A. Brill, I. Samina, H. Yadin, Y. Weisman, S. Pokamunski, R. King, V. Deubel, and Y. Stram**. 2003. Phylogenetic

relationships of West Nile viruses isolated from birds and horses in Israel from 1997 to 2001. Virus Genes **26**:135-141.

14. **Banninger, G. and N. C. Reich**. 2004. STAT2 nuclear trafficking. J. Biol. Chem. **279**:39199-39206.

15. **Baqar, S., C. G. Hayes, J. R. Murphy, and D. M. Watts**. 1993. Vertical transmission of West Nile virus by Culex and Aedes species mosquitoes. Am. J. Trop. Med. Hyg. **48**:757-762.

16. **Beasley, D. W., C. T. Davis, H. Guzman, D. L. Vanlandingham, A. P. Travassos Da Rosa, R. E. Parsons, S. Higgs, R. B. Tesh, and A. D. Barrett**. 2003. Limited evolution of West Nile virus has occurred during its southwesterly spread in the United States. Virology **309**:190-195.

17. **Beasley, D. W., C. T. Davis, M. Whiteman, B. Granwehr, R. M. Kinney, and A. D. Barrett**. 2004. Molecular determinants of virulence of West Nile virus in North America. Arch. Virol. Suppl35-41.

18. **Beasley, D. W., L. Li, M. T. Suderman, and A. D. Barrett**. 2002. Mouse neuroinvasive phenotype of West Nile virus strains varies depending upon virus genotype. Virology **296**:17-23.

19. **Beasley, D. W., M. C. Whiteman, S. Zhang, C. Y. Huang, B. S. Schneider, D. R. Smith, G. D. Gromowski, S. Higgs, R. M. Kinney, and A. D. Barrett**. 2005. Envelope protein glycosylation status influences mouse neuroinvasion

phenotype of genetic lineage 1 West Nile virus strains. J. Virol. **79**:8339-8347.

20. **Bell, J. K., G. E. Mullen, C. A. Leifer, A. Mazzoni, D. R. Davies, and D. M. Segal**. 2003. Leucine-rich repeats and pathogen recognition in Toll-like receptors. Trends Immunol. **24**:528-533.

21. **Berezin VV, Semenov BF, Reschetnikov IA, and Baschkirtsev VN**. 1972. Importance of birds in the natural cycle of arboviruses transmitted by mosquitoes in the Volga delta., p. 310-313. *In* Cherepanov IA (ed.), Transcontinental connections of migrating birds and their role in arbovirus distribution. Novosibirsk, Russia: Nauka.

22. **Bernard, K. A., J. G. Maffei, S. A. Jones, E. B. Kauffman, G. Ebel, A. P. Dupuis, K. A. Ngo, D. C. Nicholas, D. M. Young, P. Y. Shi, V. L. Kulasekera, M. Eidson, D. J. White, W. B. Stone, and L. D. Kramer**. 2001. West Nile virus infection in birds and mosquitoes, New York State, 2000. Emerg. Infect. Dis. **7**:679-685.

23. **Berthet, F. X., H. G. Zeller, M. T. Drouet, J. Rauzier, J. P. Digoutte, and V. Deubel**. 1997. Extensive nucleotide changes and deletions within the envelope glycoprotein gene of Euro-African West Nile viruses. J. Gen. Virol. **78 (Pt 9)**:2293-2297.

24. **Best, S. M., K. L. Morris, J. G. Shannon, S. J. Robertson, D. N. Mitzel, G. S. Park, E. Boer, J. B. Wolfinbarger, and M. E. Bloom**. 2005. Inhibition of interferon-stimulated JAK-STAT signaling by a tick-borne flavivirus and identification of NS5 as an interferon antagonist. J. Virol. **79**:12828-12839.

25. **Blackburn, N. K., F. Reyers, W. L. Berry, and A. J. Shepherd**. 1989. Susceptibility of dogs to West Nile virus: a survey and pathogenicity trial. J. Comp Pathol. **100**:59-66.

26. **Blackmore, C. G., L. M. Stark, W. C. Jeter, R. L. Oliveri, R. G. Brooks, L. A. Conti, and S. T. Wiersma**. 2003. Surveillance results from the first West Nile virus transmission season in Florida, 2001. Am. J. Trop. Med. Hyg. **69**:141-150.

27. **Blackwell, J. L. and M. A. Brinton**. 1995. BHK cell proteins that bind to the 3' stem-loop structure of the West Nile virus genome RNA. J. Virol. **69**:5650-5658.

28. **Blackwell, J. L. and M. A. Brinton**. 1997. Translation elongation factor-1 alpha interacts with the 3' stem-loop region of West Nile virus genomic RNA. J. Virol. **71**:6433-6444.

29. **Bode, J. G., S. Ludwig, C. A. Freitas, F. Schaper, M. Ruhl, S. Melmed, P. C. Heinrich, and D. Haussinger**. 2001. The MKK6/p38 mitogen-activated

protein kinase pathway is capable of inducing SOCS3 gene expression and inhibits IL-6-induced transcription. Biol. Chem. **382**:1447-1453.

30. **Borisevich, V., A. Seregin, R. Nistler, D. Mutabazi, and V. Yamshchikov**. 2006. Biological properties of chimeric West Nile viruses. Virology.

31. **Bovee, M. L., W. E. Marissen, M. Zamora, and R. E. Lloyd**. 1998. The predominant elF4G-specific cleavage activity in poliovirus-infected HeLa cells is distinct from 2A protease. Virology **245**:229-240.

32. **Brault, A. C., S. A. Langevin, R. A. Bowen, N. A. Panella, B. J. Biggerstaff, B. R. Miller, and K. Nicholas**. 2004. Differential virulence of West Nile strains for American crows. Emerg. Infect. Dis. **10**:2161-2168.

33. **Brazma, A., P. Hingamp, J. Quackenbush, G. Sherlock, P. Spellman, C. Stoeckert, J. Aach, W. Ansorge, C. A. Ball, H. C. Causton, T. Gaasterland, P. Glenisson, F. C. Holstege, I. F. Kim, V. Markowitz, J. C. Matese, H. Parkinson, A. Robinson, U. Sarkans, S. Schulze-Kremer, J. Stewart, R. Taylor, J. Vilo, and M. Vingron**. 2001. Minimum information about a microarray experiment (MIAME)-toward standards for microarray data. Nat. Genet. **29**:365-371.

34. **Brierley, M. M. and E. N. Fish**. 2005. Stats: multifaceted regulators of transcription. J. Interferon Cytokine Res. **25**:733-744.

35. **Brinton, M. A.** 2002. The molecular biology of West Nile Virus: a new invader of the western hemisphere. Annu. Rev. Microbiol. **56**:371-402.

36. **Buckley, A., A. Dawson, S. R. Moss, S. A. Hinsley, P. E. Bellamy, and E. A. Gould**. 2003. Serological evidence of West Nile virus, Usutu virus and Sindbis virus infection of birds in the UK. J. Gen. Virol. **84**:2807-2817.

37. **Burt, F. J., A. A. Grobbelaar, P. A. Leman, F. S. Anthony, G. V. Gibson, and R. Swanepoel**. 2002. Phylogenetic relationships of southern African West Nile virus isolates. Emerg. Infect. Dis. **8**:820-826.

38. **Campbell, G. L., A. A. Marfin, R. S. Lanciotti, and D. J. Gubler**. 2002. West Nile virus. Lancet Infect. Dis. **2**:519-529.

39. **Cebulla, C. M., D. M. Miller, and D. D. Sedmak**. 1999. Viral inhibition of interferon signal transduction. Intervirology **42**:325-330.

40. **Ceianu, C. S., A. Ungureanu, G. Nicolescu, C. Cernescu, L. Nitescu, G. Tardei, A. Petrescu, D. Pitigoi, D. Martin, V. Ciulacu-Purcarea, A. Vladimirescu, and H. M. Savage**. 2001. West nile virus surveillance in Romania: 1997-2000. Viral Immunol. **14**:251-262.

41. **Centers for Diseaes Control.** 2005. West Nile Virus Entomology. Division of Vector-Borne Infectious Diseases, Centers for Disease Control. www.cdc.gov/ncidod/dvbid/westnile/mosquitoSpecies.htm. 3-11-2007.

42. **Centers for Disease Control**. 2002. Intrauterine West Nile virus infection--New York, 2002. MMWR Morb. Mortal. Wkly. Rep. **51**:1135-1136.

43. **Centers for Disease Control**. 2002. Laboratory-Acquired West Nile Virus Infections --- United States, 2002. MMWR Morb. Mortal. Wkly. Rep. **51**:1133-1135.

44. **Centers for Disease Control**. 2002. Possible West Nile virus transmission to an infant through breast-feeding--Michigan, 2002. MMWR Morb. Mortal. Wkly. Rep. **51**:877-878.

45. **Centers for Disease Control**. 2004. Possible dialysis-related west nile virus transmission--Georgia, 2003. MMWR Morb. Mortal. Wkly. Rep. **53**:738-739.

46. **Centers for Disease Control.** 2004. West Nile Virus: Information and Guidance for Clinicians. Division of Vector-Borne Infectious Diseases, Centers for Disease Control. http://www.cdc.gov/ncidod/dvbid/westnile/clinicians/. 3-24-2007.

47. **Centers for Disease Control.** 2005. West Nile Virus Vertebrate Ecology. Division of Vector-Borne Infectious Diseases, Centers for Disease Control. http://www.cdc.gov/ncidod/dvbid/westnile/birdspecies.htm. 3-11-2007.

48. **Centers for Disease Control.** 2007. West Nile Virus Statistics, Surveillance, and Control. Division of Vector-Borne Infectious Diseases, Centers for Disease

Control. http://www.cdc.gov/ncidod/dvbid/westnile/surv&control.htm#surveillance. 3-24-2007.

49. **Chan-Tack, K. M. and G. Forrest**. 2005. Failure of interferon alpha-2b in a patient with West Nile virus meningoencephalitis and acute flaccid paralysis. Scand. J. Infect. Dis. **37**:944-946.

50. **Chastel, C., H. Launay, G. Rogues, and J. C. Beaucournu**. 1980. [Arbovirus infections in Spain: serological survey on small mammals]. Bull. Soc. Pathol. Exot. Filiales. **73**:384-390.

51. **Chu, J. J., B. G. Choo, J. W. Lee, and M. L. Ng**. 2003. Actin filaments participate in West Nile (Sarafend) virus maturation process. J. Med. Virol. **71**:463-472.

52. **Chu, J. J. and M. L. Ng**. 2004. Infectious Entry of West Nile Virus Occurs through a Clathrin-Mediated Endocytic Pathway. J. Virol. **78**:10543-10555.

53. **Clemens, M. J.** 2005. Translational control in virus-infected cells: models for cellular stress responses. Semin. Cell Dev. Biol. **16**:13-20.

54. **Cohen, J. K., A. M. Kilpatrick, F. C. Stroud, K. Paul, F. Wolf, and J. G. Else**. 2007. Seroprevalence of West Nile virus in nonhuman primates as related to mosquito abundance at two national primate research centers. Comp Med. **57**:115-119.

55. **Crance, J. M., N. Scaramozzino, A. Jouan, and D. Garin**. 2003. Interferon, ribavirin, 6-azauridine and glycyrrhizin: antiviral compounds active against pathogenic flaviviruses. Antiviral Res. **58**:73-79.

56. **Daffis, S., M. A. Samuel, B. C. Keller, M. Gale Jr., and M. S. Diamond**. 2007. Cell-specific IRF-3 responses protect against West Nile virus infection by IFN-dependent and independent mechanisms. PLoS Pathog. (*In Press*).

57. **Davis, L. E., R. DeBiasi, D. E. Goade, K. Y. Haaland, J. A. Harrington, J. B. Harnar, S. A. Pergam, M. K. King, B. K. DeMasters, and K. L. Tyler**. 2006. West Nile virus neuroinvasive disease. Ann. Neurol. **60**:286-300.

58. **Day, C. W., D. F. Smee, J. G. Julander, V. F. Yamshchikov, R. W. Sidwell, and J. D. Morrey**. 2005. Error-prone replication of West Nile virus caused by ribavirin. Antiviral Res. **67**:38-45.

59. **Denhardt, D. T.** 1996. Signal-transducing protein phosphorylation cascades mediated by Ras/Rho proteins in the mammalian cell: the potential for multiplex signalling. Biochem. J. **318 (Pt 3)**:729-747.

60. **Diamond, M. S., T. G. Roberts, D. Edgil, B. Lu, J. Ernst, and E. Harris**. 2000. Modulation of Dengue virus infection in human cells by alpha, beta, and gamma interferons. J. Virol. **74**:4957-4966.

61. **Diamond, M. S., B. Shrestha, E. Mehlhop, E. Sitati, and M. Engle**. 2003. Innate and Adaptive Immune Responses Determine Protection against

Disseminated Infection by West Nile Encephalitis Virus. Viral Immunol. **16**:259-278.

62. **Diamond, M. S., E. M. Sitati, L. D. Friend, S. Higgs, B. Shrestha, and M. Engle**. 2003. A critical role for induced IgM in the protection against West Nile virus infection. J. Exp. Med. **198**:1853-1862.

63. **Dietrich, G., J. A. Montenieri, N. A. Panella, S. Langevin, S. E. Lasater, K. Klenk, J. C. Kile, and N. Komar**. 2005. Serologic evidence of west nile virus infection in free-ranging mammals, Slidell, Louisiana, 2002. Vector. Borne. Zoonotic. Dis. **5**:288-292.

64. **Draganescu, N., R. Iftimovici, V. Iacobescu, E. Girjabu, A. Busila, D. Cvasniuc, G. Tudor, C. Lapusneanu, and M. Manastireanu**. 1975. Investigations on the presence of antibodies to several flaviviruses in humans and some domestic animals in a biotope with a high frequency of migratory birds. Virologie. **26**:103-108.

65. **Drummond, R.** 2006. West Nile virus in horses. Vet. Rec. **159**:895.

66. **Dupuis, A. P., P. P. Marra, and L. D. Kramer**. 2003. Serologic evidence of West Nile virus transmission, Jamaica, West Indies. Emerg. Infect. Dis. **9**:860-863.

67. **Ebel, G. D., J. Carricaburu, D. Young, K. A. Bernard, and L. D. Kramer**. 2004. Genetic and phenotypic variation of West Nile virus in New York, 2000-2003. Am. J. Trop. Med. Hyg. **71**:493-500.

68. **Ebel, G. D., I. Rochlin, J. Longacker, and L. D. Kramer**. 2005. Culex restuans (Diptera: Culicidae) relative abundance and vector competence for West Nile Virus. J. Med. Entomol. **42**:838-843.

69. **Farajollahi, A., W. J. Crans, D. Nickerson, P. Bryant, B. Wolf, A. Glaser, and T. G. Andreadis**. 2005. Detection of West Nile virus RNA from the louse fly Icosta americana (Diptera: Hippoboscidae). J. Am. Mosq. Control Assoc. **21**:474-476.

70. **Farfan-Ale, J. A., B. J. Blitvich, M. A. Lorono-Pino, N. L. Marlenee, E. P. Rosado-Paredes, J. E. Garcia-Rejon, L. F. Flores-Flores, L. Chulim-Perera, M. Lopez-Uribe, G. Perez-Mendoza, I. Sanchez-Herrera, W. Santamaria, J. Moo-Huchim, D. J. Gubler, B. C. Cropp, C. H. Calisher, and B. J. Beaty**. 2004. Longitudinal studies of West Nile virus infection in avians, Yucatan State, Mexico. Vector Borne Zoonotic. Dis. **4**:3-14.

71. **Feki, I., C. Marrakchi, M. Ben Hmida, F. Belahsen, M. Ben Jemaa, I. Maaloul, F. Kanoun, S. Ben Hamed, and C. Mhiri**. 2005. Epidemic West Nile virus encephalitis in Tunisia. Neuroepidemiology **24**:1-7.

72. **Fernandez-Salas, I., J. F. Contreras-Cordero, B. J. Blitvich, J. I. Gonzalez-Rojas, A. Cavazos-Alvarez, N. L. Marlenee, A. Elizondo-Quiroga, M. A. Lorono-Pino, D. J. Gubler, B. C. Cropp, C. H. Calisher, and B. J. Beaty**. 2003. Serologic evidence of West Nile Virus infection in birds, Tamaulipas State, Mexico. Vector Borne Zoonotic. Dis. **3**:209-213.

73. **Fontenille, D., F. Rodhain, J. P. Digoutte, C. Mathiot, J. Morvan, and P. Coulanges**. 1989. [Transmission cycles of the West-Nile virus in Madagascar, Indian Ocean]. Ann. Soc. Belg. Med. Trop. **69**:233-243.

74. **Foy, E., K. Li, C. Wang, R. Sumpter, Jr., M. Ikeda, S. M. Lemon, and M. Gale, Jr.** 2003. Regulation of interferon regulatory factor-3 by the hepatitis C virus serine protease. Science **300**:1145-1148.

75. **Fredericksen, B. L. and M. Gale, Jr.** 2006. West Nile Virus Evades Activation of Interferon Regulatory Factor 3 through RIG-I-Dependent and -Independent Pathways without Antagonizing Host Defense Signaling. J. Virol. **80**:2913-2923.

76. **Fredericksen, B. L., M. Smith, M. G. Katze, P. Y. Shi, and M. Gale, Jr.** 2004. The host response to West Nile Virus infection limits viral spread through the activation of the interferon regulatory factor 3 pathway. J. Virol. **78**:7737-7747.

77. **Gale, M., Jr. and M. G. Katze**. 1998. Molecular mechanisms of interferon resistance mediated by viral-directed inhibition of PKR, the interferon-induced protein kinase. Pharmacol. Ther. **78**:29-46.

78. **Gancz, A. Y., I. K. Barker, R. Lindsay, A. Dibernardo, K. McKeever, and B. Hunter**. 2004. West Nile virus outbreak in North American owls, Ontario, 2002. Emerg. Infect. Dis. **10**:2135-2142.

79. **Gancz, A. Y., D. G. Campbell, I. K. Barker, R. Lindsay, and B. Hunter**. 2004. Detecting West Nile virus in owls and raptors by an antigen-capture assay. Emerg. Infect. Dis. **10**:2204-2206.

80. **Garcia-Sastre, A.** 2002. Mechanisms of inhibition of the host interferon alpha/beta-mediated antiviral responses by viruses. Microbes. Infect. **4**:647-655.

81. **Gatto, L., C. Berlato, V. Poli, S. Tininini, I. Kinjyo, A. Yoshimura, M. A. Cassatella, and F. Bazzoni**. 2004. Analysis of SOCS-3 promoter responses to interferon gamma. J. Biol. Chem. **279**:13746-13754.

82. **George, S., P. N. Yergolkar, H. Kamala, and C. S. Kamala**. 1990. Outbreak of encephalitis in Bellary District of Karnataka & adjoining areas of Andhra Pradesh. Indian J. Med. Res. **91**:328-330.

83. **Ghosh, S. N., M. K. Goverdhan, P. S. Sathe, S. C. Chelliah, S. V. Naik, P. V. Godbole, and K. Banerjee**. 1990. Protective effect of 6-MFA, a fungal

interferon inducer against Japanese encephalitis virus in bonnet macaques. Indian J. Med. Res. **91**:408-413.

84. **Gibbs, S. E., A. B. Allison, M. J. Yabsley, D. G. Mead, B. R. Wilcox, and D. E. Stallknecht**. 2006. West Nile virus antibodies in avian species of Georgia, USA: 2000-2004. Vector Borne Zoonotic. Dis. **6**:57-72.

85. **Gibbs, S. E., N. L. Marlenee, J. Romines, D. Kavanaugh, J. L. Corn, and D. E. Stallknecht**. 2006. Antibodies to West Nile virus in feral swine from Florida, Georgia, and Texas, USA. Vector. Borne. Zoonotic. Dis. **6**:261-265.

86. **Glavits, R., E. Ferenczi, E. Ivanics, T. Bakonyi, T. Mato, P. Zarka, and V. Palya**. 2005. Co-occurrence of West Nile Fever and circovirus infection in a goose flock in Hungary. Avian Pathol. **34**:408-414.

87. **Godsey, M. S., Jr., M. S. Blackmore, N. A. Panella, K. Burkhalter, K. Gottfried, L. A. Halsey, R. Rutledge, S. A. Langevin, R. Gates, K. M. Lamonte, A. Lambert, R. S. Lanciotti, C. G. Blackmore, T. Loyless, L. Stark, R. Oliveri, L. Conti, and N. Komar**. 2005. West Nile virus epizootiology in the southeastern United States, 2001. Vector Borne Zoonotic. Dis. **5**:82-89.

88. **Godsey, M. S., Jr., R. Nasci, H. M. Savage, S. Aspen, R. King, A. M. Powers, K. Burkhalter, L. Colton, D. Charnetzky, S. Lasater, V. Taylor, and C. T.**

Palmisano. 2005. West Nile virus-infected mosquitoes, Louisiana, 2002. Emerg. Infect. Dis. **11**:1399-1404.

89. **Goldblum, N., W. JASINSKA-KLINGBERG, M. A. Klingberg, K. MARBERG, and V. V. STERK**. 1956. The natural history of West Nile Fever. I. Clinical observations during an epidemic in Israel. Am. J. Hyg. **64**:259-269.

90. **Goodbourn, S., L. Didcock, and R. E. Randall**. 2000. Interferons: cell signalling, immune modulation, antiviral response and virus countermeasures. J. Gen. Virol. **81**:2341-2364.

91. **Grandvaux, N., M. J. Servant, B. tenOever, G. C. Sen, S. Balachandran, G. N. Barber, R. Lin, and J. Hiscott**. 2002. Transcriptional profiling of interferon regulatory factor 3 target genes: direct involvement in the regulation of interferon-stimulated genes. J. Virol. **76**:5532-5539.

92. **Gresikova, M., M. Sekeyova, and E. Prazniakova**. 1975. Isolation and identification of group B arboviruses from the blood of birds captured in Czechoslovakia. Acta Virol. **19**:162-164.

93. **Guo, J. T., J. Hayashi, and C. Seeger**. 2005. West nile virus inhibits the signal transduction pathway of alpha interferon. J. Virol. **79**:1343-1350.

94. **Hall, R. A., D. J. Nisbet, K. B. Pham, A. T. Pyke, G. A. Smith, and A. A. Khromykh**. 2003. DNA vaccine coding for the full-length infectious Kunjin

virus RNA protects mice against the New York strain of West Nile virus. Proc. Natl. Acad. Sci. U. S. A **100**:10460-10464.

95. **Hanada, T., T. Yoshida, I. Kinjyo, S. Minoguchi, H. Yasukawa, S. Kato, H. Mimata, Y. Nomura, Y. Seki, M. Kubo, and A. Yoshimura**. 2001. A mutant form of JAB/SOCS1 augments the cytokine-induced JAK/STAT pathway by accelerating degradation of wild-type JAB/CIS family proteins through the SOCS-box. J. Biol. Chem. **276**:40746-40754.

96. **Hanna, S. L., T. C. Pierson, M. D. Sanchez, A. A. Ahmed, M. M. Murtadha, and R. W. Doms**. 2005. N-linked glycosylation of west nile virus envelope proteins influences particle assembly and infectivity. J. Virol. **79**:13262-13274.

97. **Hannoun C, Corniou B, and Mouchet J**. 1972. Role of migrating birds in arbovirus transfer between Africa and Europe., p. 167-172. *In* Cherepanov IA (ed.), Transcontinental connections of migratory birds and their role in the distribution of arboviruses. Novosibirsk, Russia: Nauka.

98. **Harinasuta, C., C. Wasi, and S. Vithanomsat**. 1984. The effect of interferon on Japanese encephalitis virus in vitro. Southeast Asian J. Trop. Med. Public Health **15**:564-568.

99. **Hayes, C. G., S. Baqar, T. Ahmed, M. A. Chowdhry, and W. K. Reisen**. 1982. West Nile virus in Pakistan. 1. Sero-epidemiological studies in Punjab Province. Trans. R. Soc. Trop. Med. Hyg. **76**:431-436.

100. **Hayes, E. B. and D. J. Gubler**. 2006. West Nile virus: epidemiology and clinical features of an emerging epidemic in the United States. Annu. Rev. Med. **57**:181-194.

101. **Heinz-Taheny, K. M., J. J. Andrews, M. J. Kinsel, A. P. Pessier, M. E. Pinkerton, K. Y. Lemberger, R. J. Novak, G. J. Dizikes, E. Edwards, and N. Komar**. 2004. West Nile virus infection in free-ranging squirrels in Illinois. J. Vet. Diagn. Invest **16**:186-190.

102. **Hilton, D. J.** 1999. Negative regulators of cytokine signal transduction. Cell Mol. Life Sci. **55**:1568-1577.

103. **Hilton, D. J., R. T. Richardson, W. S. Alexander, E. M. Viney, T. A. Willson, N. S. Sprigg, R. Starr, S. E. Nicholson, D. Metcalf, and N. A. Nicola**. 1998. Twenty proteins containing a C-terminal SOCS box form five structural classes. Proc. Natl. Acad. Sci. U. S. A **95**:114-119.

104. **Hjortsberg, L., C. Lindvall, M. Corcoran, V. Arulampalam, D. Chan, L. Thyrell, M. Nordenskjold, D. Grander, and K. Pokrovskaja**. 2007. Phosphoinositide 3-kinase regulates a subset of interferon-alpha-stimulated genes. Exp. Cell Res. **313**:404-414.

105. **Ho, H. H. and L. B. Ivashkiv**. 2006. Role of STAT3 in type I interferon responses. Negative regulation of STAT1-dependent inflammatory gene activation. J. Biol. Chem. **281**:14111-14118.

106. **Ho, L. J., L. F. Hung, C. Y. Weng, W. L. Wu, P. Chou, Y. L. Lin, D. M. Chang, T. Y. Tai, and J. H. Lai**. 2005. Dengue virus type 2 antagonizes IFN-alpha but not IFN-gamma antiviral effect via down-regulating Tyk2-STAT signaling in the human dendritic cell. J. Immunol. **174**:8163-8172.

107. **Horscroft, N., D. Bellows, I. Ansari, V. C. Lai, S. Dempsey, D. Liang, R. Donis, W. Zhong, and Z. Hong**. 2005. Establishment of a subgenomic replicon for bovine viral diarrhea virus in Huh-7 cells and modulation of interferon-regulated factor 3-mediated antiviral response. J. Virol. **79**:2788-2796.

108. **Hrnicek, M. J. and M. E. Mailliard**. 2004. Acute west nile virus in two patients receiving interferon and ribavirin for chronic hepatitis C. Am. J. Gastroenterol. **99**:957.

109. **Hubalek, Z. and J. Halouzka**. 1999. West Nile fever--a reemerging mosquito-borne viral disease in Europe. Emerg. Infect. Dis. **5**:643-650.

110. **Hurlbut, H. S., F. Rizk, R. M. Taylor, and T. H. Work**. 1956. A study of the ecology of West Nile virus in Egypt. Am. J. Trop. Med. Hyg. **5**:579-620.

111. **Ilangumaran, S., S. Ramanathan, and R. Rottapel**. 2004. Regulation of the immune system by SOCS family adaptor proteins. Semin. Immunol. **16**:351-365.

112. **Isaacs, A. and J. Lindenmann**. 1957. Virus interference. I. The interferon. Proc. R. Soc. Lond B Biol. Sci. **147**:258-267.

113. **Isaacs, A. and M. A. Westwood**. 1959. Duration of protective action of interferon against infection with West Nile virus. Nature **184(Suppl 16)**:1232-1233.

114. **Iwamoto, M., D. B. Jernigan, A. Guasch, M. J. Trepka, C. G. Blackmore, W. C. Hellinger, S. M. Pham, S. Zaki, R. S. Lanciotti, S. E. Lance-Parker, C. A. DiazGranados, A. G. Winquist, C. A. Perlino, S. Wiersma, K. L. Hillyer, J. L. Goodman, A. A. Marfin, M. E. Chamberland, and L. R. Petersen**. 2003. Transmission of West Nile virus from an organ donor to four transplant recipients. N. Engl. J. Med. **348**:2196-2203.

115. **Jacobson, E. R., P. E. Ginn, J. M. Troutman, L. Farina, L. Stark, K. Klenk, K. L. Burkhalter, and N. Komar**. 2005. West Nile virus infection in farmed American alligators (Alligator mississippiensis) in Florida. J. Wildl. Dis. **41**:96-106.

116. **Johnson, C. L. and M. Gale, Jr.** 2006. CARD games between virus and host get a new player. Trends Immunol. **27**:1-4.

117. **Jones, D. T., W. R. Taylor, and J. M. Thornton**. 1992. The rapid generation of mutation data matrices from protein sequences. Comput. Appl. Biosci. **8**:275-282.

118. **Jones, M., A. Davidson, L. Hibbert, P. Gruenwald, J. Schlaak, S. Ball, G. R. Foster, and M. Jacobs**. 2005. Dengue Virus Inhibits Alpha Interferon Signaling by Reducing STAT2 Expression. J. Virol. **79**:5414-5420.

119. **Jones, S. A.** 2005. Directing transition from innate to acquired immunity: defining a role for IL-6. J. Immunol. **175**:3463-3468.

120. **Jordan, I., T. Briese, N. Fischer, J. Y. Lau, and W. I. Lipkin**. 2000. Ribavirin inhibits West Nile virus replication and cytopathic effect in neural cells. J. Infect. Dis. **182**:1214-1217.

121. **Jozan, M., R. Evans, R. McLean, R. Hall, B. Tangredi, L. Reed, and J. Scott**. 2003. Detection of West Nile Virus infection in birds in the United States by blocking ELISA and immunohistochemistry. Vector Borne Zoonotic. Dis. **3**:99-110.

122. **Jupp, P. G.** 2001. The ecology of West Nile virus in South Africa and the occurrence of outbreaks in humans. Ann. N. Y. Acad. Sci. **951**:143-152.

123. **Juricova, Z.** 1992. [Arbovirus antibodies in wild game caught in Moravia]. Vet. Med. (Praha) **37**:633-636.

124. **Kalil, A. C., M. P. Devetten, S. Singh, B. Lesiak, D. P. Poage, K. Bargenquast, P. Fayad, and A. G. Freifeld**. 2005. Use of interferon-alpha in patients with West Nile encephalitis: report of 2 cases. Clin. Infect. Dis. **40**:764-766.

125. **Kato, H., O. Takeuchi, S. Sato, M. Yoneyama, M. Yamamoto, K. Matsui, S. Uematsu, A. Jung, T. Kawai, K. J. Ishii, O. Yamaguchi, K. Otsu, T. Tsujimura, C. S. Koh, Reis E Sousa, Y. Matsuura, T. Fujita, and S. Akira**. 2006. Differential roles of MDA5 and RIG-I helicases in the recognition of RNA viruses. Nature **441**:101-105.

126. **Katsoulidis, E., Y. Li, H. Mears, and L. C. Platanias**. 2005. The p38 mitogen-activated protein kinase pathway in interferon signal transduction. J. Interferon Cytokine Res. **25**:749-756.

127. **Katze, M. G., Y. He, and M. Gale, Jr.** 2002. Viruses and interferon: a fight for supremacy. Nat. Rev. Immunol. **2**:675-687.

128. **Kaur, S., S. Uddin, and L. C. Platanias**. 2005. The PI3' kinase pathway in interferon signaling. J. Interferon Cytokine Res. **25**:780-787.

129. **Kawai, T. and S. Akira**. 2007. Antiviral signaling through pattern recognition receptors. J. Biochem. (Tokyo) **141**:137-145.

130. **Keller, B. C., B. L. Fredericksen, M. A. Samuel, R. E. Mock, P. W. Mason, M. S. Diamond, and M. Gale, Jr.** 2006. Resistance to alpha/beta interferon is a

determinant of West Nile virus replication fitness and virulence. J. Virol. **80**:9424-9434.

131. **Khromykh, A. A. and E. G. Westaway**. 1994. Completion of Kunjin virus RNA sequence and recovery of an infectious RNA transcribed from stably cloned full-length cDNA. J. Virol. **68**:4580-4588.

132. **Kile, J. C., N. A. Panella, N. Komar, C. C. Chow, A. MacNeil, B. Robbins, and M. L. Bunning**. 2005. Serologic survey of cats and dogs during an epidemic of West Nile virus infection in humans. J. Am. Vet. Med. Assoc. **226**:1349-1353.

133. **Kilpatrick, A. M., L. D. Kramer, M. J. Jones, P. P. Marra, and P. Daszak**. 2006. West Nile virus epidemics in North America are driven by shifts in mosquito feeding behavior. PLoS. Biol. **4**:e82.

134. **Klein, C., I. Kimiagar, L. Pollak, R. Gandelman-Marton, A. Itzhaki, R. Milo, and J. M. Rabey**. 2002. Neurological features of West Nile virus infection during the 2000 outbreak in a regional hospital in Israel. J. Neurol. Sci. **200**:63-66.

135. **Klenk, K. and N. Komar**. 2003. Poor replication of West Nile virus (New York 1999 strain) in three reptilian and one amphibian species. Am. J. Trop. Med. Hyg. **69**:260-262.

136. **Komar, N., S. Langevin, S. Hinten, N. Nemeth, E. Edwards, D. Hettler, B. Davis, R. Bowen, and M. Bunning**. 2003. Experimental infection of North American birds with the New York 1999 strain of West Nile virus. Emerg. Infect. Dis. **9**:311-322.

137. **Komar, N., N. A. Panella, S. A. Langevin, A. C. Brault, M. Amador, E. Edwards, and J. C. Owen**. 2005. Avian hosts for West Nile virus in St. Tammany Parish, Louisiana, 2002. Am. J. Trop. Med. Hyg. **73**:1031-1037.

138. **Komar, O., M. B. Robbins, K. Klenk, B. J. Blitvich, N. L. Marlenee, K. L. Burkhalter, D. J. Gubler, G. Gonzalvez, C. J. Pena, A. T. Peterson, and N. Komar**. 2003. West Nile virus transmission in resident birds, Dominican Republic. Emerg. Infect. Dis. **9**:1299-1302.

139. **Kostiukov, M. A., A. N. Alekseev, V. P. Bulychev, and Z. E. Gordeeva**. 1986. [Experimental evidence for infection of Culex pipiens L. mosquitoes by West Nile fever virus from Rana ridibunda Pallas and its transmission by bites]. Med. Parazitol. (Mosk)76-78.

140. **Kramer, L. D., J. Li, and P. Y. Shi**. 2007. West Nile virus. Lancet Neurol. **6**:171-181.

141. **Krebs, D. L. and D. J. Hilton**. 2001. SOCS proteins: negative regulators of cytokine signaling. Stem Cells **19**:378-387.

142. **Krishnan, M. N., B. Sukumaran, U. Pal, H. Agaisse, J. L. Murray, T. W. Hodge, and E. Fikrig**. 2007. Rab 5 is required for the cellular entry of Dengue and West Nile Viruses. J. Virol.

143. **Kuchtey, R. W., G. S. Kosmorsky, D. Martin, and M. S. Lee**. 2003. Uveitis associated with west nile virus infection. Arch. Ophthalmol. **121**:1648-1649.

144. **Kumar, H., T. Kawai, H. Kato, S. Sato, K. Takahashi, C. Coban, M. Yamamoto, S. Uematsu, K. J. Ishii, O. Takeuchi, and S. Akira**. 2006. Essential role of IPS-1 in innate immune responses against RNA viruses. J. Exp. Med. **203**:1795-1803.

145. **L'vov, D. K., A. F. Dzharkenov, D. N. L'vov, V. A. Aristova, A. I. Kovtunov, V. L. Gromashevskii, O. I. Vyshemirskii, I. V. Galkina, S. V. Al'khovskii, E. I. Samokhvalov, A. G. Prilipov, P. G. Deriabin, E. I. Odolevskii, and R. M. Ibragimov**. 2002. [Isolation of the West Nile fever virus from the great cormorant Phalacrocorax carbo, the crow Corvus corone, and Hyalomma marginatum ticks associated with them in natural and synanthroic biocenosis in the Volga delta (Astrakhan region, 2001)]. Vopr. Virusol. **47**:7-12.

146. **La Rocca, S. A., R. J. Herbert, H. Crooke, T. W. Drew, T. E. Wileman, and P. P. Powell**. 2005. Loss of interferon regulatory factor 3 in cells infected with

classical swine fever virus involves the N-terminal protease, Npro. J. Virol. **79**:7239-7247.

147. **Lanciotti, R. S., G. D. Ebel, V. Deubel, A. J. Kerst, S. Murri, R. Meyer, M. Bowen, N. McKinney, W. E. Morrill, M. B. Crabtree, L. D. Kramer, and J. T. Roehrig**. 2002. Complete genome sequences and phylogenetic analysis of West Nile virus strains isolated from the United States, Europe, and the Middle East. Virology **298**:96-105.

148. **Lanciotti, R. S., J. T. Roehrig, V. Deubel, J. Smith, M. Parker, K. Steele, B. Crise, K. E. Volpe, M. B. Crabtree, J. H. Scherret, R. A. Hall, J. S. MacKenzie, C. B. Cropp, B. Panigrahy, E. Ostlund, B. Schmitt, M. Malkinson, C. Banet, J. Weissman, N. Komar, H. M. Savage, W. Stone, T. McNamara, and D. J. Gubler**. 1999. Origin of the West Nile virus responsible for an outbreak of encephalitis in the northeastern United States. Science **286**:2333-2337.

149. **Lay-Rogues, G., M. Valle, C. Chastel, and J. C. Beaucournu**. 1983. [Small wild mammals and arboviruses in Italy]. Bull. Soc. Pathol. Exot. Filiales. **76**:333-345.

150. **Le Bon, A., V. Durand, E. Kamphuis, C. Thompson, S. Bulfone-Paus, C. Rossmann, U. Kalinke, and D. F. Tough**. 2006. Direct stimulation of T

cells by type I IFN enhances the CD8+ T cell response during cross-priming. J. Immunol. **176**:4682-4689.

151. **Le Bon, A., N. Etchart, C. Rossmann, M. Ashton, S. Hou, D. Gewert, P. Borrow, and D. F. Tough**. 2003. Cross-priming of CD8+ T cells stimulated by virus-induced type I interferon. Nat. Immunol. **4**:1009-1015.

152. **Le Bon, A., C. Thompson, E. Kamphuis, V. Durand, C. Rossmann, U. Kalinke, and D. F. Tough**. 2006. Cutting edge: enhancement of antibody responses through direct stimulation of B and T cells by type I IFN. J. Immunol. **176**:2074-2078.

153. **Lee, M. S. and Y. J. Kim**. 2007. Signaling Pathways Downstream of Pattern-Recognition Receptors and Their Cross Talk. Annu. Rev. Biochem.

154. **Leung, S., S. A. Qureshi, I. M. Kerr, J. E. Darnell, Jr., and G. R. Stark**. 1995. Role of STAT2 in the alpha interferon signaling pathway. Mol. Cell Biol. **15**:1312-1317.

155. **Li, W. and M. A. Brinton**. 2001. The 3' stem loop of the West Nile virus genomic RNA can suppress translation of chimeric mRNAs. Virology **287**:49-61.

156. **Li, W., Y. Li, N. Kedersha, P. Anderson, M. Emara, K. M. Swiderek, G. T. Moreno, and M. A. Brinton**. 2002. Cell proteins TIA-1 and TIAR interact with the 3' stem-loop of the West Nile virus complementary minus-strand RNA and facilitate virus replication. J. Virol. **76**:11989-12000.

157. **Li, Y. P., K. J. Handberg, H. R. Juul-Madsen, M. F. Zhang, and P. H. Jorgensen**. 2007. Transcriptional profiles of chicken embryo cell cultures following infection with infectious bursal disease virus. Arch. Virol. **152**:463-478.

158. **Lichtensteiger, C. A., K. Heinz-Taheny, T. S. Osborne, R. J. Novak, B. A. Lewis, and M. L. Firth**. 2003. West Nile virus encephalitis and myocarditis in wolf and dog. Emerg. Infect. Dis. **9**:1303-1306.

159. **Lin, C. C., C. M. Chou, Y. L. Hsu, J. C. Lien, Y. M. Wang, S. T. Chen, S. C. Tsai, P. W. Hsiao, and C. J. Huang**. 2004. Characterization of two mosquito STATs, AaSTAT and CtSTAT. Differential regulation of tyrosine phosphorylation and DNA binding activity by lipopolysaccharide treatment and by Japanese encephalitis virus infection. J. Biol. Chem. **279**:3308-3317.

160. **Lin, R. J., B. L. Chang, H. P. Yu, C. L. Liao, and Y. L. Lin**. 2006. Blocking of interferon-induced Jak-Stat signaling by Japanese encephalitis virus NS5 through a protein tyrosine phosphatase-mediated mechanism. J. Virol. **80**:5908-5918.

161. **Lin, R. J., C. L. Liao, E. Lin, and Y. L. Lin**. 2004. Blocking of the alpha interferon-induced jak-stat signaling pathway by Japanese encephalitis virus infection. J. Virol. **78**:9285-9294.

162. **Lindenbach, B. D. and C. M. Rice**. 2001. Flaviviridae: the viruses and their replication, p. 991-1041. *In* D. M. Knipe and P. M. Howley (eds.), Fields Virology. Lippincott Williams & Wilkins, Philadelphia.

163. **Lindsay, R., I. Barker, G. Nayar, M. Drebot, S. Calvin, C. Scammell, C. Sachvie, T. S. Fleur, A. Dibernardo, M. Andonova, and H. Artsob**. 2003. Rapid antigen-capture assay to detect West Nile virus in dead corvids. Emerg. Infect. Dis. **9**:1406-1410.

164. **Liu, W. J., X. J. Wang, V. V. Mokhonov, P. Y. Shi, R. Randall, and A. A. Khromykh**. 2005. Inhibition of Interferon Signaling by the New York 99 Strain and Kunjin Subtype of West Nile Virus Involves Blockage of STAT1 and STAT2 Activation by Nonstructural Proteins. J. Virol. **79**:1934-1942.

165. **Lo, M. K., M. Tilgner, and P. Y. Shi**. 2003. Potential high-throughput assay for screening inhibitors of west nile virus replication. J. Virol. **77**:12901-12906.

166. **Loo, Y. M., D. M. Owen, K. Li, A. K. Erickson, C. L. Johnson, P. M. Fish, D. S. Carney, T. Wang, H. Ishida, M. Yoneyama, T. Fujita, T. Saito, W. M. Lee, C. H. Hagedorn, D. T. Lau, S. A. Weinman, S. M. Lemon, and M. Gale, Jr.** 2006. Viral and therapeutic control of IFN-beta promoter stimulator 1 during hepatitis C virus infection. Proc. Natl. Acad. Sci. U. S. A **103**:6001-6006.

167. **Ludwig, G. V., P. P. Calle, J. A. Mangiafico, B. L. Raphael, D. K. Danner, J. A. Hile, T. L. Clippinger, J. F. Smith, R. A. Cook, and T. McNamara**. 2002. An outbreak of West Nile virus in a New York City captive wildlife population. Am. J. Trop. Med. Hyg. **67**:67-75.

168. **Lutfalla, G., S. J. Holland, E. Cinato, D. Monneron, J. Reboul, N. C. Rogers, J. M. Smith, G. R. Stark, K. Gardiner, K. E. Mogensen, and .** 1995. Mutant U5A cells are complemented by an interferon-alpha beta receptor subunit generated by alternative processing of a new member of a cytokine receptor gene cluster. EMBO J. **14**:5100-5108.

169. **Lvov, D. K., A. A. Timopheeva, V. A. Smirnov, V. L. Gromashevsky, G. A. Sidorova, L. P. Nikiforov, A. A. Sazonov, A. P. Andreev, T. M. Skvortzova, L. K. Beresina, and V. A. Aristova**. 1975. Ecology of tick-borne viruses in colonies of birds in the USSR. Med. Biol. **53**:325-330.

170. **Mackenzie, J. M., M. K. Jones, and E. G. Westaway**. 1999. Markers for trans-Golgi membranes and the intermediate compartment localize to induced membranes with distinct replication functions in flavivirus-infected cells. J. Virol. **73**:9555-9567.

171. **Mackenzie, J. M., A. A. Khromykh, M. K. Jones, and E. G. Westaway**. 1998. Subcellular localization and some biochemical properties of the flavivirus Kunjin nonstructural proteins NS2A and NS4A. Virology **245**:203-215.

172. **Mackenzie, J. M. and E. G. Westaway**. 2001. Assembly and maturation of the flavivirus Kunjin virus appear to occur in the rough endoplasmic reticulum and along the secretory pathway, respectively. J. Virol. **75**:10787-10799.

173. **MacKenzie, J. S., D. J. Gubler, and L. R. Petersen**. 2004. Emerging flaviviruses: the spread and resurgence of Japanese encephalitis, West Nile and dengue viruses. Nat. Med. **10**:S98-S109.

174. **Madic, J., D. Huber, and B. Lugovic**. 1993. Serologic survey for selected viral and rickettsial agents of brown bears (Ursus arctos) in Croatia. J. Wildl. Dis. **29**:572-576.

175. **Mans, N. Z., S. E. Yurgionas, M. C. Garvin, R. E. Gary, J. D. Bresky, A. C. Galaitsis, and O. A. Ohajuruka**. 2004. West Nile virus in mosquitoes of Northern Ohio, 2001-2002. Am. J. Trop. Med. Hyg. **70**:562-565.

176. **Markoff, L.** 2003. 5'- and 3'-noncoding regions in flavivirus RNA. Adv. Virus Res. **59**:177-228.

177. **McBride, K. M. and N. C. Reich**. 2003. The ins and outs of STAT1 nuclear transport. Sci. STKE. **2003**:RE13.

178. **McIntosh, B., P. Jupp, I. Dossantos, and G. Meenehan**. 1976. Epidemics of West Nile and Sindbis Viruses in South Africa with Culex (Culex) Univittatus Theobald as Vector. South African Journal of Science **72**:295-300.

179. **McKendry, R., J. John, D. Flavell, M. Muller, I. M. Kerr, and G. R. Stark**. 1991. High-frequency mutagenesis of human cells and characterization of a mutant unresponsive to both alpha and gamma interferons. Proc. Natl. Acad. Sci. U. S. A **88**:11455-11459.

180. **McLean, R. G., S. R. Ubico, D. Bourne, and N. Komar**. 2002. West Nile virus in livestock and wildlife. Curr. Top. Microbiol. Immunol. **267**:271-308.

181. **Medlock, J. M., K. R. Snow, and S. Leach**. 2005. Potential transmission of West Nile virus in the British Isles: an ecological review of candidate mosquito bridge vectors. Med. Vet. Entomol. **19**:2-21.

182. **Meyer, T. and U. Vinkemeier**. 2004. Nucleocytoplasmic shuttling of STAT transcription factors. Eur. J. Biochem. **271**:4606-4612.

183. **Meylan, E. and J. Tschopp**. 2006. Toll-like receptors and RNA helicases: two parallel ways to trigger antiviral responses. Mol. Cell **22**:561-569.

184. **Miller, B. R., R. S. Nasci, M. S. Godsey, H. M. Savage, J. J. Lutwama, R. S. Lanciotti, and C. J. Peters**. 2000. First field evidence for natural vertical transmission of West Nile virus in Culex univittatus complex mosquitoes from Rift Valley province, Kenya. Am. J. Trop. Med. Hyg. **62**:240-246.

185. **Morales, M. A., M. Barrandeguy, C. Fabbri, J. B. Garcia, A. Vissani, K. Trono, G. Gutierrez, S. Pigretti, H. Menchaca, N. Garrido, N. Taylor, F.**

Fernandez, S. Levis, and D. Enria. 2006. West Nile virus isolation from equines in Argentina, 2006. Emerg. Infect. Dis. **12**:1559-1561.

186. **Morrey, J. D., C. W. Day, J. G. Julander, L. M. Blatt, D. F. Smee, and R. W. Sidwell**. 2004. Effect of interferon-alpha and interferon-inducers on West Nile virus in mouse and hamster animal models. Antivir. Chem. Chemother. **15**:101-109.

187. **Morrey, J. D., C. W. Day, J. G. Julander, A. L. Olsen, R. W. Sidwell, C. D. Cheney, and L. M. Blatt**. 2004. Modeling hamsters for evaluating West Nile virus therapies. Antiviral Res. **63**:41-50.

188. **Morvan, J., T. Besselaar, D. Fontenille, and P. Coulanges**. 1990. Antigenic variations in West Nile virus strains isolated in Madagascar since 1978. Res. Virol. **141**:667-676.

189. **Mostashari, F., M. L. Bunning, P. T. Kitsutani, D. A. Singer, D. Nash, M. J. Cooper, N. Katz, K. A. Liljebjelke, B. J. Biggerstaff, A. D. Fine, M. C. Layton, S. M. Mullin, A. J. Johnson, D. A. Martin, E. B. Hayes, and G. L. Campbell**. 2001. Epidemic West Nile encephalitis, New York, 1999: results of a household-based seroepidemiological survey. Lancet **358**:261-264.

190. **Mouchet, J., J. Rageau, C. Laumond, C. Hannoun, D. Beytout, J. Oudar, B. Corniou, and A. Chippaux**. 1970. [Epidemiology of West Nile virus: study

of a focus in Camargue. V. The fector: Culex modestus Ficalbi Diptera; Culicidae]. Ann. Inst. Pasteur (Paris) **118**:839-855.

191. **Mukhopadhyay, S., B. S. Kim, P. R. Chipman, M. G. Rossmann, and R. J. Kuhn**. 2003. Structure of West Nile virus. Science **302**:248.

192. **Mumcuoglu, K. Y., C. Banet-Noach, M. Malkinson, U. Shalom, and R. Galun**. 2005. Argasid ticks as possible vectors of West Nile virus in Israel. Vector Borne Zoonotic. Dis. **5**:65-71.

193. **Munoz-Jordan, J. L., M. Laurent-Rolle, J. Ashour, L. Martinez-Sobrido, M. Ashok, W. I. Lipkin, and A. Garcia-Sastre**. 2005. Inhibition of Alpha/Beta Interferon Signaling by the NS4B Protein of Flaviviruses. J. Virol. **79**:8004-8013.

194. **Munoz-Jordan, J. L., G. G. Sanchez-Burgos, M. Laurent-Rolle, and A. Garcia-Sastre**. 2003. Inhibition of interferon signaling by dengue virus. Proc. Natl. Acad. Sci. U. S. A.

195. **Nasci, R. S., H. M. Savage, D. J. White, J. R. Miller, B. C. Cropp, M. S. Godsey, A. J. Kerst, P. Bennett, K. Gottfried, and R. S. Lanciotti**. 2001. West Nile virus in overwintering Culex mosquitoes, New York City, 2000. Emerg. Infect. Dis. **7**:742-744.

196. **Nicholson, S. E., D. De Souza, L. J. Fabri, J. Corbin, T. A. Willson, J. G. Zhang, A. Silva, M. Asimakis, A. Farley, A. D. Nash, D. Metcalf, D. J.**

Hilton, N. A. Nicola, and M. Baca. 2000. Suppressor of cytokine signaling-3 preferentially binds to the SHP-2-binding site on the shared cytokine receptor subunit gp130. Proc. Natl. Acad. Sci. U. S. A **97**:6493-6498.

197. **Nicholson, S. E., T. A. Willson, A. Farley, R. Starr, J. G. Zhang, M. Baca, W. S. Alexander, D. Metcalf, D. J. Hilton, and N. A. Nicola**. 1999. Mutational analyses of the SOCS proteins suggest a dual domain requirement but distinct mechanisms for inhibition of LIF and IL-6 signal transduction. EMBO J. **18**:375-385.

198. **Nimnual, A. and D. Bar-Sagi**. 2002. The two hats of SOS. Sci. STKE. **2002**:E36.

199. **Nir, Y., R. Goldwasser, Y. Lasowski, and A. Avivi**. 1967. Isolation of arboviruses from wild birds in Israel. Am. J. Epidemiol. **86**:372-378.

200. **Nisole, S., J. P. Stoye, and A. Saib**. 2005. TRIM family proteins: retroviral restriction and antiviral defence. Nat. Rev. Microbiol. **3**:799-808.

201. **Osterrieth, P. M. and P. Deleplanque-Liegeois**. 1961. [The presence of antibodies against viruses transmitted by arthropods in the chimpanzee (Pan troglodites). Comparison of their immune state with that of man.]. Ann. Soc. Belg. Med. Trop. **41**:63-72.

202. **Paddock, C. D., W. L. Nicholson, J. Bhatnagar, C. S. Goldsmith, P. W. Greer, E. B. Hayes, J. A. Risko, C. Henderson, C. G. Blackmore, R. S.**

Lanciotti, G. L. Campbell, and S. R. Zaki. 2006. Fatal hemorrhagic fever caused by West Nile virus in the United States. Clin. Infect. Dis. **42**:1527-1535.

203. **Palmer, M. V., W. C. Stoffregen, D. G. Rogers, A. N. Hamir, J. A. Richt, D. D. Pedersen, and W. R. Waters**. 2004. West Nile virus infection in reindeer (Rangifer tarandus). J. Vet. Diagn. Invest **16**:219-222.

204. **Paul, S. D., P. K. Rajagopalan, and M. A. Sreenivasan**. 1970. Isolation of the West Nile virus from the frugivorous bat, Rousettus leschenaulti. Indian J. Med. Res. **58**:1169-1171.

205. **Pavri, K. M. and K. R. Singh**. 1965. ISOLATION OF WEST NILE VIRUS FROM CULEX FATIGANS MOSQUITOES FROM WESTERN INDIA. Indian J. Med. Res. **53**:501-505.

206. **Pealer, L. N., A. A. Marfin, L. R. Petersen, R. S. Lanciotti, P. L. Page, S. L. Stramer, M. G. Stobierski, K. Signs, B. Newman, H. Kapoor, J. L. Goodman, and M. E. Chamberland**. 2003. Transmission of West Nile virus through blood transfusion in the United States in 2002. N. Engl. J. Med. **349**:1236-1245.

207. **Platanias, L. C.** 2005. Mechanisms of type-I- and type-II-interferon-mediated signalling. Nat. Rev. Immunol. **5**:375-386.

208. **Platonov, A. E., G. A. Shipulin, O. Y. Shipulina, E. N. Tyutyunnik, T. I. Frolochkina, R. S. Lanciotti, S. Yazyshina, O. V. Platonova, I. L. Obukhov, A. N. Zhukov, Y. Y. Vengerov, and V. I. Pokrovskii**. 2001. Outbreak of West Nile virus infection, Volgograd Region, Russia, 1999. Emerg. Infect. Dis. **7**:128-132.

209. **Pogodina, V. V., M. P. Frolova, G. V. Malenko, G. I. Fokina, G. V. Koreshkova, L. L. Kiseleva, N. G. Bochkova, and N. M. Ralph**. 1983. Study on West Nile virus persistence in monkeys. Arch. Virol. **75**:71-86.

210. **Rappole, J. H., S. R. Derrickson, and Z. Hubalek**. 2000. Migratory birds and spread of West Nile virus in the Western Hemisphere. Emerg. Infect. Dis. **6**:319-328.

211. **Ratho, R. K., S. Sethi, and S. R. Prasad**. 1999. Prevalence of Japanese encephalitis and West Nile viral infections in pig population in and around Chandigarh. J. Commun. Dis. **31**:113-116.

212. **Ratterree, M. S., A. P. da Rosa, R. P. Bohm, Jr., F. B. Cogswell, K. M. Phillippi, K. Caillouet, S. Schwanberger, R. E. Shope, and R. B. Tesh**. 2003. West Nile virus infection in nonhuman primate breeding colony, concurrent with human epidemic, southern Louisiana. Emerg. Infect. Dis. **9**:1388-1394.

213. **Ratterree, M. S., R. A. Gutierrez, A. P. Travassos Da Rosa, B. J. Dille, D. W. Beasley, R. P. Bohm, S. M. Desai, P. J. Didier, L. G. Bikenmeyer, G. J. Dawson, T. P. Leary, G. Schochetman, K. Phillippi-Falkenstein, J. Arroyo, A. D. Barrett, and R. B. Tesh**. 2004. Experimental infection of rhesus macaques with west nile virus: level and duration of viremia and kinetics of the antibody response after infection. J. Infect. Dis. **189**:669-676.

214. **Reed, L. J. and H. Muench**. 1938. A simple method of estimating fifty per cent endpoints. The American Journal of Hygiene **27**:493-497.

215. **Reisen, W. K., C. G. Hayes, K. Azra, S. Niaz, F. Mahmood, T. Parveen, and P. F. Boreham**. 1982. West Nile virus in Pakistan. II. Entomological studies at Changa Manga National Forest, Punjab Province. Trans. R. Soc. Trop. Med. Hyg. **76**:437-448.

216. **Rice, C. M.** 1996. Flaviviridae: The viruses and their replication, p. 931-960. *In* B. N. Fields, D. M. Knipe, and P. M. Howley (eds.), Fields Virology. Lippincott Williams & Wilkins, Philadelphia.

217. **Rodrigues, F. M., S. N. Guttikar, and B. D. Pinto**. 1981. Prevalence of antibodies to Japanese encephalitis and West Nile viruses among wild birds in the Krishna-Godavari Delta, Andhra Pradesh, India. Trans. R. Soc. Trop. Med. Hyg. **75**:258-262.

218. **Rossi, S. L., Q. Zhao, V. K. O'Donnell, and P. W. Mason**. 2005. Adaptation of West Nile virus replicons to cells in culture and use of replicon-bearing cells to probe antiviral action. Virology **331**:457-470.

219. **Rottenberg, M. and K. Kristensson**. 2002. Effects of interferon-gamma on neuronal infections. Viral Immunol. **15**:247-260.

220. **Sabio, I. J., A. J. Mackay, A. Roy, and L. D. Foil**. 2006. Detection of West Nile virus RNA in pools of three species of ceratopogonids (Diptera: Ceratopogonidae) collected in Louisiana. J. Med. Entomol. **43**:1020-1022.

221. **Samuel, C. E.** 2001. Antiviral actions of interferons. Clin. Microbiol. Rev. **14**:778-809, table.

222. **Samuel, M. A. and M. S. Diamond**. 2005. Alpha/beta interferon protects against lethal West Nile virus infection by restricting cellular tropism and enhancing neuronal survival. J. Virol. **79**:13350-13361.

223. **Samuel, M. A., K. Whitby, B. C. Keller, A. Marri, W. Barchet, B. R. Williams, R. H. Silverman, M. Gale, Jr., and M. S. Diamond**. 2006. PKR and RNase L contribute to protection against lethal West Nile Virus infection by controlling early viral spread in the periphery and replication in neurons. J. Virol. **80**:7009-7019.

224. **Santaella, J., R. McLean, J. S. Hall, J. S. Gill, R. A. Bowen, H. H. Hadow, and L. Clark**. 2005. West Nile virus serosurveillance in Iowa white-tailed deer (1999-2003). Am. J. Trop. Med. Hyg. **73**:1038-1042.

225. **Sasaki, A., H. Yasukawa, A. Suzuki, S. Kamizono, T. Syoda, I. Kinjyo, M. Sasaki, J. A. Johnston, and A. Yoshimura**. 1999. Cytokine-inducible SH2 protein-3 (CIS3/SOCS3) inhibits Janus tyrosine kinase by binding through the N-terminal kinase inhibitory region as well as SH2 domain. Genes Cells **4**:339-351.

226. **Savage, H. M., C. Ceianu, G. Nicolescu, N. Karabatsos, R. Lanciotti, A. Vladimirescu, L. Laiv, A. Ungureanu, C. Romanca, and T. F. Tsai**. 1999. Entomologic and avian investigations of an epidemic of West Nile fever in Romania in 1996, with serologic and molecular characterization of a virus isolate from mosquitoes. Am. J. Trop. Med. Hyg. **61**:600-611.

227. **Sayao, A. L., O. Suchowersky, A. Al Khathaami, B. Klassen, N. R. Katz, R. Sevick, P. Tilley, J. Fox, and D. Patry**. 2004. Calgary experience with West Nile virus neurological syndrome during the late summer of 2003. Can. J. Neurol. Sci. **31**:194-203.

228. **Scherbik, S. V., J. M. Paranjape, B. M. Stockman, R. H. Silverman, and M. A. Brinton**. 2006. RNase L plays a role in the antiviral response to West Nile virus. J. Virol. **80**:2987-2999.

229. **Schmidt, J. R. and M. I. Said**. 1964. ISOLATION OF WEST NILE VIRUS FROM THE AFRICAN BIRD ARGASID, ARGAS REFLEXUS HERMANNI, IN EGYPT. J. Med. Entomol. **39**:83-86.

230. **Scholle, F. and P. W. Mason**. 2005. West Nile virus replication interferes with both poly(I:C)-induced interferon gene transcription and response to interferon treatment. Virology.

231. **Schultz, U., B. Kaspers, and P. Staeheli**. 2004. The interferon system of non-mammalian vertebrates. Dev. Comp Immunol. **28**:499-508.

232. **Sen, G. C.** 2001. Viruses and interferons. Annu. Rev. Microbiol. **55**:255-281.

233. **Shi, P. Y., W. Li, and M. A. Brinton**. 1996. Cell proteins bind specifically to West Nile virus minus-strand 3' stem-loop RNA. J. Virol. **70**:6278-6287.

234. **Shi, P. Y., M. Tilgner, and M. K. Lo**. 2002. Construction and characterization of subgenomic replicons of New York strain of West Nile virus. Virology **296**:219-233.

235. **Shi, P. Y., M. Tilgner, M. K. Lo, K. A. Kent, and K. A. Bernard**. 2002. Infectious cDNA clone of the epidemic west nile virus from New York City. J. Virol. **76**:5847-5856.

236. **Shirato, K., H. Miyoshi, A. Goto, Y. Ako, T. Ueki, H. Kariwa, and I. Takashima**. 2004. Viral envelope protein glycosylation is a molecular

determinant of the neuroinvasiveness of the New York strain of West Nile virus. J. Gen. Virol. **85**:3637-3645.

237. **Shrestha, B., M. A. Samuel, and M. S. Diamond**. 2006. CD8+ T cells require perforin to clear West Nile virus from infected neurons. J. Virol. **80**:119-129.

238. **Shrestha, B., T. Wang, M. A. Samuel, K. Whitby, J. Craft, E. Fikrig, and M. S. Diamond**. 2006. Gamma interferon plays a crucial early antiviral role in protection against West Nile virus infection. J. Virol. **80**:5338-5348.

239. **Shuai, K. and B. Liu**. 2005. Regulation of gene-activation pathways by PIAS proteins in the immune system. Nat. Rev. Immunol. **5**:593-605.

240. **Silva, A. M., M. Whitmore, Z. Xu, Z. Jiang, X. Li, and B. R. Williams**. 2004. Protein kinase R (PKR) interacts with and activates mitogen-activated protein kinase kinase 6 (MKK6) in response to double-stranded RNA stimulation. J. Biol. Chem. **279**:37670-37676.

241. **Sioud, M.** 2006. Innate sensing of self and non-self RNAs by Toll-like receptors. Trends Mol. Med. **12**:167-176.

242. **Sitati, E. M. and M. S. Diamond**. 2006. CD4+ T-cell responses are required for clearance of West Nile virus from the central nervous system. J. Virol. **80**:12060-12069.

243. **Sixl, W., M. Batikova, D. Stunzner, M. Sekeyova, B. Sixl-Voigt, and M. Gresikova**. 1973. Haemagglutination-inhibiting antibodies against arboviruses in animal sera, collected in some regions in Austria. II. Zentralbl. Bakteriol. [Orig. A] **224**:303-308.

244. **Skolnik, E. Y., C. H. Lee, A. Batzer, L. M. Vicentini, M. Zhou, R. Daly, M. J. Myers, Jr., J. M. Backer, A. Ullrich, M. F. White, and .** 1993. The SH2/SH3 domain-containing protein GRB2 interacts with tyrosine-phosphorylated IRS1 and Shc: implications for insulin control of ras signalling. EMBO J. **12**:1929-1936.

245. **Smithburn, K. C., T. P. Hughes, A. W. Burke, and J. H. Paul**. 1940. A neurotropic virus isolated from the blood of a native of Uganda. Am. J. Trop. Med. **20**:471-492.

246. **Solomon, T., M. H. Ooi, D. W. Beasley, and M. Mallewa**. 2003. West Nile encephalitis. BMJ **326**:865-869.

247. **Song, M. M. and K. Shuai**. 1998. The suppressor of cytokine signaling (SOCS) 1 and SOCS3 but not SOCS2 proteins inhibit interferon-mediated antiviral and antiproliferative activities. J. Biol. Chem. **273**:35056-35062.

248. **Steele, K. E., M. J. Linn, R. J. Schoepp, N. Komar, T. W. Geisbert, R. M. Manduca, P. P. Calle, B. L. Raphael, T. L. Clippinger, T. Larsen, J. Smith, R. S. Lanciotti, N. A. Panella, and T. S. McNamara**. 2000.

Pathology of fatal West Nile virus infections in native and exotic birds during the 1999 outbreak in New York City, New York. Vet. Pathol. **37**:208-224.

249. **Steinman, A., C. Banet-Noach, S. Tal, O. Levi, L. Simanov, S. Perk, M. Malkinson, and N. Shpigel**. 2003. West Nile virus infection in crocodiles. Emerg. Infect. Dis. **9**:887-889.

250. **Stone, W. B., J. C. Okoniewski, J. E. Therrien, L. D. Kramer, E. B. Kauffman, and M. Eidson**. 2004. VecTest as diagnostic and surveillance tool for West Nile virus in dead birds. Emerg. Infect. Dis. **10**:2175-2181.

251. **Stout, W. E., A. G. Cassini, J. K. Meece, J. M. Papp, R. N. Rosenfield, and K. D. Reed**. 2005. Serologic evidence of West Nile virus infection in three wild raptor populations. Avian Dis. **49**:371-375.

252. **Styer, L. M., K. A. Bernard, and L. D. Kramer**. 2006. Enhanced early West Nile virus infection in young chickens infected by mosquito bite: effect of viral dose. Am. J. Trop. Med. Hyg. **75**:337-345.

253. **Sumpter, R., Jr., C. Wang, E. Foy, Y. M. Loo, and M. Gale, Jr.** 2004. Viral evolution and interferon resistance of hepatitis C virus RNA replication in a cell culture model. J. Virol. **78**:11591-11604.

254. **Taylor, J. L., C. Schoenherr, and S. E. Grossberg**. 1980. Protection against Japanese encephalitis virus in mice and hamsters by treatment with

carboxymethylacridanone, a potent interferon inducer. J. Infect. Dis. **142**:394-399.

255. **Ternovoi, V. A., E. V. Protopopova, S. G. Surmach, M. V. Gazetdinov, S. I. Zolotykh, A. M. Shestopalov, E. V. Pavlenko, G. N. Leonova, and V. B. Loktev**. 2006. [The genotyping of the West Nile virus in birds in the far eastern region of Russia in 2002-2004]. Mol. Gen. Mikrobiol. Virusol.30-35.

256. **Ternovoi, V. A., M. I. Shchelkanov, A. M. Shestopalov, V. A. Aristova, E. V. Protopopova, V. L. Gromashevskii, A. V. Druziaka, A. A. Slavskii, S. I. Zolotykh, V. B. Loktev, and D. K. L'vov**. 2004. [Detection of West Nile virus in birds in the territories of Baraba and Kulunda lowlands (West Siberian migration way) during summer-autumn of 2002]. Vopr. Virusol. **49**:52-56.

257. **Tesh, R. B., R. Parsons, M. Siirin, Y. Randle, C. Sargent, H. Guzman, T. Wuithiranyagool, S. Higgs, D. L. Vanlandingham, A. A. Bala, K. Haas, and B. Zerinque**. 2004. Year-round West Nile virus activity, Gulf Coast region, Texas and Louisiana. Emerg. Infect. Dis. **10**:1649-1652.

258. **Thompson, J. D., D. G. Higgins, and T. J. Gibson**. 1994. CLUSTAL W: improving the sensitivity of progressive multiple sequence alignment

through sequence weighting, position-specific gap penalties and weight matrix choice. Nucleic Acids Res. **22**:4673-4680.

259. **Tilgner, M., T. S. Deas, and P. Y. Shi**. 2005. The flavivirus-conserved penta-nucleotide in the 3' stem-loop of the West Nile virus genome requires a specific sequence and structure for RNA synthesis, but not for viral translation. Virology **331**:375-386.

260. **Tomori, O., A. Fagbami, and A. Fabiyi**. 1978. Isolations of West Nile virus from man in Nigeria. Trans. R. Soc. Trop. Med. Hyg. **72**:103-104.

261. **Tough, D. F.** 2004. Type I interferon as a link between innate and adaptive immunity through dendritic cell stimulation. Leuk. Lymphoma **45**:257-264.

262. **U.S.Geological Society.** 2006. USGS National Wildlife Health Center - West Nile Virus Project. U.S.Geological Survey. http://www.nwhc.usgs.gov/disease_information/west_nile_virus/index.jsp. 3-10-2007.

263. **Uze, G. and D. Monneron**. 2007. IL-28 and IL-29: Newcomers to the interferon family. Biochimie.

264. **Valentino, L. and J. Pierre**. 2006. JAK/STAT signal transduction: regulators and implication in hematological malignancies. Biochem. Pharmacol. **71**:713-721.

265. **van den Hurk, A. F., D. J. Nisbet, P. N. Foley, S. A. Ritchie, J. S. MacKenzie, and N. W. Beebe**. 2002. Isolation of arboviruses from mosquitoes (Diptera: Culicidae) collected from the Gulf Plains region of northwest Queensland, Australia. J. Med. Entomol. **39**:786-792.

266. **Vidy, A., J. El Bougrini, M. K. Chelbi-Alix, and D. Blondel**. 2007. The Nucleocytoplasmic Rabies Virus P Protein Counteracts Interferon Signaling by Inhibiting both Nuclear Accumulation and DNA Binding of STAT1. J. Virol. **81**:4255-4263.

267. **Vithanomsat, S., C. Wasi, C. Harinasuta, and P. Thongcharoen**. 1984. The effect of interferon on flaviviruses in vitro: a preliminary study. Southeast Asian J. Trop. Med. Public Health **15**:27-31.

268. **Wang, F., Y. Ma, J. W. Barrett, X. Gao, J. Loh, E. Barton, H. W. Virgin, and G. McFadden**. 2004. Disruption of Erk-dependent type I interferon induction breaks the myxoma virus species barrier. Nat. Immunol. **5**:1266-1274.

269. **Wang, T., T. Town, L. Alexopoulou, J. F. Anderson, E. Fikrig, and R. A. Flavell**. 2004. Toll-like receptor 3 mediates West Nile virus entry into the brain causing lethal encephalitis. Nat. Med.

270. **Weber, F., G. Kochs, and O. Haller**. 2004. Inverse interference: how viruses fight the interferon system. Viral Immunol. **17**:498-515.

271. **Weiskittel, P. D.** 2004. West Nile virus infection in a renal transplant recipient. Nephrol. Nurs. J. **31**:327-329.

272. **Westaway, E. G., J. M. Mackenzie, M. T. Kenney, M. K. Jones, and A. A. Khromykh**. 1997. Ultrastructure of Kunjin virus-infected cells: colocalization of NS1 and NS3 with double-stranded RNA, and of NS2B with NS3, in virus-induced membrane structures. J. Virol. **71**:6650-6661.

273. **Westaway, E. G., J. M. Mackenzie, and A. A. Khromykh**. 2003. Kunjin RNA replication and applications of Kunjin replicons. Adv. Virus Res. **59**:99-140.

274. **Wicker, J. A., M. C. Whiteman, D. W. Beasley, C. T. Davis, S. Zhang, B. S. Schneider, S. Higgs, R. M. Kinney, and A. D. Barrett**. 2006. A single amino acid substitution in the central portion of the West Nile virus NS4B protein confers a highly attenuated phenotype in mice. Virology.

275. **Woodall, J. P., J. D. Gillett, P. S. Corbet, M. P. Weinbren, and M. C. Williams**. 1961. The isolation of West Nile virus from the bird-biting mosquito Mansonia metallica in Uganda. Ann. Trop. Med. Parasitol. **55**:398-402.

276. **Work, T. H., H. S. Hurlbut, and R. M. Taylor**. 1953. Isolation of West Nile virus from hooded crow and rock pigeon in the Nile delta. Proc. Soc. Exp. Biol. Med. **84**:719-722.

277. **Xiao, S. Y., H. Guzman, H. Zhang, A. P. Travassos Da Rosa, and R. B. Tesh**. 2001. West Nile virus infection in the golden hamster (Mesocricetus auratus): a model for West Nile encephalitis. Emerg. Infect. Dis. **7**:714-721.

278. **Yaeger, M., K. J. Yoon, K. Schwartz, and L. Berkland**. 2004. West Nile virus meningoencephalitis in a Suri alpaca and Suffolk ewe. J. Vet. Diagn. Invest **16**:64-66.

279. **Yamshchikov, G., V. Borisevich, A. Seregin, E. Chaporgina, M. Mishina, V. Mishin, C. W. Kwok, and V. Yamshchikov**. 2004. An attenuated West Nile prototype virus is highly immunogenic and protects against the deadly NY99 strain: a candidate for live WN vaccine development. Virology **330**:304-312.

280. **Yasukawa, H., H. Misawa, H. Sakamoto, M. Masuhara, A. Sasaki, T. Wakioka, S. Ohtsuka, T. Imaizumi, T. Matsuda, J. N. Ihle, and A. Yoshimura**. 1999. The JAK-binding protein JAB inhibits Janus tyrosine kinase activity through binding in the activation loop. EMBO J. **18**:1309-1320.

281. **Yoneyama, M., M. Kikuchi, T. Natsukawa, N. Shinobu, T. Imaizumi, S. Akira, M. Miyagishi, K. Taira, and T. Fujita**. 2004. CARD-containing DExD/H box RNA helicase, RIG-I, plays an essential role for double-stranded RNA-induced innate antiviral responses. SUBMITTED.

282. **Yoneyama, M., M. Kikuchi, T. Natsukawa, N. Shinobu, T. Imaizumi, M. Miyagishi, K. Taira, S. Akira, and T. Fujita**. 2004. The RNA helicase RIG-I has an essential function in double-stranded RNA-induced innate antiviral responses. Nat. Immunol.

283. **Zhang, J. G., A. Farley, S. E. Nicholson, T. A. Willson, L. M. Zugaro, R. J. Simpson, R. L. Moritz, D. Cary, R. Richardson, G. Hausmann, B. J. Kile, S. B. Kent, W. S. Alexander, D. Metcalf, D. J. Hilton, N. A. Nicola, and M. Baca**. 1999. The conserved SOCS box motif in suppressors of cytokine signaling binds to elongins B and C and may couple bound proteins to proteasomal degradation. Proc. Natl. Acad. Sci. U. S. A **96**:2071-2076.

Vitae

Brian Christopher Keller was born November 25, 1977 in Oberlin, Kansas to James and Sherry Keller. He has a younger sister, Krista, who lives in Olathe, Kansas with her husband Andrew Dueringer. After graduating from Douglass High School, Douglass, Kansas in 1996 he entered Kansas State University where he received the degree of Bachelor of Science in Microbiology with a Secondary Major in International Studies and a Minor in French. During his undergraduate years, Brian was awarded a Goldwater Scholarship and studied abroad in Botswana (1998) and at l'Université Blaise Pascal in Clermont-Ferrand, France (2000). He graduated from Kansas State University in 2001 and joined the Medical Scientist Training Program (M.D./Ph.D.) at the University of Texas Southwestern Medical Center shortly, thereafter. Prior to his arrival in Dallas, he married Amber Donelle Rucker of Douglass, Kansas. They now have a beautiful 19 month old daughter, Anna.

Permanent Address: 1823 Austin Avenue

Grand Prairie, TX 75051